Norwegian University
of Life Sciences

Master's Thesis 2022 30 ECTS

The Faculty of Environmental Sciences and Natural Resource Management

Biogeochemical Cycling and Retention of Fe in Boreal Lakes

Therese Merete Børseth

Natural Resource Management

Acknowledgements

This thesis concludes my master's degree in Natural Resource Management at the Norwegian University of Life Sciences (NMBU). The study was conducted in collaboration with Vannområde Øyeren [the River Basin Sub-District Øyeren], Statsforvalteren i Oslo og Viken [The County Governor of Oslo and Viken], and the Norwegian Institute for Nature Research (NINA), whose guidance and financial support were instrumental to the project.

First and foremost, I would like to express my gratitude to my supervisor Gunnhild Riise (MINA) for including me in the project and for her continuous assistance and involvement at every step of the process. I would also like to give special thanks to my co-advisors Kristian Moseby (Vannområde Øyeren), for his important support and contributions, Ståle Haaland (MINA), who offered invaluable feedback and advice, and Terje Wivestad (Statsforvalteren i Oslo og Viken) and Stein Johnsen (NINA), who generously provided knowledge and expertise.

I am very grateful for my fellow master's student Sigrid Hårstad Pålsrud, not only for her partnership in this project, but also for her hard work in the field while I was unable to move back to Norway during the pandemic.

Finally, many thanks to Eivind Molversmyr for his guidance and time during laboratory work.

Abstract

An observed trend of increasing iron (Fe) concentrations in boreal freshwaters has been attributed to changes in the biogeochemical cycling of Fe. To better understand the drivers behind this trend, as well as any potential negative impacts on ecosystems, the biogeochemical cycling of Fe in a lake in south eastern Norway was studied between May and September 2021.

The study lake Vindlandstjernet is a small and shallow lake located upstream from its much larger recipient Lake Øyeren. Increased Fe concentrations have previously been reported in the study lake's catchment area, so it was of interest to investigate whether the lake acts as a sink or a source of Fe. The objectives of this study were therefore to (1) examine the seasonal variations of Fe in a boreal lake at different depths, to (2) examine the retention and cycling of Fe in a boreal lake under different runoff and stratification conditions, and to (3) examine potential effects of increased Fe concentrations on aquatic fauna. Further, it was hypothesised that (i) thermal stratification affects the distribution and cycling of Fe in the water column of the lake, and that (ii) the lake is a source of Fe during high flow.

The weather prior to and during the study period were characterised as warm and dry. During early spring, the lake's catchment area received very little precipitation compared to normal, which would have led to reduced runoff. The catchment received more precipitation than normal in May, where Fe concentrations saw an upwards trend along with dissolved organic carbon (DOC) and Fe (oxy)hydroxide associated parameters. The lake was thermally stratified in June and July resulting in hypoxic and anoxic conditions in the hypolimnion. Thermal stratification and reducing conditions led to the remobilisation of Fe to the water column and the accumulation of several water parameters at the bottom layer of the lake. A heavy rainfall event at the end of July diluted most parameters, including Fe. By mid-August, the lake had experienced some circulation, likely encouraged by the heavy rainfall event, with increased particulate Fe concentrations evenly distributed in the water column.

The results from this study confirm the first hypothesis that thermal stratification affects the distribution and cycling of Fe in the water column. Further, the results indicate that the lake acts as a Fe sink in the catchment, but more data on the total Fe budget of the lake would be needed to reject the second hypothesis. It is not clear how much the lake contributed as a Fe source to its outlet stream during high flow due to significant Fe mobilisation nearby in the catchment.

Sammendrag

En økende trend i jernkonsentrasjoner i boreale vassdrag har blitt sett på i sammenheng med endringer i den biogeokjemiske syklusen til jern. For å bedre kunne forstå driverne bak denne trenden, samt eventuelle negative konsekvenser for økosystemer, så har den biogeokjemiske omsetningen og tilbakeholdelsen av jern i en innsjø på Sør-Østlandet i Norge blitt undersøkt mellom mai og september 2021.

Studieområdet er Vindlandstjernet, en liten og grunn innsjø som ligger oppstrøms Øyeren. Tidligere undersøkelser har rapportert om økte jernkonsentrasjoner i innsjøens vassdrag, så det var av interesse å undersøke om innsjøen lagrer eller eksporterer jern. Målet med dette prosjektet var derfor å (1) undersøke sesongvariasjoner i jern ved ulike dyp i en boreal innsjø, å (2) undersøke tilbakeholdelse og omsetning av jern under ulike sjiktnings- og avrenningsforhold, og å (3) undersøke potensielle effekter av økte jernkonsentrasjoner på ferskvannsfauna. Videre ble det predikert at (i) temperatursjiktninger påvirker fordelingen og omsetningen til jern i vannsøylen, og at (ii) innsjøen er en jernkilde under høye avrenningsforhold.

Været før og under studieperioden var varmt og tørt. Innsjøens nedbørsfelt hadde svært lite nedbør i forhold til normalverdien, som sannsynligvis ga mindre avrenning. I mai hadde nedbørsfeltet mer nedbør enn vanlig, hvor jernkonsentrasjonen i innsjøen hadde en økende trend sammen med parametere tilknyttet løst organisk karbon (DOC) og jernhydroksid. Innsjøen var sjiktet i juni og juli som ga lave konsentrasjoner av oksygen i bunnvannet. Temperatursjiktning og reduserende forhold førte til en remobilisering av jern til vannsøylen og en akkumulering av flere vannparametere i bunnvannet. Kraftig nedbør i slutten av juli tynnet ut nesten alle parameterne, inkludert jern. I løpet av august hadde innsjøen gått gjennom en sirkulasjon som følge av kraftig nedbør, med økte partikulære jernkonsentrasjoner jevnt fordelt i vannsøylen.

Resultatene fra dette prosjektet bekrefter den første prediksjonen om at temperatursjiktninger påvirker fordelingen og omsetningen til jern i vannsøylen. Videre tyder resultatene på at innsjøen generelt lagrer jern, men mer data er nødvendig for å kunne avkrefte den andre prediksjonen. Det er fremdeles uklart hvorvidt innsjøen eksporterte jern til utløpsbekken ved høy avrenning, da det finnes flere potensielle kilder.

List of Figures

List of Tables

Table of Contents

List of Appendices

1. Introduction

1.1 Background

1.1.1 Increasing trend of iron (Fe) concentrations in boreal freshwaters

Many studies have reported on a strong increase of iron (Fe) concentrations in northern European and American freshwaters. In the United Kingdom (UK), Neal et al. (2008) found an average increase of 100% between 1984 and 2006 in upland freshwaters. In Swedish rivers, Fe concentrations have on average doubled since 1972 (Kritzberg and Ekström, 2012). Many water bodies in North America have seen a significant increase from 1990 (Björnerås et al., 2017), and in Finland Sarkkola et al. (2013) found a 21-74% increase in surface waters between 1995 and 2006.

The increase in Fe concentrations in boreal freshwaters has been attributed to changes in the biogeochemical cycling of Fe. These changes have been linked to an increased export of natural organic matter (NOM) in catchments (Neal et al., 2008), higher temperatures (Ekström et al., 2016), more frequent and extreme precipitation events (Knorr et al., 2009; Kritzberg and Ekström, 2012; Sarkkola et al., 2013; Weyhenmeyer et al., 2014), land use changes (Kritzberg and Ekström, 2012; Finstad et al., 2016; Kritzberg, 2017), and reduced atmospheric acid deposition (Neal et al., 2008; Weyhenmeyer et al., 2014; Björnerås et al., 2017).

1.1.2 The biogeochemical cycle of Fe in boreal lakes and catchments

The mobility and bioavailability of Fe in aquatic systems are heavily influenced by its speciation, which depends on the relative importance of many different competing processes, such as ion exchange, redox reactions, adsorption/desorption, precipitation/dissolution and complexation/dissociation (Shaked et al., 2004).

Redox reactions is a key process affecting the distribution of Fe in freshwater catchments because of the difference in solubility and mobility of Fe(II) and Fe(III) (Mortimer, 1941). In most lakes and lotic systems, Fe will quickly oxidise to its trivalent state Fe(III) and precipitate into the sediment as a solid Fe (oxy)hydroxide (Warren and Haack, 2001). In anoxic conditions, Fe will readily reduce to the much more soluble Fe(II) (Mortimer, 1941). In boreal lakes, where soil and bedrock tend to be abundant in Fe (Björnerås et al., 2021), the reduction and release of accumulated sedimentary Fe can, therefore, be an internal source during anoxic conditions (Shaked et al., 2004).

Boreal catchments often have a high export of organic matter (OM), which will form stable complexes with Fe (Weber et al., 2006). Fe (oxy)hydroxides and Fe-OM complexes are therefore the most common Fe phases in boreal freshwater systems (Björnerås et al., 2021). Although aqueous concentrations of Fe are usually low in oxic non-acidic freshwaters due to the tendency of Fe(III) to precipitate, organic complexation of Fe will greatly enhance Fe solubility (Jansen et al., 2002). In boreal catchments, Fe-OM complexes allow Fe to stay in solution under conditions where it would normally precipitate, which can increase Fe concentrations in the water column (Maloney et al., 2005).

Depending on the type of organic ligand complexed with Fe, photochemical reactions in the euphotic zone by photon absorption and ligand to metal charge transfer (LMCT) can reduce Fe(III) to the more soluble Fe(II) (Lueder et al., 2020). Fe (oxy)hydroxides precipitates can also be photochemically reduced by LMCT, leading to mineral dissolution in the sediment (Waite and Morel, 1984). These processes are however dependent on pH (Fig. 1). Moreover, Fe reducing/oxidising bacteria also play an important role in freshwaters (Heikkinen et al., 2022).

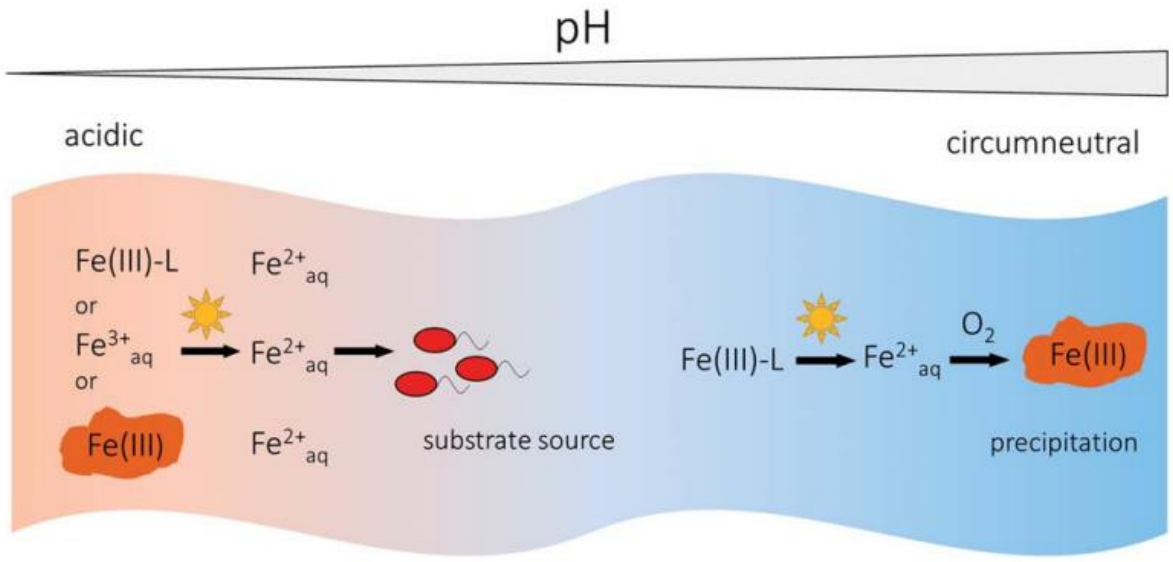

Figure 1. *Photochemical Fe processes in a downstream water course with a pH gradient. Dissolved organically complexed Fe (Fe(III)-L), dissolved inorganic Fe(III) species (Fe^{3+}_{aq}), and precipitated Fe(III) (oxy)hydroxides (Fe(III)) can be reduced to Fe^{2+}_{aq} photochemically under acidic conditions, which can be used as substrate for Fe oxidising bacteria. Under circumneutral pH conditions, smaller parts of Fe(III)-L can be reduced photochemically, but will mostly re-oxidise and precipitate. Taken from Lueder, et al (2020).*

The transport of Fe in boreal catchments consists of many key aspects (Fig. 2). Fe usually originates from weathered bedrock and soil rich in Fe, where catchments dominated by peatlands have higher concentrations than catchments dominated by woodland (Heikkinen et al., 2022). Areas with no vegetation cover will often be more prone to erosion, especially during flood events (Björkvald et al., 2008).

Anthropogenic activities will exacerbate the export from Fe rich sources, through for example peat extraction or mining (Heikkinen et al., 2022). The transport of Fe will also depend on the land cover characteristics of the catchment. In areas dominated by peatland, Fe is mainly transported in the form of dissolved organic Fe-Phosphorus colloids (Heikkinen et al., 2022). In areas dominated by woodlands, Fe is normally transported as Fe-OM complexes, and is therefore closely tied to the transport of OM and particulates which will increase during high discharge (Björkvald et al., 2008).

Fe concentrations in boreal catchments and lakes will often go through seasonal variations. During winter, anoxic conditions can increase Fe concentrations by releasing dissolved Fe species into the water (Goulet and Pick, 2001). Following snow melt, spring floods will lead to a higher export of OM and particulate matter, which can also increase Fe concentrations, especially in woodland catchments (Björkvald et al., 2008). In dimictic lakes, a thermal stratification during summer stagnation can lead to anoxic conditions in the hypolimnion, which will release dissolved Fe(II) from the sediment (Shaked et al., 2004).

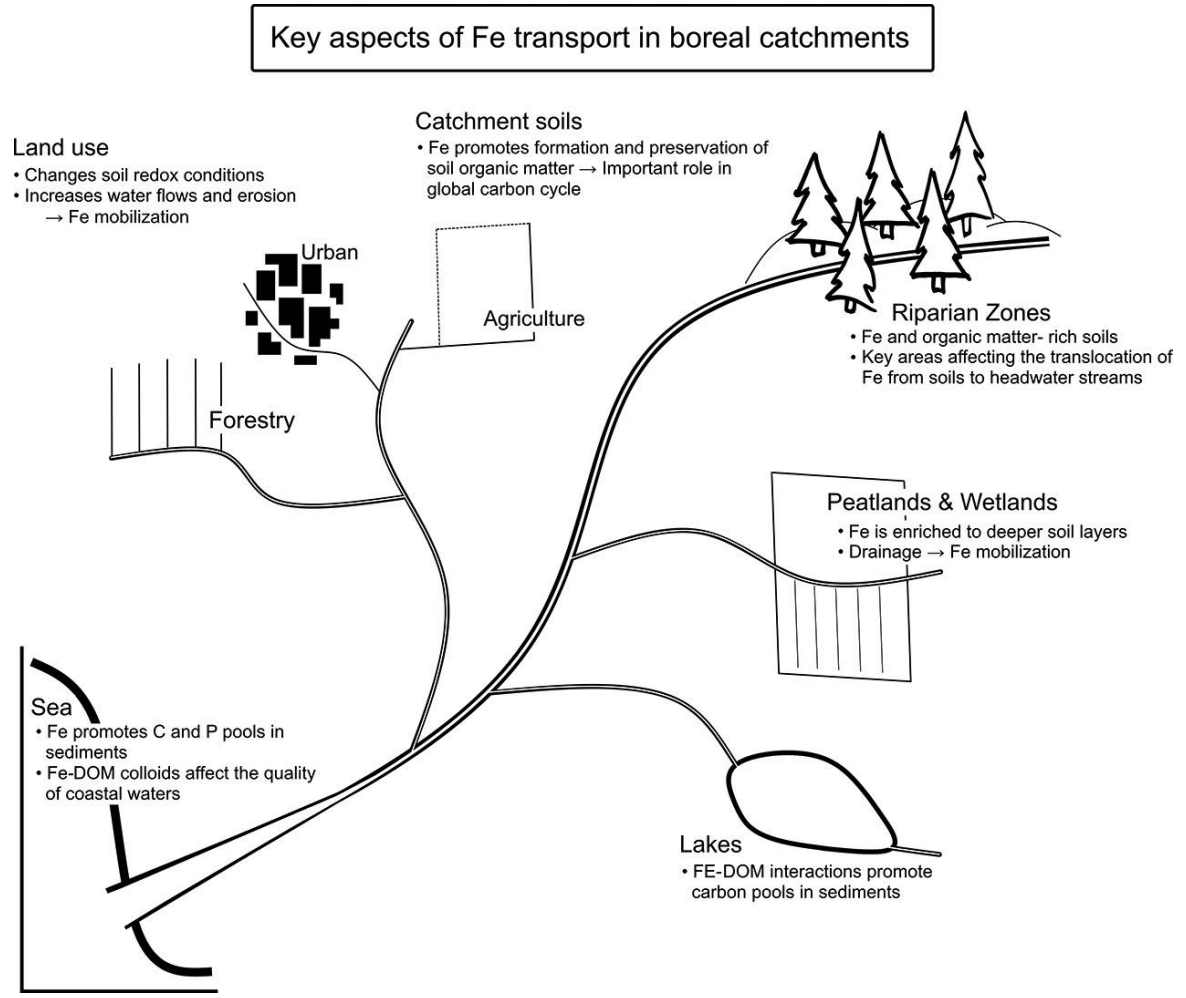

Figure 2. *Key aspects of Fe transport in boreal catchments. Land use can change redox conditions in soil and increase water flows and erosion. Riparian zones are rich in organic matter, while peatlands and wetlands are Fe-enriched in deeper soil layers. Lakes can act as carbon sinks through Fe-OM complexes in sediments. Taken from Heikkinen, et al. (2022).*

1.1.3 Drivers behind increasing Fe concentrations

The vegetation cover in the Northern Hemisphere has recently experienced a 'greening' trend following higher temperatures and changes in land use, which has increased the export of OM to freshwaters (Finstad et al., 2016; Kritzberg, 2017). A reduction in atmospheric acid deposition has also changed the soil and water acidity of many boreal catchments (Gavin et al., 2018). Because the mobility of OM is supressed in acidic conditions, the export of OM has further increased (Evans et al., 2005; Haaland et al., 2010; Kokorite et al., 2012). Additionally, a wetter climate has led to more catchment runoff which also enhances the mobility of OM (Hongve et al., 2004). These changes have resulted in an increase in OM concentrations and

water colour in many boreal freshwaters (Monteith et al., 2007; Kritzberg et al., 2020), which has recently been coupled with the observed increase of Fe concentrations (Kritzberg and Ekström, 2012; Weyhenmeyer et al., 2014; Xiao and Riise, 2021).

High concentrations of Fe(III) will turn freshwater into a darker brown colour (Shapiro, 1966), which is exacerbated by Fe-DOM complexes (Weyhenmeyer et al., 2014). Less transparency can in turn reduce photosynthesis and increase microbial activity in a lake (Couture et al., 2015; Arzel et al., 2020), leading to reducing conditions and even more Fe in solution. Moreover, following the reduction in atmospheric acid deposition, less Fe will be bound to sulfides in soil and Fe(III) reducing bacteria can more effectively compete against SO_4^{2-} reducing bacteria for organic substrates (Björnerås et al., 2017).

More frequent and extreme precipitation events will not only increase the export of Fe-OM complexes from the catchment, but can also enhance the release of Fe (Björnerås et al., 2017). Changes in precipitation have directly changed redox conditions in boreal catchments (Knorr et al., 2009; Kritzberg and Ekström, 2012; Sarkkola et al., 2013). Water saturated soils and a raised groundwater table leads to reducing conditions where Fe(II) will readily form and mobilise. Increased precipitation has also resulted in a shorter water retention time (WRT) in lakes, meaning Fe will have less time to settle into the sediment and instead flush further down the catchment (Weyhenmeyer et al., 2014). This is further exacerbated in catchments with a high export of OM, as Fe-OM complexes will keep Fe in solution for a longer period of time.

Higher temperatures in boreal regions are also a driver of increased Fe concentrations. Along with more rainfall, a warmer climate may enhance weathering rates and groundwater discharge resulting in an increased export of Fe associated minerals in catchments (Smedberg et al., 2006). In a catchment in Sweden, Ekström et al. (2016) found that the most significant increase in Fe concentrations correlated with increases in water discharge following earlier snow melt. Moreover, they also pointed out that higher temperatures can increase the activity of Fe reducing bacteria allowing for more Fe(II) to mobilise.

1.1.4 Ecosystem impacts

Fe is an essential micronutrient for many organisms and plays a central role in all of earth's surface systems (Weber et al., 2006). It is tightly connected to significant processes such as the biogeochemical cycling of carbon, nitrogen, and phosphorous (Björnerås et al., 2017). As an example, Fe plays an important role as a carbon sink by promoting the preservation of organic

matter in freshwater and marine sediments (Lalonde et al., 2011). Changes in Fe concentrations and its biogeochemical cycle can therefore have significant effects on a myriad of important processes.

High Fe concentrations can lead to direct and indirect negative impacts in freshwaters. Fe compounds can disturb the metabolism and osmoregulation of aquatic organisms, and change the structure and quality of benthic habitats and food resources (Vuori, 1995). Dissolved Fe(II) can also have direct toxic effects on biota, by for example causing respiratory disorders or reduced growth in fish (Cunha et al., 2019). Moreover, a lower water transparency will limit photosynthesis and phytoplankton productivity in lakes, which can affect other species in the food web (Arzel et al., 2020). Lower transparency can also promote thermal stratification, which can cause anoxic conditions in the benthic zone (Couture et al., 2015).

1.2 Scope of the Study

As the concentration of Fe continues to increase in boreal freshwaters, it is important to fully understand the drivers behind this trend, as well as potential impacts on ecosystems. With this in mind, the biogeochemical cycling and retention of Fe has been investigated in the small lake Vindlandstjernet in south-eastern Norway. The lake was selected for this study because of previous reports of increased Fe concentrations in the lake's catchment area, which was investigated in relation to the noble crayfish (*Astacus astacus*).

In order to better understand the lake's biogeochemical cycling and retention of Fe, several water parameters have been sampled between May and September 2021 and analysed in relation to seasonal variations and catchment runoff. To reach the aim of this study, the following research objectives were formulated:

i. To examine the seasonal variations of Fe in a boreal lake at different depths
ii. To examine the retention and cycling of Fe in a boreal lake under different runoff and thermal stratification conditions
iii. To examine potential effects of increased Fe concentrations on aquatic fauna

Although the lake Vindlandstjernet is very shallow, it is also humic and may therefore follow the trend of other boreal lakes that have seen an increased warming of surface layers, which would induce a stronger thermal stratification during summer. A strong thermal stratification could lead to a remobilisation of Fe in the water column. As more frequent and extreme

precipitation events have impacted the water retention time of many boreal lakes, Vindlandstjernet might see a high export of Fe under increased runoff conditions due to being shallow. Therefore, it is hypothesised that (1) thermal stratification affects the distribution and cycling of Fe in the water column of the lake; and that (2) the lake is a source of Fe during high flow.

1.3 Structure

Chapter 1 includes a background on current trends and issues, a short theoretical background, as well as the aim, objectives, and hypothesis of the study.

Chapter 2 includes information on the study area, methodologies used during sampling and chemical analyses, and the methodology used for statistical analyses.

Chapter 3 includes the results from water sampling, data analyses, and statistical analyses. A complete overview of raw data from chemical and statistical analyses is available in the appendices.

Chapter 4 includes a discussion of the results, which focuses on the research objectives and answering the hypotheses.

Chapter 5 includes a conclusion of the study and the results discussed in Chapter 4.

2. Methods

2.1 Study Area

Vindlandstjernet is located 162 m above sea level and is about 0.24 km^2 large (NVE, 2021a.). It is a very shallow lake with an approximate 3.5 m – 4 m maxium depth. The lake's catchment area (Fig. 3) mainly consists of woodland (92%) with some agricultural landscape (0.8%), and bogland (3%) (NVE, 2021b.). The topography consists of thick marine deposits and bedrock of mylonite, phyllonite, gabbro, amphibolite, and highly deformed gneiss (NGU, 2021). Vindlandstjernet is currently classified as a humus-rich lake low in calcium (Vann-nett, 2021). The lake has an abundance of floating, submerged and emergent macrophytes near the riparian zone (Fig. 4 and 5). The lake is especially overgrown with macrophytes and riparian vegetation near its northern outlet stream (UT) and southern inlet stream (IN1) (Fig. 3).

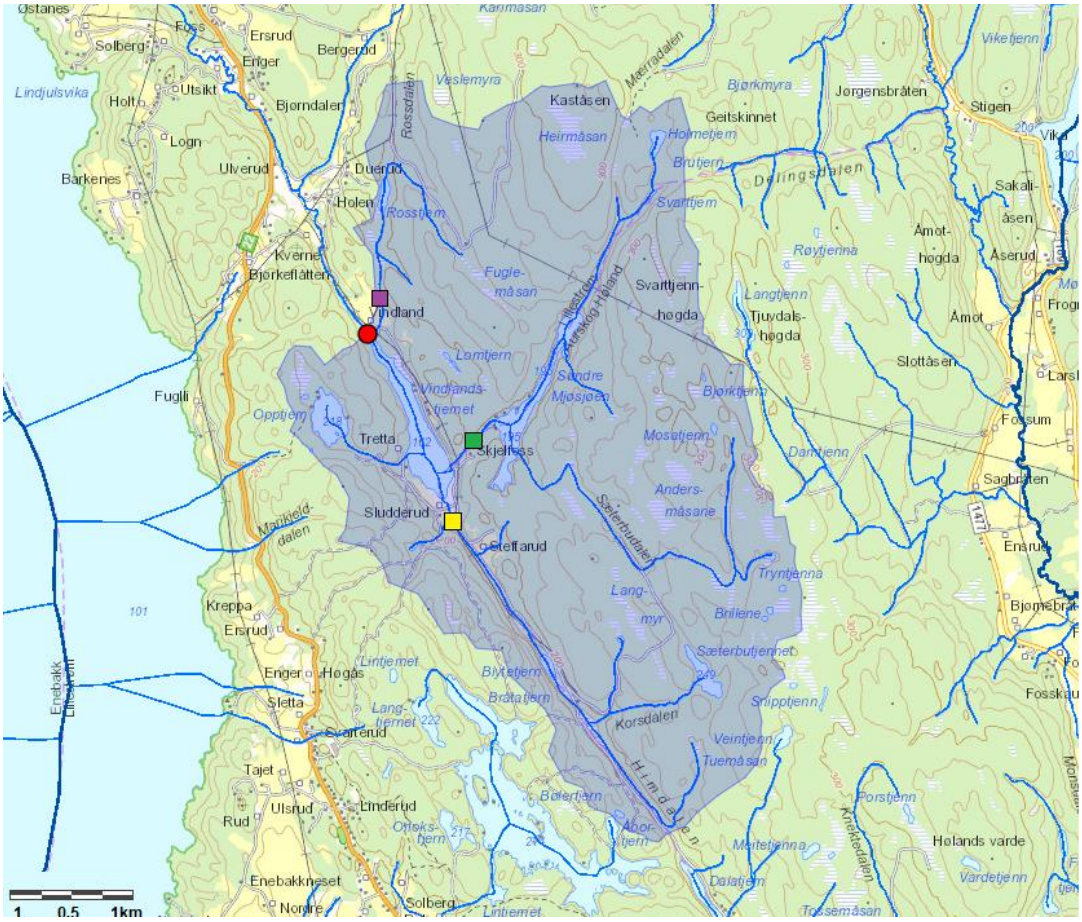

Figure 3. *The lake Vindlandstjernet and its catchment area (blue filled area). Yellow box: the lake's inlet stream (IN1) used as reference for the study; Green box: inlet stream (IN2); Purple box: inlet stream (IN3); Red dot: the lake's outlet stream (UT). Data from the streams can be found in a study by Pålsrud (2022). Map obtained from NVE, (2021b) and edited.*

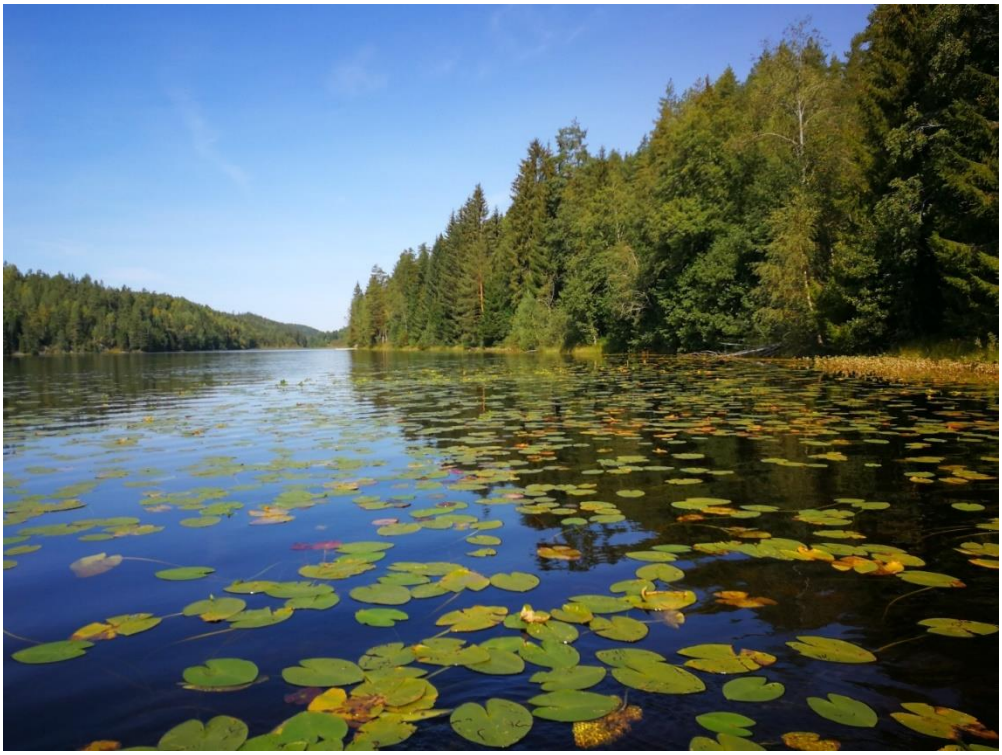

Figure 4. *Riparian and aquatic vegetation at the lake. Photo: Therese M. Børseth.*

Figure 5. *View towards the north of the lake. The surrounding area mainly consists of woodland with some bogland, agricultural landscape, and occasional buildings. Photo: Therese M. Børseth.*

Vindlandstjernet is situated in the Ulverudåa watercourse, upstream from its much larger recipient the lake Øyeren (84 km^2) within the Øyeren catchment area in south eastern Norway (Fig. 6). Ulverudåa includes many small streams, rivers and lakes. The area's ecological status, according to the European Union (EU) Water Framework Directive, is currently considered moderate due to moderate concentrations of pH, total alkalinity, and labile aluminium, while its chemical status is not defined (Vann-nett, 2021). It receives some nonpoint pollution from nearby agriculture and wastewater/drainage systems and is possibly affected by atmospheric acid deposition.

The Øyeren catchment stretches across 1285 km^2 and is the home of many species, including fish species only found in this part of Norway. Around 114 endangered and rare species have been recorded in the internationally protected Ramsar nature reserve north of the catchment. Moreover, the area includes 7 large drinking water sources (Vannområdet Øyeren, n.d.).

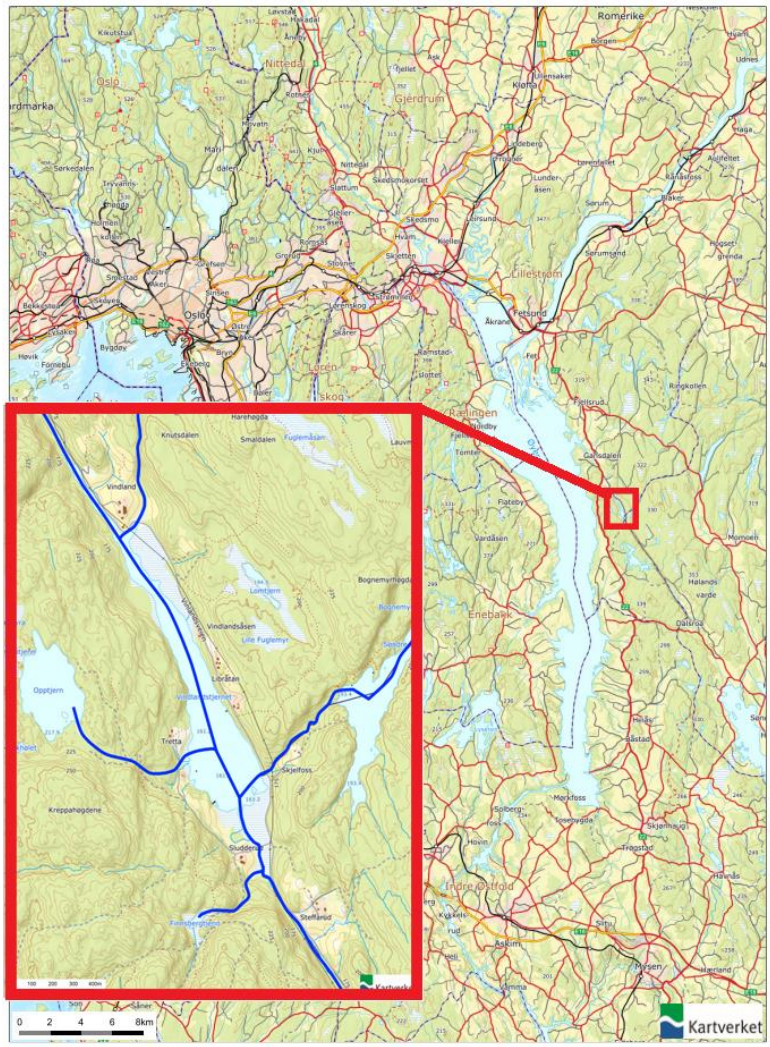

Figure 6. *Vindlandstjernet, within the Ulverudåa watercourse, is situated east of Oslo next to its much larger recipient the lake Øyeren. Map obtained from Kartverket (2021).*

2.2 Water Sampling

Water samples were collected *in situ* every two weeks between May and September 2021 at the same location in the lake (59.8192404, 11.272255) (Fig. 7). The samples were taken along a vertical profile in the lake at 0.5 m, 1 m, 2 m, and 3 m using a Rüttner water sampler. As it was difficult to find the deepest point of the lake (3.5 m – 4 m), it was decided to prioritise collecting samples from 3 m for consistency. The first day of sampling (05.05.2021) the deepest point found was at 2.5 m. 500 ml bottles were cleaned three times with lake water from the same depth about to be sampled. 50 ml vials were also used for metal samples to be analysed using Inductively Coupled Plasma analysis (ICP-OES Agilent 5100). One 500 ml bottle filled with Milli-Q water was used as control. The samples were transported in a cooling box and processed as soon as possible according to Norwegian standards.

Oxygen, temperature, and conductivity were measured *in situ.* Temperature was also continuously measured throughout the entire sampling period (see Chapter 2.3.9).

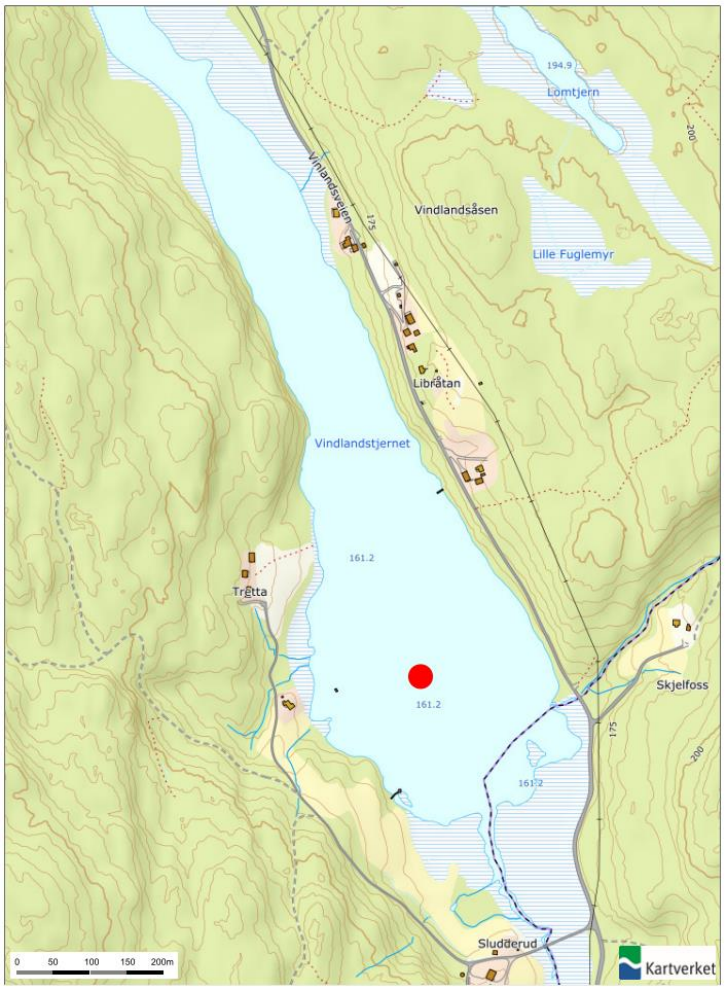

Figure 7. *The lake Vindlandstjernet. The red dot marks where water samples were collected between May and September 2021 (59.8192404, 11.272255). Map obtained from Kartverket (2021) and edited.*

2.3 Physical and Chemical Analyses

Filtered samples went through a vacuum filtration system using a Whatman GF/C Microfiber Glass Filter and a 0.45 μm membrane filter. Untreated samples were filled in 10 ml scintillation vials and frozen for later analysis of Total phosphorous (Tot-P) and Total nitrogen (Tot-N). The remaining samples were processed at the laboratory within 12 hours of being collected according to Norwegian standards.

2.3.1 Total nitrogen (Tot-N)

Total nitrogen (Tot-N) was measured according to Norwegian standards (NS 4743) using Flow Injection Analysis (FIA) (FIA Star 5023 Spectrophotometer with 5023 Detector Controller and 5010 analyser from Tecator). The samples are oxidised by potassium peroxydisulfate to convert nitrogen to nitrate and autoclaved at 1 ATM for 30 min at 121°C, before being coupled with N-(1-naphtyl)-Ethylene Diamine Dihydrochloride to form a purple azo dye, which is measured at 540 nm. The detection limit is 0.01 mg/L.

2.3.2 Chloride (Cl^-), nitrate-nitrogen (NO_3-N) and sulfate (SO_4^{2-})

Cl^-, NO_3-N and SO_4^{-2} were measured according to the Norwegian standards (NS-EN ISO 10304-1). The samples are filtered and analysed by ion chromatography using an electrical conductometer as the detector (XYZ auto sampler, ASX-500 Zellweger analytics). The detection limit is between 0.01 and 0.03 mg/L.

2.3.3 Turbidity and colour

Turbidity was measured on the day of sampling according to Norwegian standards (NS 7027) on unfiltered samples using a turbidity meter (2100AN IS Turbimeter) and expressed as Formazin Nephelometric Units (FNU).

Water colour was measured on the day of sampling according to Norwegian standards (NS 4787) using a spectrophotometer (Shimadzu UV-VIS Spectrophotometer UV1201). The samples are filtered using a 0.45 μm membrane filter. The colour is determined by measuring absorbance at 410 nm using 5 cm cuvettes. Colour is expressed in mg Pt/L by comparing it to a platina standard solution. The absorbance at 254 nm was also measured using 1 cm cuvettes.

2.3.4 Dissolved organic carbon (DOC)

DOC was analysed using filtered samples according to Norwegian standards (NS-EN 1484). DOC is the fraction of organic carbon which can pass through a 0.45 µm membrane filter. Prior to the analysis, inorganic carbon is removed from the sample using an acid and sparging with an inert gas. The organic carbon in the sample is then oxidised to form CO_2 using a platinum-catalyser at 680°C, which is then detected by the TOC instrument system (Shimadzu Total Organic Carbon Analyzer, TOC-V CPN). The method is applied in the 0.3 – 1000 mg/L carbon range.

2.3.5 Total phosphorous (Tot-P) and orthophosphate (PO_4-P)

Total phosphorous and orthophosphate were measured according to Norwegian standards (NS-EN 1189). The samples were oxidised using potassium peroxydisulfate and autoclaved for 30 minutes to convert phosphorus to orthophosphate. Orthophosphate reacts with ascorbic acid and antimony molybdate to form an antimony-phosphomolybdate complex. Reduction with ascorbic acid forms a blue colour which is measured spectrophotometrically at 880 nm using 2 cm cuvettes (Hitachi UH5300). The average detection limit is 0.456 µg/L. Unfiltered samples were used to measure total phosphorus and filtered samples were used to measure orthophosphate. To convert PO_4-P to PO_4^{3-}, the value was divided by 0.3261.

2.3.6 Ammonium (NH_4-N)

The concentration of ammonium was determined according to the modified Norwegian standard NS 4746. In alkaline solution, ammonium and hypochlorite reacts and forms monochloramine, which in the presence of salicylic acid forms a blue complex. The sample is then measured using a spectrophotometer (Hitachi UH5300) at 655 nm with 2 cm cuvettes. The detection limit is 0.02 mg/L. To convert NH_4-N to NH_4, the value was multiplied with 1.2878.

2.3.7 Aluminium (Al), calcium (Ca), iron (Fe), potassium (K), magnesium (Mg), manganese (Mn), sodium (Na), sulfur (S), and silicon (Si)

Aluminium, calcium, iron, potassium, magnesium, manganese, sodium, sulfur and silicon were measured using inductively coupled plasma atomic emission spectroscopy (ICP-OES Agilent 5100). Nitric acid was added to the samples before being analysed. The limit of detection (LOD) and limit of quantification (LOQ) of the filtered and unfiltered samples can be found in Appendix B.

2.3.8 pH and alkalinity

The pH was measured on the day of sampling according to Norwegian standards (NS 4720), using a Metrohm 914 pH/Conductometer at room temperature. The pH meter was calibrated against two standard solutions with pH 4 and pH 7 before use.

Alkalinity was measured according to Norwegian standards (NS-EN ISO 9963-1) through titration by adding HCl until reaching a pH 4.5 endpoint. A 665 Dosimat with an Orion 8172BNWP pH electrode connected to the Metrohm 914 pH/Conductometer was used.

2.3.9 Oxygen, conductivity, and temperature

Oxygen, temperature, and conductivity was measured *in situ* using a handheld WTW portable multiparameter. On the 11th of August, the meter did not work. Oxygen data is therefore missing for that day, while conductivity was measured at the laboratory within 12 hours of the samples being collected. Temperature was continuously logged throughout the sampling period using a MX2202 HOBO temperature logger.

2.4 Weather and Climate Data

Weather and climate data were obtained from the Norwegian Meteorological Institute's database at Seklima (The Norwegian Meteorological Institute, 2021). Precipitation data and snow depth data were obtained from the Enebakk – Barbøl station (ID SN4040) (59.75, 11.1535). The Enebakk – Barbøl station is 9.9 km away from the lake. Temperature data was obtained from the FV169 Åserud station (ID SN2560) (59.8388, 11.3625). The Åserud station is 5.5 km away from the lake.

Temperature data is measured as an arithmetic mean of 24-hour values between February and September 2021. Precipitation data is measured as total precipitation in mm per 24 hours between February and September 2021. The mean monthly temperature and mean monthly precipitation between 1991 – 2021 were obtained from the same stations mentioned above, where temperature was measured as an arithmetic mean of 24-hour values and total precipitation in mm per month.

Data of total monthly water supply from rain and snowmelt, and runoff data, were obtained from The Norwegian Water Resource and Energy Directorate (NVE) using SeNorge (NVE,

2021c). Total monthly water supply is calculated using the Snow Map model, which is based on the Hydrologiska Byråns Vattenbalansavdelning (HBV) model. The deviation from the normal total monthly water supply (1981 – 2010) is characterised by NVE as either "very large", "large", "normal", "low", or "very low". Runoff data is presented as the mean monthly runoff, and calculated using a gridded HBV model, as precipitation minus evaporation and change in the amount of water stored in soil/snow from the day before.

2.5 Data Processing and Statistical Analyses

Data from physical and chemical analyses were processed in Microsoft Office Excel (version 2204) and analysed using the integrated development environment (IDE) RStudio (version 2022.02.2+485) and the statistical software MiniTab (version 21.1). For consistency, only data from 0.5 m, 1 m, 2 m, and 3 m depths were used for statistical analyses.

Contour plots were created to graphically present stratification and seasonal variations of parameters at different depths during the sampling period. Pearson's correlation coefficient was used to look at associations between variables, using a confidence level of 95.

A Principal Component Analysis (PCA) was performed on 20 parameters of the data set to look at variations. Prior to the analysis, the data was standardised by subtracting the mean and dividing by the standard deviation. The parameters used in the analysis were chosen based on relevancy to the study and degree of change during the sampling period. The parameters used were Fe, temperature, oxygen saturation, conductivity, turbidity, DOC, Tot-P, Mn, Al, S, Si, Cl^-, Tot-N, NH_4-N, pH, SO_4^{2-}, alkalinity, PO_4-P, and NO_3-N. Total concentrations of Fe, Mn, Al, S, and Si were separated into dissolved (<0.45 μm) and particulate (>0.45 μm) fractions. Data from each depth point (0.5 m, 1 m, 2 m, 3 m) were analysed separately.

A paired t-test was performed to look at possible statistical differences between the parameters sampled in the surface and bottom layers of the lake. Because the thermocline is expected to move further down during the seasons, data from 0.5 m and 1 m were analysed against data from 3 m. The parameters used in the analyses were Fe, Al, Mn, S, Si, oxygen saturation, pH, DOC, colour, conductivity, and temperature (N=9). Total concentrations of Fe, Mn, Al, S, and Si were separated into dissolved (<0.45 μm) and particulate (>0.45 μm) fractions. The chosen significance level was 0.05.

3. Results

3.1 Weather and Climate

Prior to and during the sampling period, the study area had temperatures similar to the mean temperatures between 1991-2021, with the summer months being somewhat warmer (Fig. 9 and Table 2). The mean precipitation in the study area was much lower than the mean precipitation between 1991-2021 in all months except for May and July (Fig. 8 and Table 1). The 28th of July stands out due to a heavy rainfall event (46 mm). August was especially dry, where the study area received 82.9 mm less precipitation than the mean between 1991-2021. Most of the snow had melted by the beginning of April (Fig. 10).

The mean runoff in the lake's catchment area was <5 mm in all months between February – August (Table 3). The total monthly water supply from rain and snowmelt ranged between <100 – 200 mm in February, March, and April, and was highest in May and July (Table 3). Based on precipitation data, temperature data, snow melt data, and the monthly deviation from the mean monthly water supply (1981 – 2010), the lake's catchment likely experienced a normal to small spring flood. Further, the data suggest that the lake's catchment may have had a discharge above the mean in May and July, and a discharge below the mean in June and August.

Table 1. *Mean monthly precipitation (mm) from February-August between 1991-2020 compared to the mean monthly precipitation (mm) in 2021. Data obtained from The Norwegian Meteorological Institute (2021).*

	Mean precipitation (mm) 1991-2020	Mean precipitation (mm) 2021	Deviation (mm)
February	56.4	35.2	-21.2
March	50.2	45.3	-4.9
April	50.6	17.8	-32.8
May	65.3	94	28.7
June	80.2	40	-40.2
July	85.1	110.1	25.0
August	97.5	14.6	-82.9

***Table 2**. Mean monthly temperature (°C) from February-August between 1991-2020 compared to the mean monthly temperature (°C) in 2021. Data obtained from The Norwegian Meteorological Institute (2021).*

	Mean temperature (°C) 1991-2020	Mean temperature (°C) 2021	Deviation (°C)
February	-3.3	-6	-2.7
March	0.1	2.5	2.4
April	5.0	4.6	-0.4
May	10.4	10.2	-0.2
June	14.6	17.2	2.6
July	16.6	19.3	2.7
August	15.1	15.4	0.3

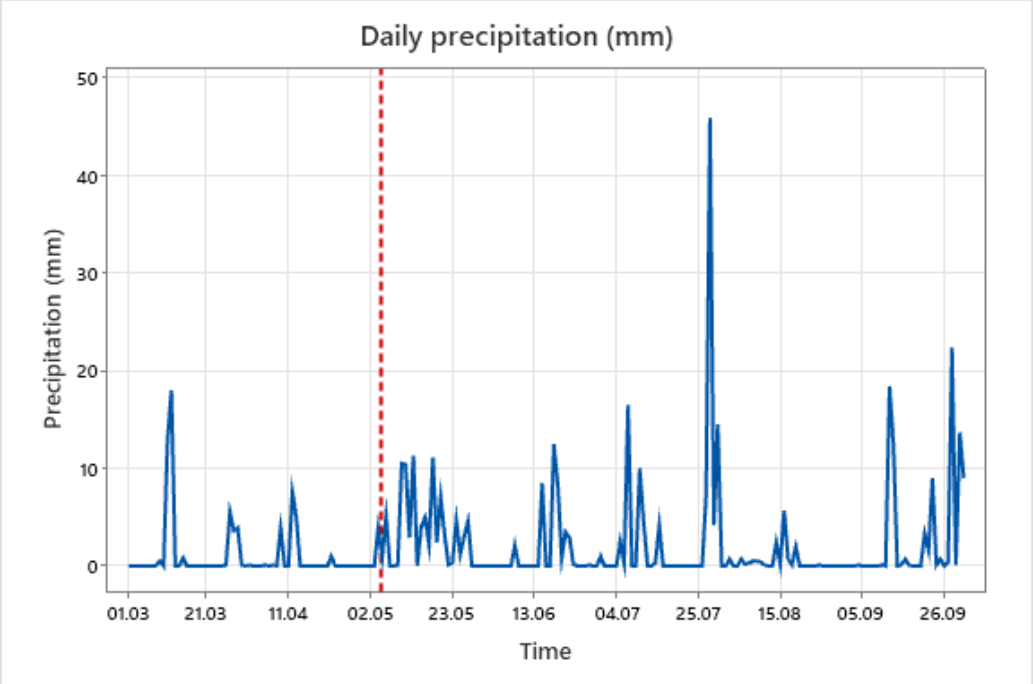

***Figure 8.** Daily total precipitation (mm) between March and October 2021. Red dotted line marks the beginning of the sampling period (05.05.2021). Data obtained from The Norwegian Meteorological Institute (2021).*

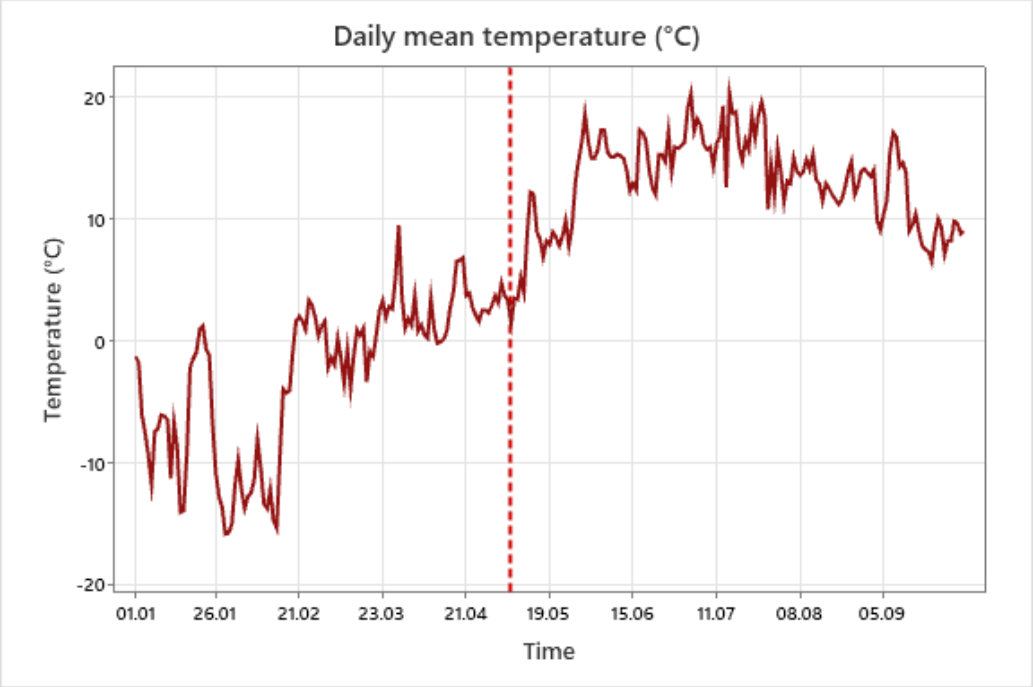

Figure 9. *Daily mean temperature (°C) between January and October 2021. Red dotted line marks the beginning of the sampling period (05.05.2021). Data obtained from The Norwegian Meteorological Institute (2021).*

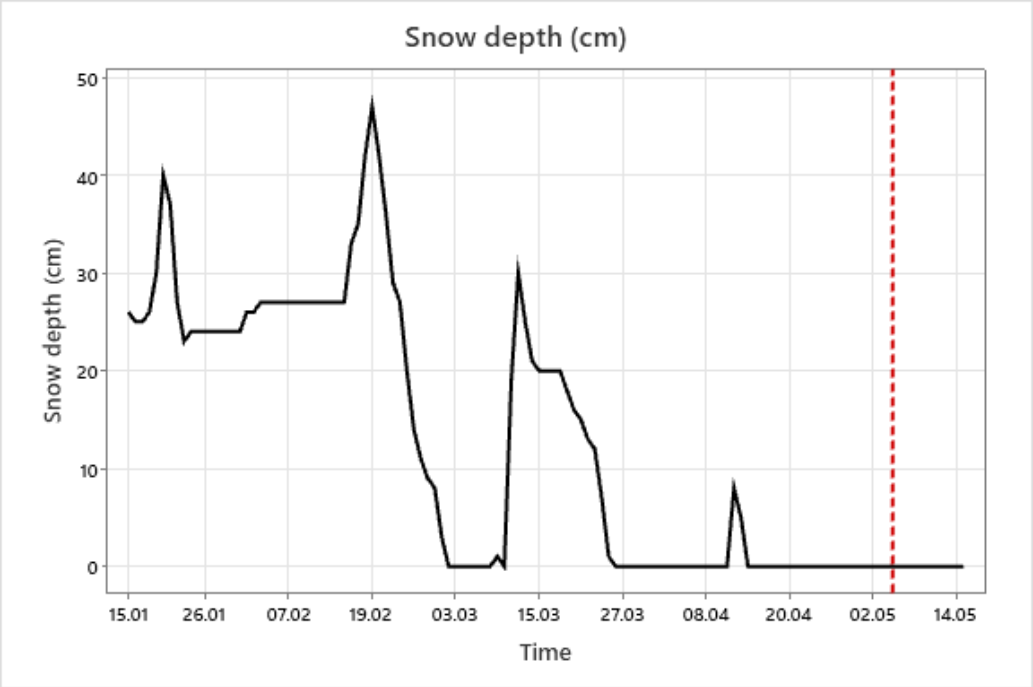

Figure 10. *Snow depth (cm) between January and May 2021. Red dotted line marks the beginning of the sampling period (05.05.2021). Data obtained from The Norwegian Meteorological Institute (2021).*

Table 3. *Mean monthly runoff (mm), total monthly water supply from rain and snow melt (mm), and the monthly deviation from the normal (1981 – 2010). The monthly deviation is characterized by NVE as either "very large", "large", "normal", "low", or "very low". A month characterised as "low" will have less total monthly water supply (mm) than the normal, while a month characterised as "large" will have more total monthly water supply than the normal. Data obtained from NVE (2021c).*

	Runoff (mm)	**Total monthly water supply from rain and snow melt (mm)**	**Monthly deviation from the normal (1981 – 2010)**
February	<5 mm	<100 - 200	Normal
March	<5 mm	<100 - 200	Normal
April	<5 mm	<100	Very low
May	<5 mm	200-300	Large
June	<5 mm	<100	Low
July	<5 mm	500-750	Large
August	<5 mm	<100	Very low

3.2 *In situ* and Laboratory Results

Results from chemical analyses as well as *in situ* and laboratory measurements are presented below. The results from statistical analyses and all raw sample data can be found in the appendices.

3.2.1 Temperature, oxygen, pH and alkalinity

The mean temperatures during the sampling period at 0.5 m, 1 m, 2 m, and 3 m were 18°C, 18°C, 16°C, and 13°C, respectively (Fig. 11). At the beginning of May, the temperature was the same (8°C) at all depths, indicating a full circulation in the water column following ice melt and a spring turnover. The temperature difference between the surface layer and bottom layer continued to increase until a peak difference of 14°C between temperatures at 0.5 m and 3.5 m in mid-July. The lake remained thermally stratified until the end of August, indicating a full circulation of the water column following autumn turnover (Fig. 12). The surface layer temperature was reduced by almost 10°C following heavy rainfall on the 28th of July, which could have encouraged an earlier mixing of the water column.

The oxygen saturation in the lake was negatively correlated to the temperature at all depths ($p < 0.05$). The mean oxygen saturation during the sampling period at 0.5 m, 1 m, 2 m, and 3 m was 93%, 92%, 88%, and 48%, respectively. During May, the oxygen saturation ranged

between 97% - 81% at all depths. As the thermal stratification of the lake grew stronger, the difference in oxygen saturation between surface and bottom water increased (Fig. 13). During June and July, the oxygen saturation at 3 m ranged between 46% - 16%. At 3.5 m, the oxygen saturation declined to 1% and 0.8% on the 16th and 30th of June, respectively. The bottom layer of the lake was therefore hypoxic and anoxic during the summer months. After surface layer temperatures declined in August following the heavy rainfall event, the water column underwent circulation which led to an increase of oxygen saturation at 3 m, from 18% at the end of July to 54% at the beginning of September (Fig. 14).

The mean pH at 0.5 m, 1 m, 2 m, and 3 m were 6.2, 6.2, 6.1, and 5.9, respectively, during the sampling period. In May, which had more precipitation than normal, the pH dropped to its lowest ranging from 5.8 – 5.7 in the water column. During the dry summer months, the pH increased at all depths of the lake. Following the heavy rainfall event on the 28th of July, the pH dropped before continuing to increase in August (Fig. 15). Temperature was positively correlated to pH ($p < 0.05$). The alkalinity remained stable throughout the sampling period, with a mean of 0.06, 0.06, 0.06, and 0.08 mmol/L at 0.5 m, 1 m, 2 m, and 3 m, respectively.

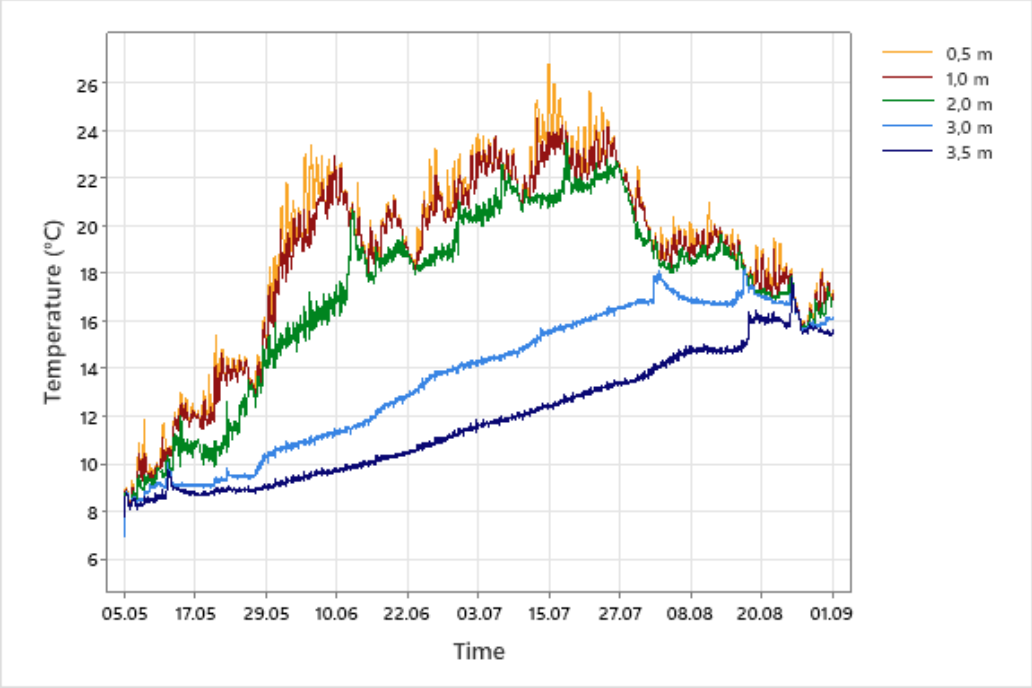

Figure 11. *Lake temperature (°C) continuously logged during the sampling period at different depths (0.5 m, 1 m, 2 m, 3 m).*

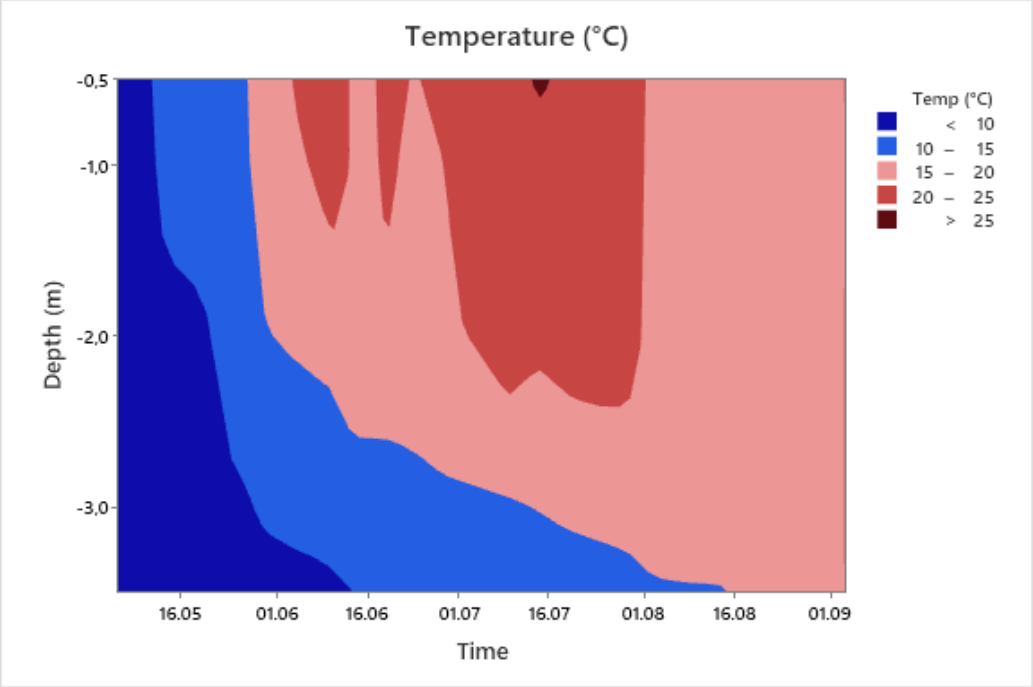

Figure 12. *Contour plot of lake temperature (°C) at different depths (0.5 m, 1 m, 2 m, 3 m).*

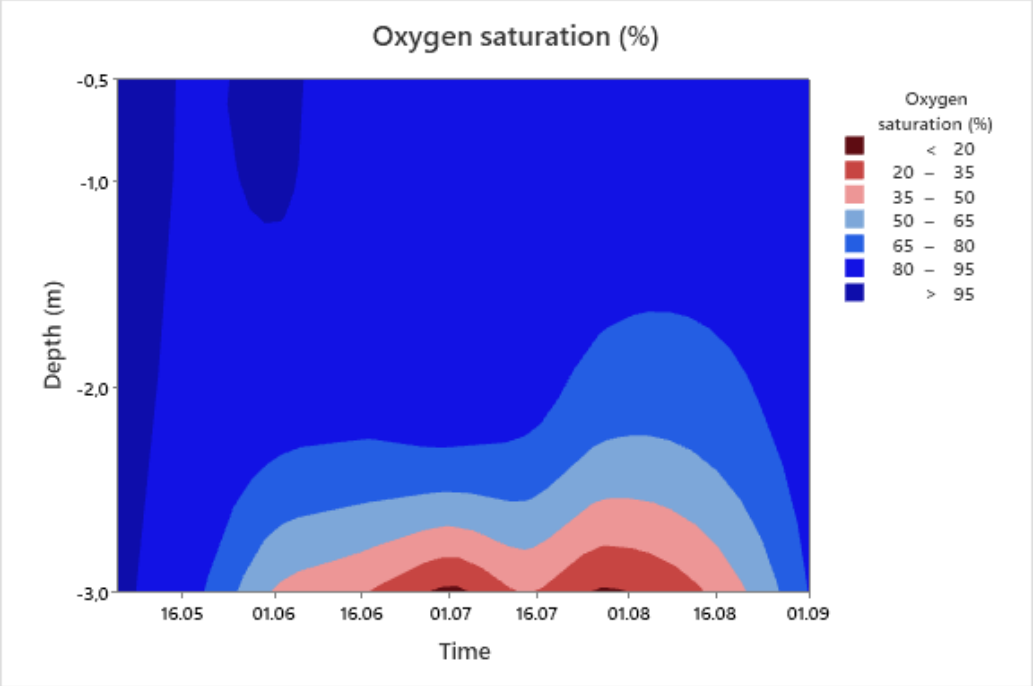

Figure 13. *Contour plot of oxygen saturation (%) at different depths (0.5 m, 1 m, 2 m, 3 m).*

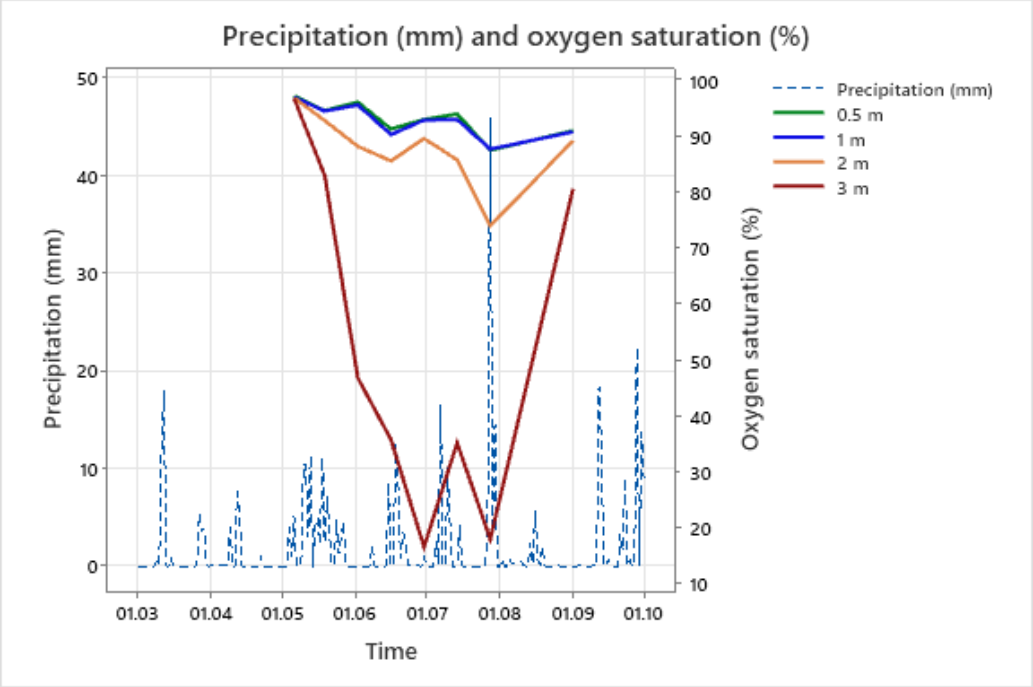

Figure 14. *Total daily precipitation (mm) in the study area and lake oxygen saturation (%) at different depths (0.5 m, 1 m, 2 m, 3 m).*

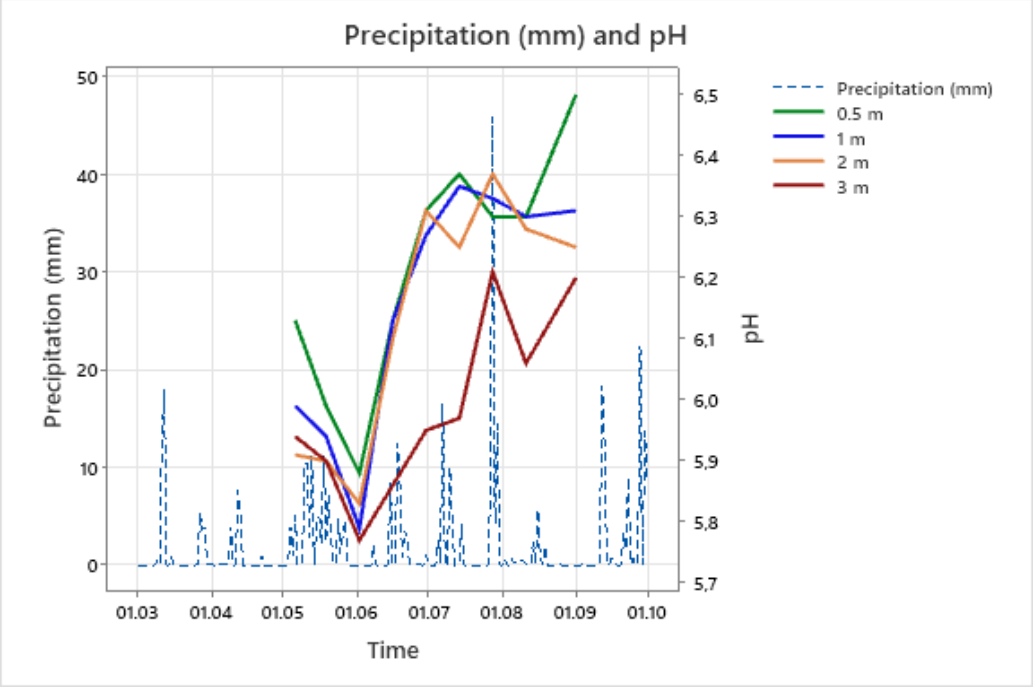

Figure 15. *Total daily precipitation (mm) in the study area and lake pH at different depths (0.5 m, 1 m, 2 m, 3 m).*

3.2.2 Fe

Total Fe concentrations, as well as dissolved Fe (<0.45 μm) and particulate Fe (>0.45 μm) concentrations, can be found in Table 4.

The particulate Fe concentrations had a mean of 0.148, 0.147, 0.154, and 0.248 mg/L at 0.5 m, 1 m, 2 m, and 3 m, respectively. On the 30th of June, particulate Fe concentrations at 3 m reached a peak of 0.650 mg/L, before declining to 0.250 mg/L on the 14th of July (Fig. 16 and 17). Following the heavy rainfall event on the 28th of July, particulate Fe concentrations increased at all depths in the lake. Particulate Fe had a very strong positive correlation to conductivity, as well as strong positive correlations to particulate Al and S, at all depths except for 3 m ($p < 0.05$).

The dissolved Fe concentrations had a mean of 0.230, 0.230, 0.240, and 0.38 mg/L at 0.5 m, 1 m, 2 m, and 3 m, respectively. On the 14th of July, dissolved Fe concentrations at 3 m reached a peak of 0.850 mg/L, before declining to 0.370 mg/L during the heavy rainfall event on the 28th of July (Fig. 18 and 19). Dissolved Fe had a strong negative correlation to SO_4^{2-} at 0.5 m and 1 m, a strong positive correlation to dissolved Mn at all depths, a negative correlation to oxygen saturation at 1 m, 2 m, and 3 m, and a strong positive correlation to Cl^- at 1 m, 2 m, and 3 m ($p < 0.05$).

Table 4. *Total Fe concentrations (Tot) with dissolved fraction (<0.45 μm) (Dis) and particulate fraction (>0.45 μm) (Part). Taken at 0.5 m, 1 m, 2 m, and 3 m between May – September 2021. Notable increases are marked in bold.*

	Dis	**Dis**	**Dis**	**Dis**	**Part**	**Part**	**Part**	**Part**	**Tot**	**Tot**	**Tot**	**Tot**
Sample date	**Fe 0.5m mg/L**	**Fe 1m mg/L**	**Fe 2m mg/L**	**Fe 3m mg/L**	**Fe 0.5m mg/L**	**Fe 1m mg/L**	**Fe 2m mg/L**	**Fe 3m mg/L**	**Fe 0.5m mg/L**	**Fe 1m mg/L**	**Fe 2m mg/L**	**Fe 3m mg/L**
05.05.21	0.16	0.17	0.17	0.17	0.11	0.10	0.12	0.09	0.27	0.27	0.29	0.26
19.05.21	0.20	0.21	0.23	0.26	0.12	0.10	0.12	0.25	0.32	0.31	0.35	0.51
02.06.21	0.19	0.19	0.20	0.27	0.12	0.14	0.12	0.17	0.31	0.33	0.32	0.44
16.06.21	0.21	0.21	0.22	0.33	0.13	0.18	0.11	0.26	0.34	0.39	0.33	0.59
30.06.21	0.18	0.19	0.19	0.35	0.14	0.15	0.14	**0.65**	0.32	0.34	0.33	**1.00**
14.07.21	0.26	0.26	0.27	**0.85**	0.12	0.13	0.13	0.25	0.38	0.39	0.40	**1.10**
28.07.21	0.27	0.27	0.27	0.37	0.16	0.11	0.11	0.14	0.43	0.38	0.38	0.51
11.08.21	0.30	0.31	0.30	0.44	0.13	0.17	0.21	0.19	0.43	0.48	0.51	0.63
01.09.21	0.30	0.26	0.27	0.36	0.30	0.24	0.33	0.23	0.60	0.50	0.60	0.59

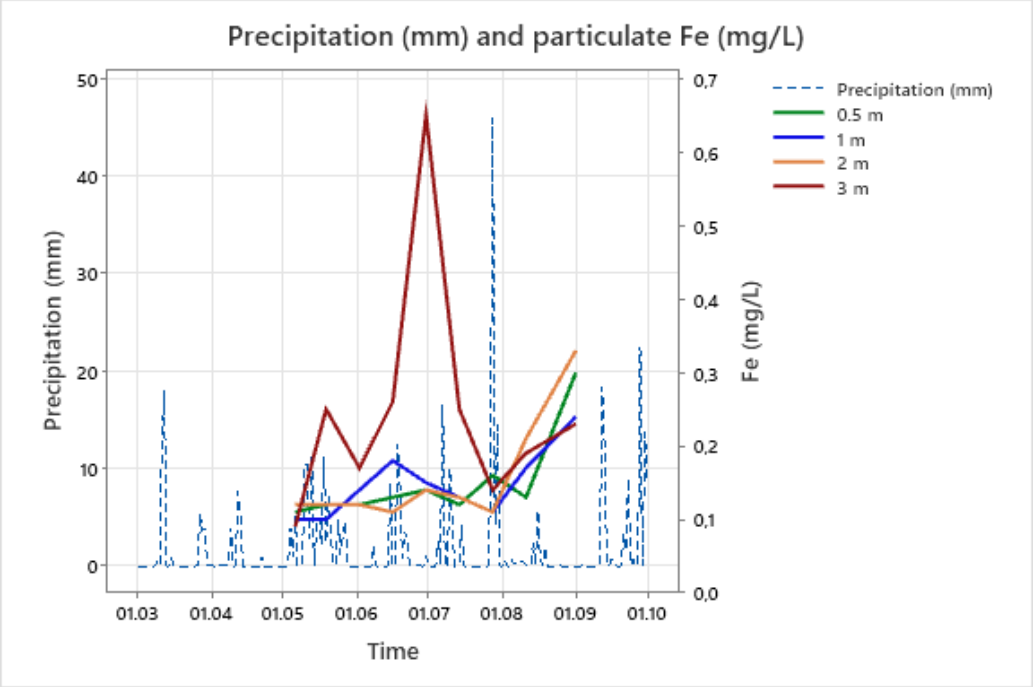

Figure 16. *Total daily precipitation (mm) in the study area and particulate Fe (mg/L) at different depths (0.5 m, 1 m, 2 m, 3 m).*

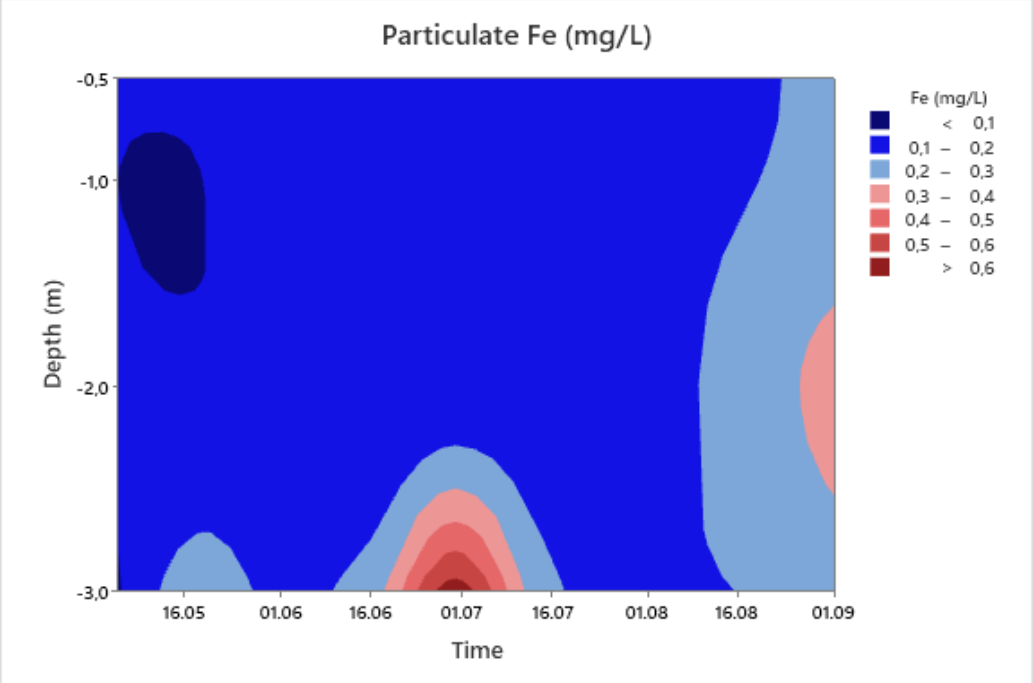

Figure 17. *Contour plot of particulate Fe (mg/L) at different depths (0.5 m, 1 m, 2 m, 3 m).*

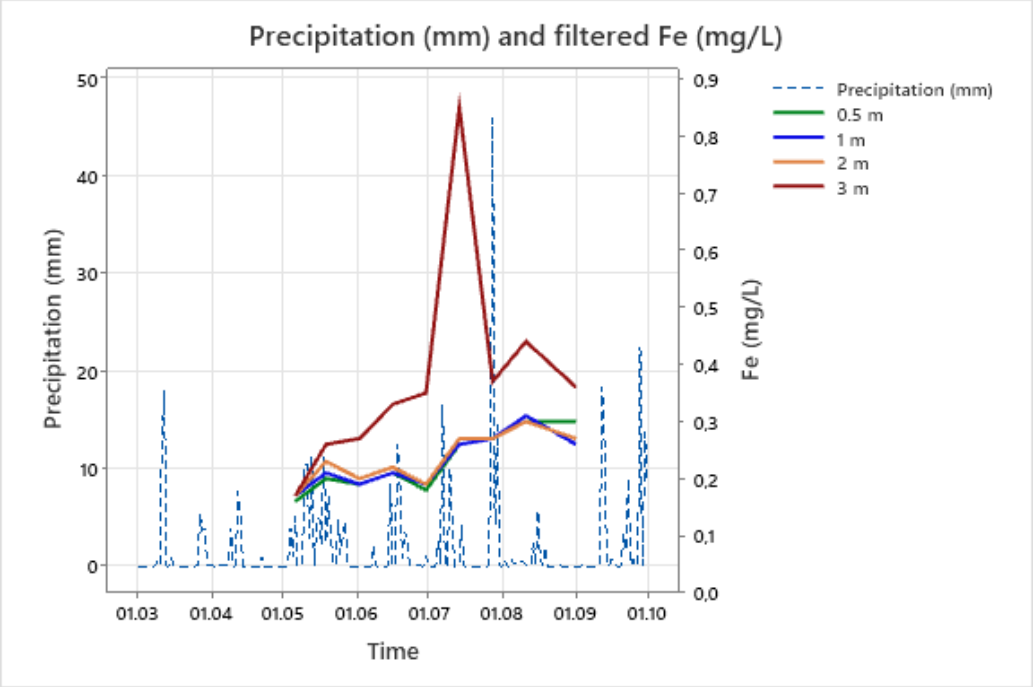

Figure 18. *Total daily precipitation (mm) in the study area and dissolved Fe (mg/L) at different depths (0.5 m, 1 m, 2 m, 3 m).*

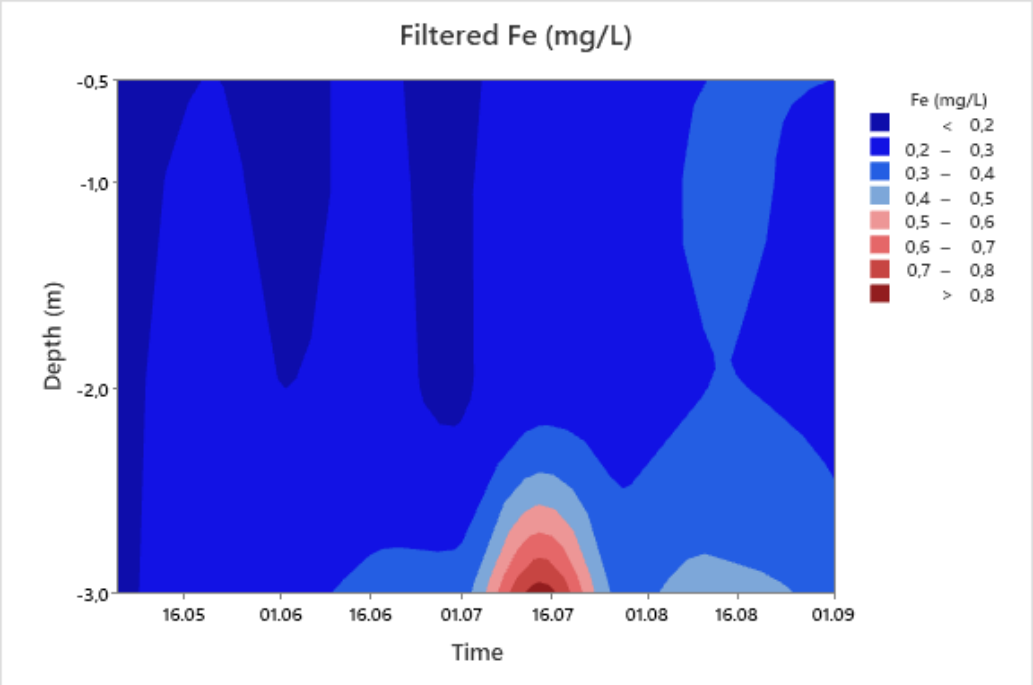

Figure 19. *Contour plot of dissolved Fe (mg/L) at different depths (0.5 m, 1 m, 2 m, 3 m).*

3.2.3 DOC, colour and turbidity

DOC concentrations increased in May before declining during the summer months and reaching its lowest point after the heavy rainfall event on the 28th of July (Fig. 20). Overall the concentration of DOC at all depths remained stable throughout the sampling period, ranging from 12.2 mg/L on the 2nd of June to 8.7 mg/L on the 28th of July.

The water colour followed a similar trend to that of DOC concentrations. However, the 14th of July stands out where the colour at 3 m increased to a peak of 100 mg Pt/L, while the colour in the rest of the water column decreased (Fig. 21). Similar to DOC concentrations, the colour also declined at all depths during the heavy rainfall event. DOC was positively correlated to colour at all depths and to dissolved Fe at 3 m ($p < 0.05$).

The turbidity of the lake ranged between 0.9 to 2.6 (FNU), and followed a similar trend to DOC and colour with an increase at 2 m and 3 m in mid-May and the beginning of July.

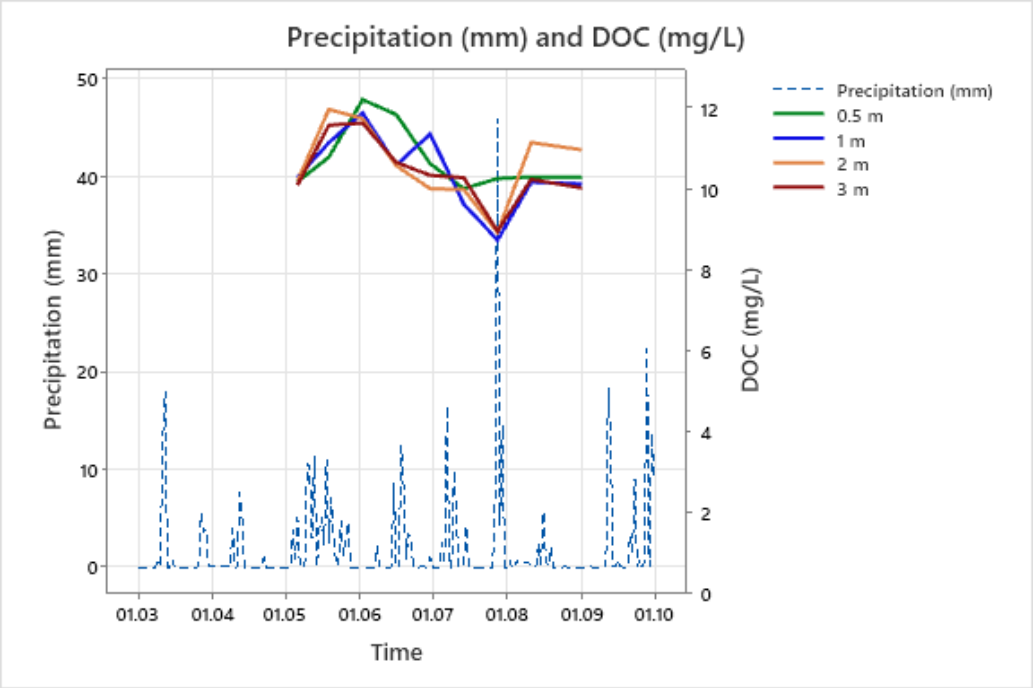

Figure 20. *Total daily precipitation (mm) in the study area and DOC (mg/L) at different depths (0.5 m, 1 m, 2 m, 3 m).*

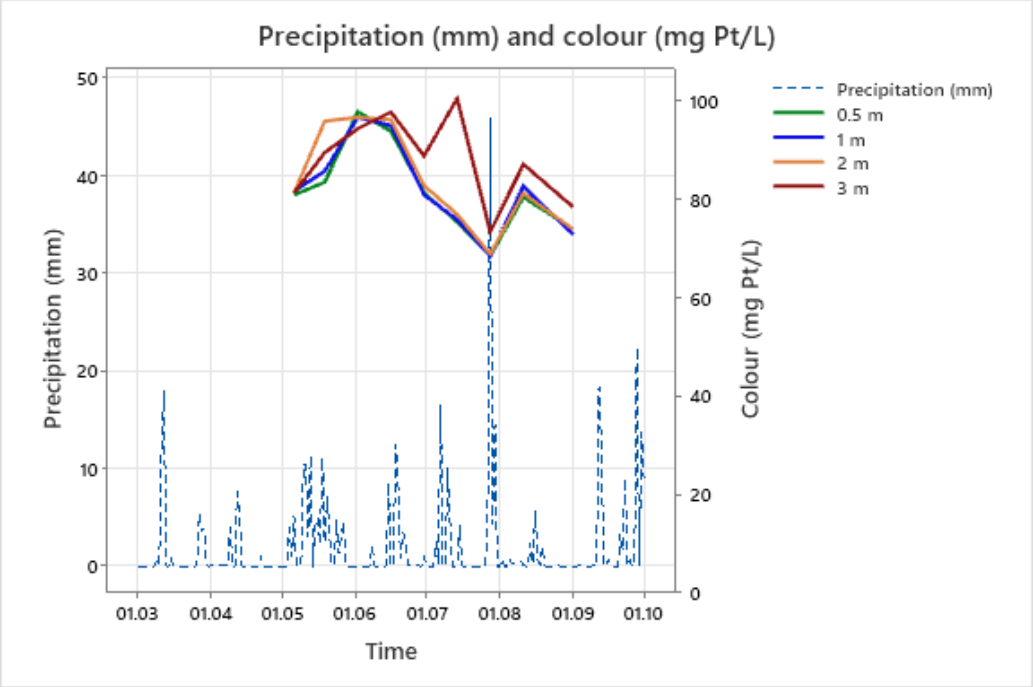

Figure 21. *Total daily precipitation (mm) in the study area and colour (mg Pt/L) at different depths (0.5 m, 1 m, 2 m, 3 m).*

3.2.4 Conductivity and Cl^-

The mean conductivity at 0.5 m, 1 m, 2 m, and 3 m was 21.6, 21.8, 21.7, and 24.6 µS/cm, respectively. In May, the conductivity was at its lowest (19 µS/cm) before increasing during the summer months. During the heavy rainfall event on the 28th of July, the conductivity reached its peak at 3 m of 28.4 µS/cm, before declining during the first half of August (Fig. 22). On the 1st of September the conductivity had increased again at all depths in the lake.

The concentration of Cl^- followed a similar trend to that of conductivity. At 3 m, Cl^- concentrations also reached its peak at 2.6 mg/L in July before declining following the heavy rainfall event (Fig. 23). Similar to conductivity, Cl^- concentrations also continued to increase in the second half of August. Conductivity had a strong positive correlation with Cl^- at all depths ($p < 0.05$).

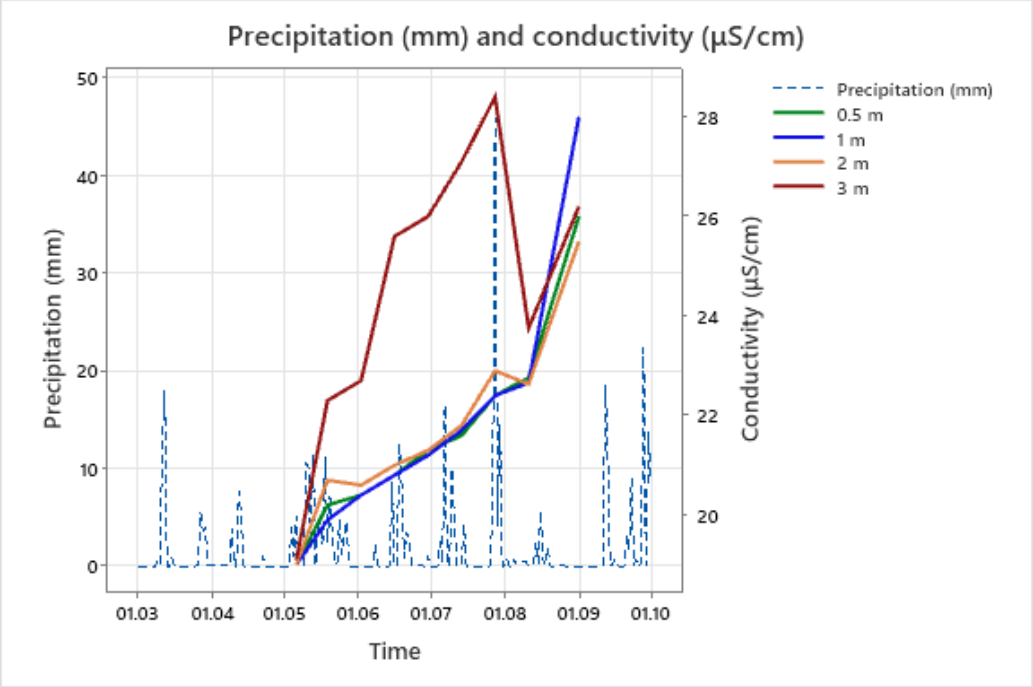

Figure 22. *Total daily precipitation (mm) in the study area and conductivity (µS/cm) at different depths (0.5 m, 1 m, 2 m, 3 m).*

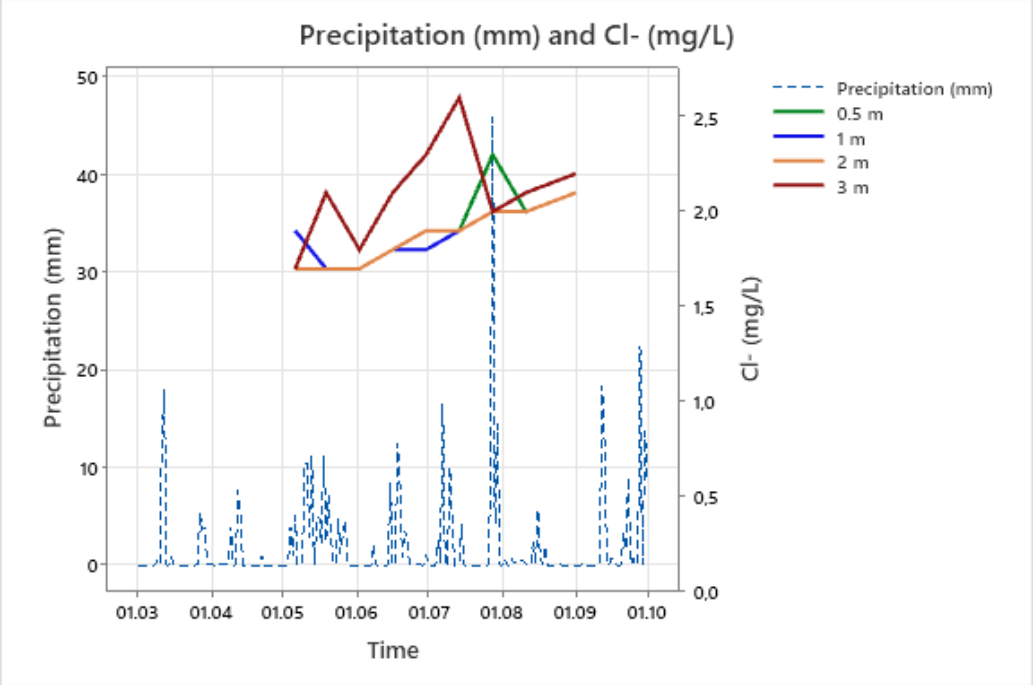

Figure 23. *Total daily precipitation (mm) in the study area and Cl^- (mg/L) at different depths (0.5 m, 1 m, 2 m, 3 m).*

3.2.5 Nutrients

Tot-P concentrations increased at 0.5 m in May and at 3 m at the end of June (Fig. 24). The mean proportion of Tot-P available as PO_4^{3-} ranged between 13% - 25% at all depths during the sampling period, where the highest concentration of PO_4^{3-} mostly occurred at 0.5 m. When Tot-P concentrations peaked at 1 m on the 19th of May, the proportion available as PO_4^{3-} was 28%. When Tot-P concentrations peaked at 3 m on the 30th of June, the proportion available as PO_4^{3-} was 2%. Dissolved Fe was negatively correlated to PO_4-P at 1 m and 2 m, particulate Fe was negatively correlated to PO_4-P at 0.5 m and 1 m, and Tot-P was positively correlated to particulate Fe at 3 m ($p < 0.05$).

Tot-N concentrations increased at 3 m in May (Fig. 25) but remained otherwise stable at all depths ranging from a mean of 0.36-0.39 mg/L during the sampling period. The mean proportion of Tot-N available as NH_4 ranged between 4-6%. When Tot-N concentrations peaked at 3 m on the 19th of May, the proportion available as NH_4 was 5%. Concentrations of NO_3-N were low during the sampling period. Between the 16th of May and the 1st of September, NO_3-N concentrations rarely went above the detection limit of 0.02 mg/L

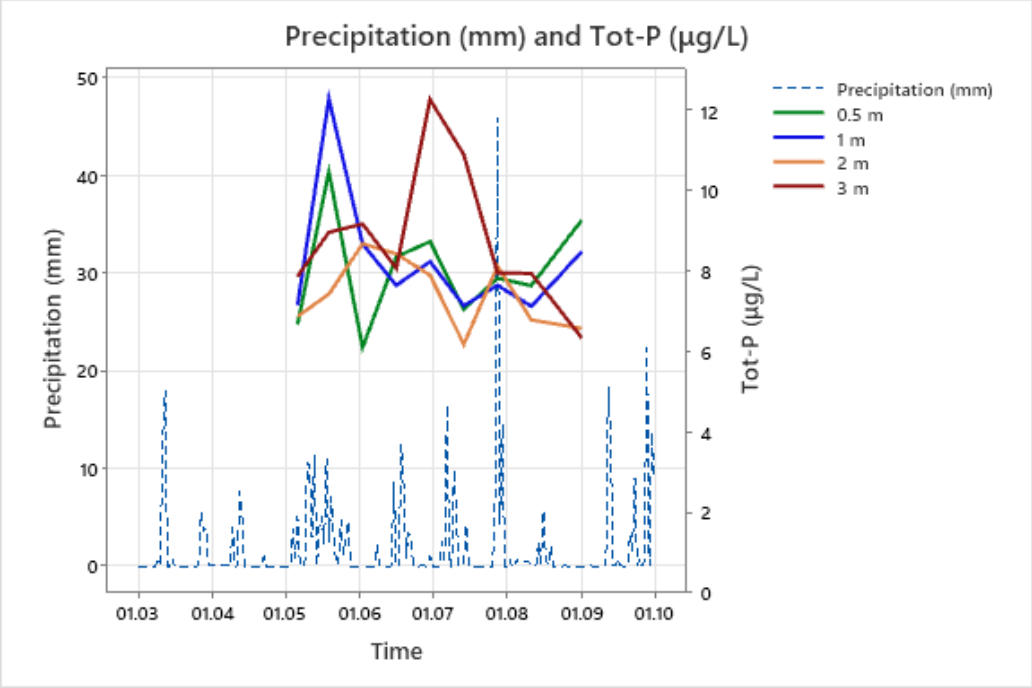

Figure 24. *Total daily precipitation (mm) in the study area and Tot-P (µg/L) at different depths (0.5 m, 1 m, 2 m, 3 m).*

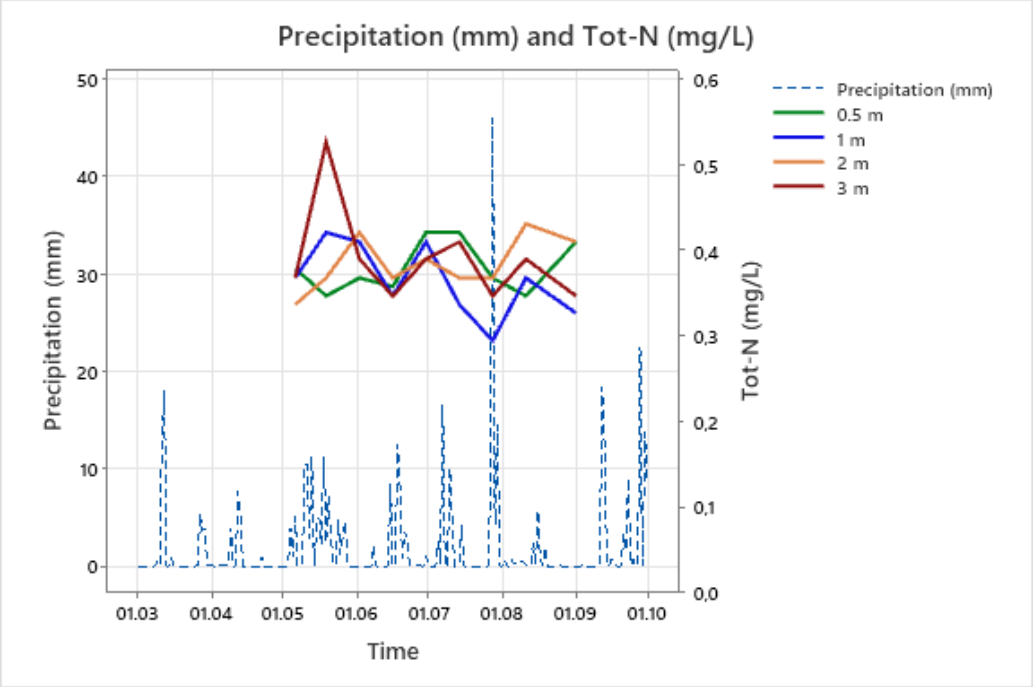

Figure 25. *Total daily precipitation (mm) in the study area and Tot-N (mg/L) at different depths (0.5 m, 1 m, 2 m, 3 m).*

3.2.6 Mn, Al, S, and Si

The dissolved Mn concentrations had a total mean of 0.015 mg/L at all depths during the sampling period, while the particulate fraction had a total mean of 0.004 mg/L (Fig. 26). Total Mn concentrations reached a peak of 0.55 mg/L at 3 m on the 14th of July, where 100% of total Mn measured consisted of dissolved Mn. Particulate Mn saw an increase at all depths during the heavy rainfall event on the 28th of July. Oxygen saturation was negatively correlated to particulate Mn at all depths, and to dissolved Mn at 3 m ($p < 0.05$).

The dissolved Al concentrations remained stable during the sampling period, ranging between a mean of 0.26-0.30 mg/L at all depths. The particulate fraction of total Al also remained stable, ranging between a mean of 0.07-0.09 mg/L at all depths. During the heavy rainfall event on the 28th of July, dissolved Al concentrations saw a decline at all depths while particulate Al remained stable (Fig. 27). Particulate Al concentrations was positively correlated to particulate Fe at all depths ($p < 0.05$).

Similar to Mn and Al, total S concentrations also remained stable during the sampling period. Dissolved S ranged between a mean of 0.55-0.60 mg/L at all depths, while particulate S ranged

between a mean of 0.03-0.05 mg/L at all depths. Dissolved S did however see an increase at 3 m to 0.83 mg/L on the 19th of May (Fig. 28). SO_4^{2-} concentrations remained stable during the sampling period, with a mean concentration of 1.4 mg/L at 0.5 m, 1 m, and 2 m, and a mean concentration of 1.5 mg/L at 3 m. On the 19th of May, SO_4^{2-} concentrations reached its peak of 2.1 mg/L at 3 m. Particulate S was positively correlated to particulate Fe at 0.5 m, 1 m, and 2 m ($p < 0.05$).

Total Si concentrations were decreasing from the beginning of the sampling period until the heavy rainfall event on the 28th of July, when particulate Si concentrations increased at all depths except for 0.5 m, and dissolved Si concentrations increased at all depths two weeks after (Fig. 29). Particulate Si ranged between a mean of 0.24-0.35 mg/L at all depths, while dissolved Si ranged between a mean of 0.72-0.76 mg/L at all depths. Dissolved Si was negatively correlated to dissolved Fe at 1 m, 2 m, and 3 m ($p < 0.05$).

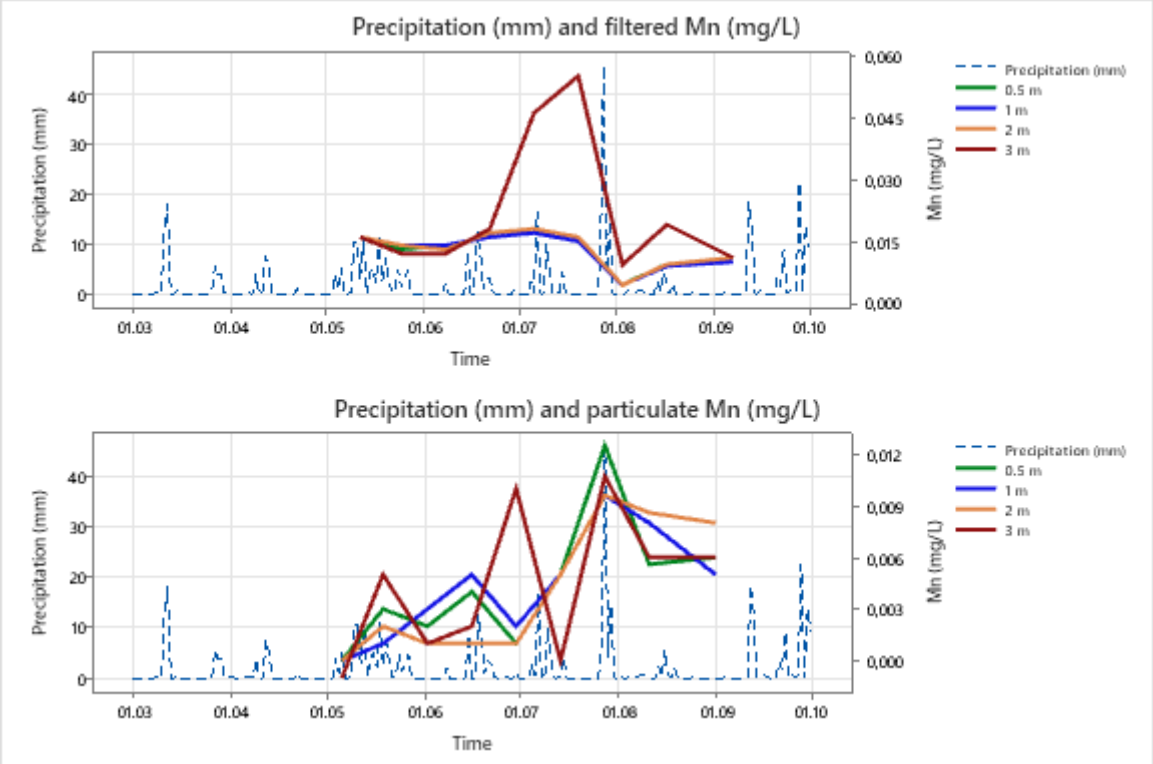

Figure 26. *Total daily precipitation (mm) in the study area and Mn (mg/L) (dissolved, particulate) at different depths (0.5 m, 1 m, 2 m, 3 m).*

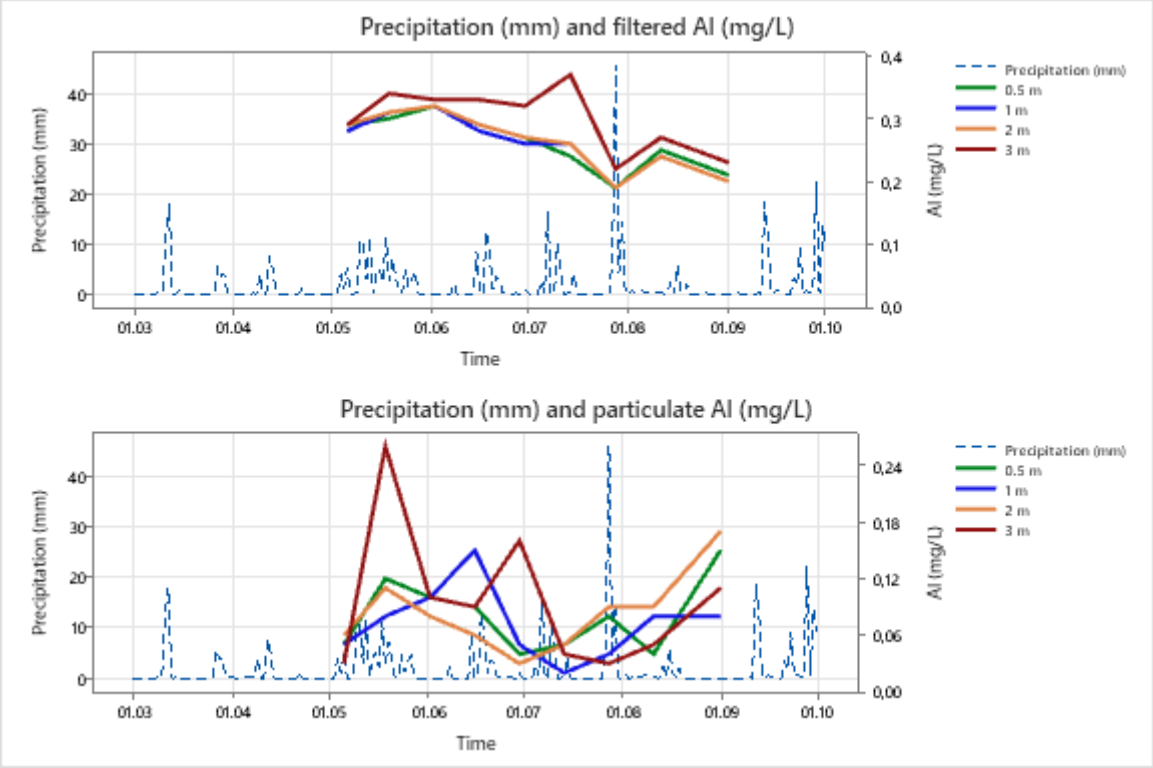

Figure 27. *Total daily precipitation (mm) in the study area and Al (mg/L) (dissolved, particulate) at different depths (0.5 m, 1 m, 2 m, 3 m).*

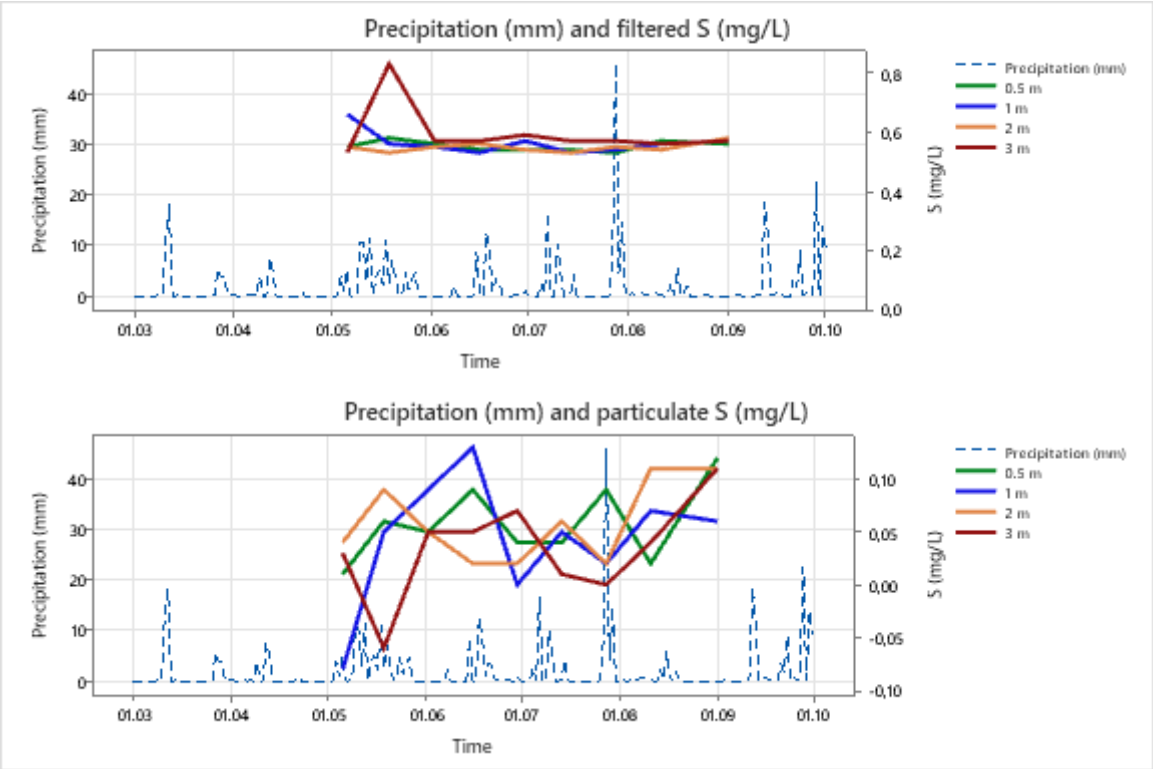

Figure 28. *Total daily precipitation (mm) in the study area and S (mg/L) (dissolved, particulate) at different depths (0.5 m, 1 m, 2 m, 3 m).*

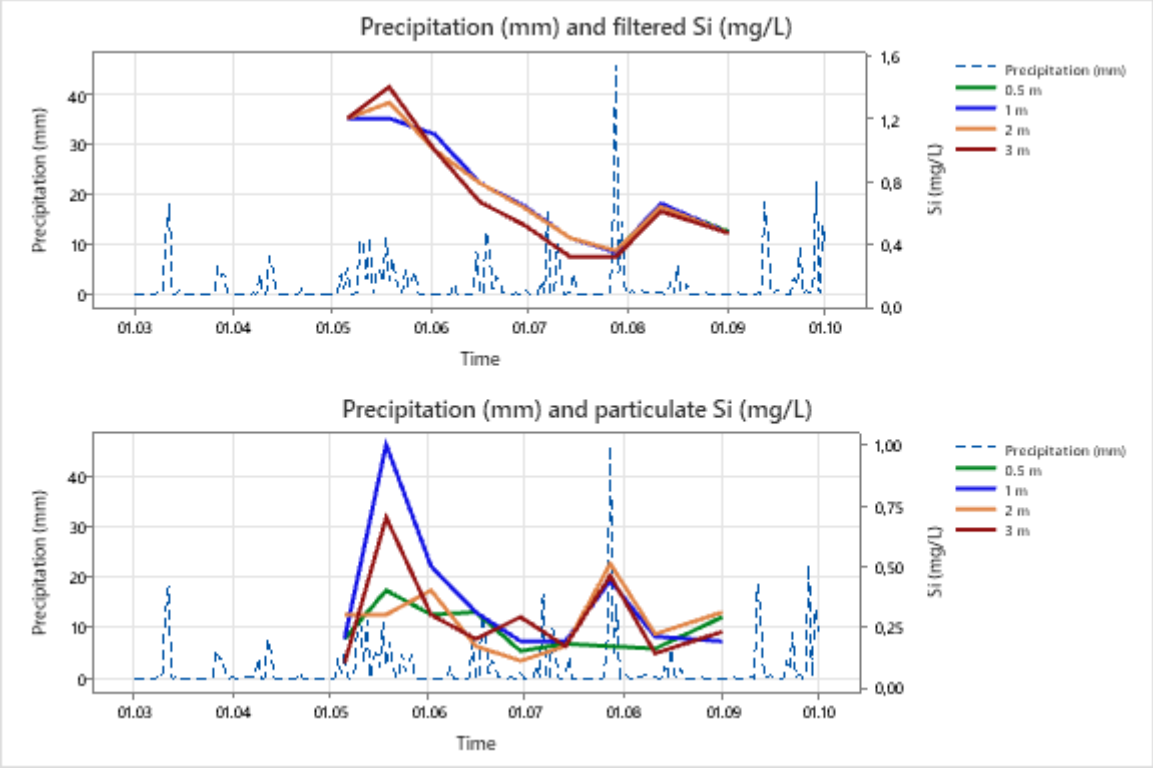

Figure 29. *Total daily precipitation (mm) in the study area and Si (mg/L) (dissolved, particulate) at different depths (0.5 m, 1 m, 2 m, 3 m).*

3.3 Statistical analyses

3.3.1 Principal Component Analysis (PCA)

A PCA was performed on 20 parameters from 0.5 m, 1 m, 2 m, and 3 m in the lake (Fig. 30-33). The complete analysis with eigenvalues and eigenvectors can be found in Appendix C.

At 0.5 m, PC1 and PC2 explained 64% and 36% of the total variation, respectively. Particulate Mn, particulate Al, alkalinity, dissolved Fe, particulate Fe, particulate S, conductivity, and SO_4^{2-} were all positively correlated with PC1, while oxygen saturation, dissolved Mn, and pH were negatively correlated. Turbidity, dissolved S, NH_4-N, NO_3-N and Tot-P were positively correlated to PC2, while Cl^-, colour, and DOC were negatively correlated.

At 1 m, PC1 and PC2 explained 73% and 27% of the total variation, respectively. Particulate S, dissolved Al, alkalinity, conductivity, particulate Al, and DOC were positively correlated to PC1, while NH_4-N, PO_4-P, dissolved S, dissolved Mn, SO_4^{2-}, and Cl^- were negatively correlated. Particulate Fe and oxygen saturation were positively correlated to PC2, while NO_3-N, turbidity, and Tot-P were negatively correlated.

At 2 m, PC1 and PC2 explained 55% and 45% of the total variation, respectively. Temperature, Tot-N, Tot-P, particulate Fe, alkalinity, and particulate Si were positively correlated to PC1, while pH, SO_4^{2-}, and dissolved S were negatively correlated. Particulate Al, particulate Mn, dissolved Fe, and particulate S were positively correlated to PC2, while dissolved S was negatively correlated.

At 3 m, PC1 and PC2 explained 43% and 33% of the total variation, respectively. Temperature, dissolved Mn, conductivity, dissolved Fe, Cl^-, and Tot-P were positively correlated to PC1, while dissolved Si, oxygen saturation, and PO_4-P were negatively correlated. Particulate S was positively correlated to PC2, while turbidity, SO_4^{2-}, dissolved S, particulate Si, particulate Al, and Tot-N were negatively correlated.

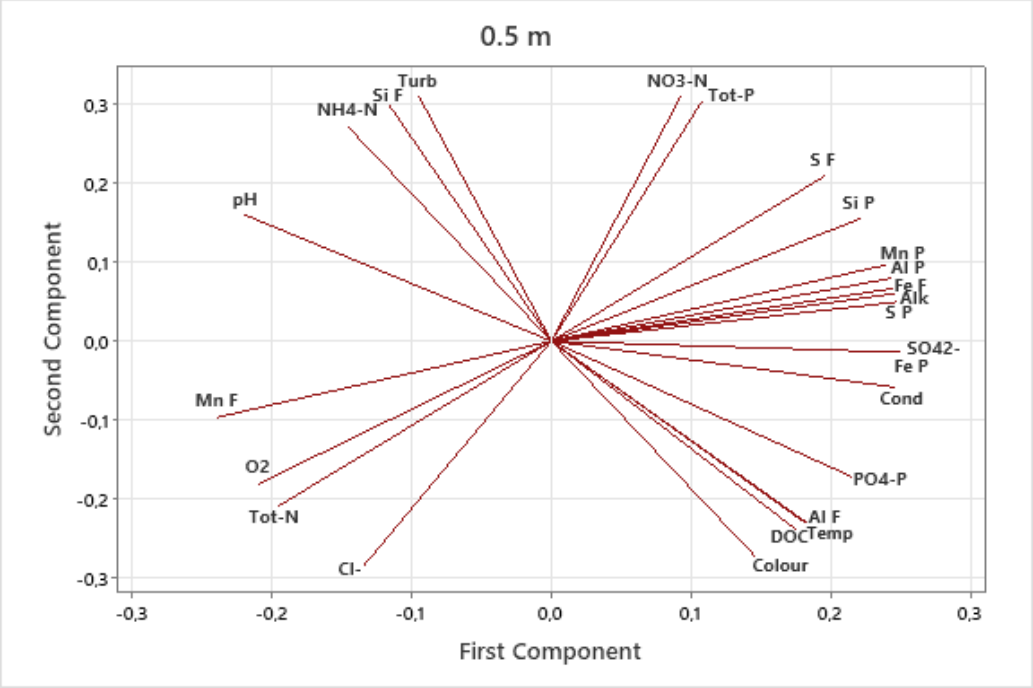

Figure 30. Principal component analysis (PCA) of dissolved Fe (Fe F), particulate Fe (Fe P), temperature (Temp), oxygen saturation (O2), conductivity (Cond), colour, turbidity (Turb), DOC, Tot-P, dissolved Mn (Mn F), particulate Mn (Mn P), dissolved Al (Al F), particulate Al (Al P), dissolved S (S F), particulate S (S P), Cl^-, Tot-N, NH_4-N, pH, alkalinity (Alk), SO_4^{2-}, dissolved Si (Si F), particulate Si (Si P), PO_4-P, and NO_3-N. Analysis was performed on parameters from 0.5 m. Values are standardised.

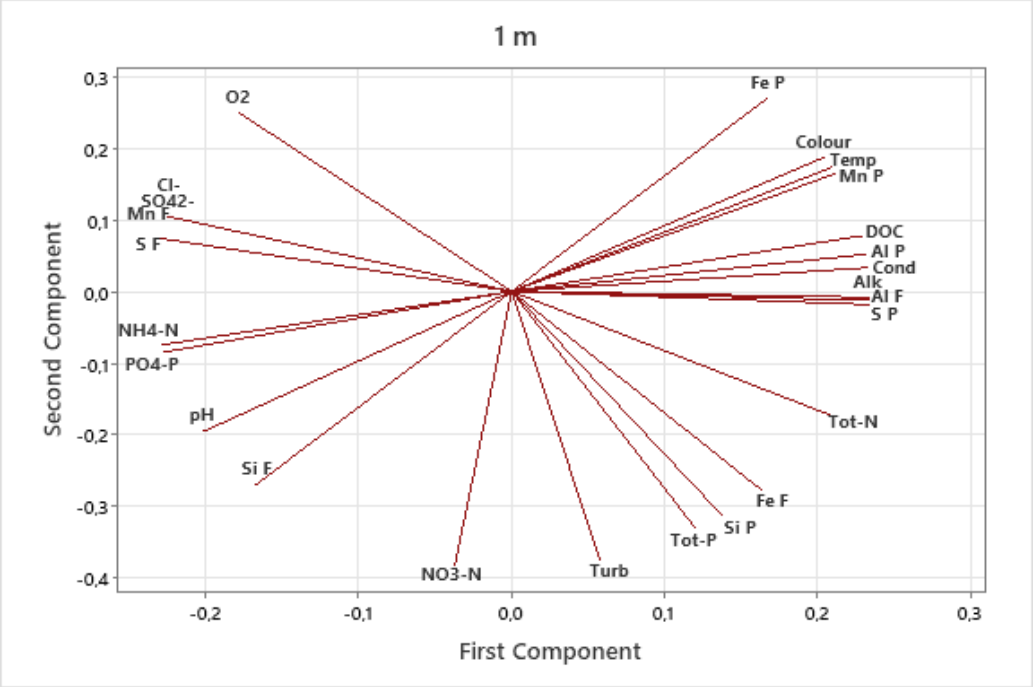

Figure 31. Principal component analysis (PCA) of dissolved Fe (Fe F), particulate Fe (Fe P), temperature (Temp), oxygen saturation (O2), conductivity (Cond), colour, turbidity (Turb), DOC, Tot-P, dissolved Mn (Mn F), particulate Mn (Mn P), dissolved Al (Al F), particulate Al (Al P), dissolved S (S F), particulate S (S P), Cl^-, Tot-N, NH_4-N, pH, alkalinity (Alk), SO_4^{2-}, dissolved Si (Si F), particulate Si (Si P), PO_4-P, and NO_3-N. Analysis was performed on parameters from 1 m. Values are standardised.

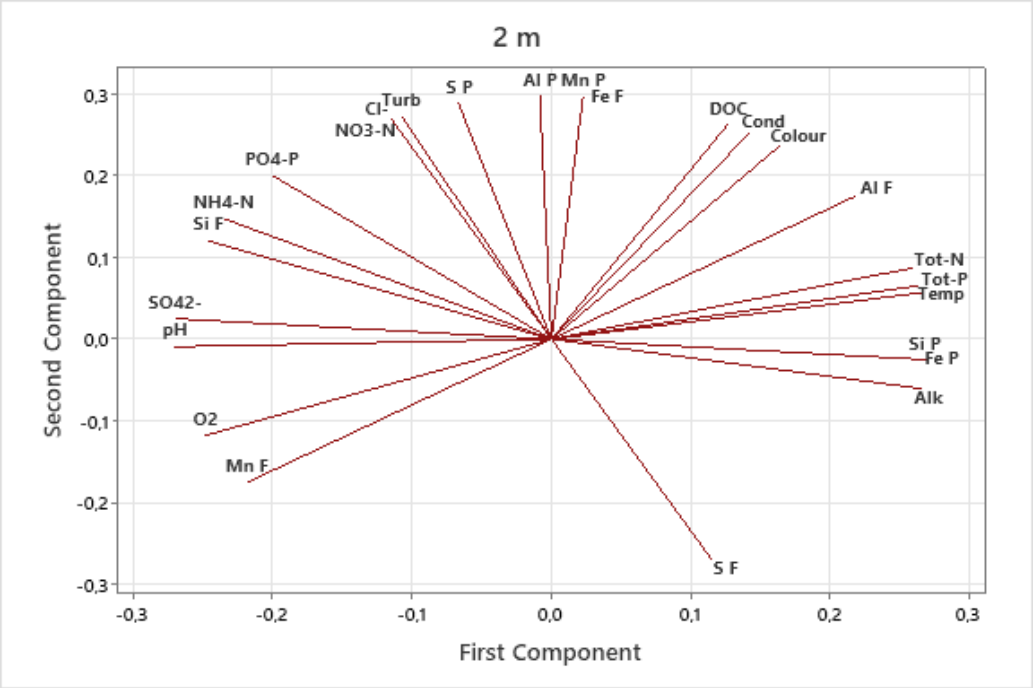

Figure 32. Principal component analysis (PCA) of dissolved Fe (Fe F), particulate Fe (Fe P), temperature (Temp), oxygen saturation (O2), conductivity (Cond), colour, turbidity (Turb), DOC, Tot-P, dissolved Mn (Mn F), particulate Mn (Mn P), dissolved Al (Al F), particulate Al (Al P), dissolved S (S F), particulate S (S P), Cl^-, Tot-N, NH_4-N, pH, alkalinity (Alk), SO_4^{2-}, dissolved Si (Si F), particulate Si (Si P), PO_4-P, and NO_3-N. Analysis was performed on parameters from 2 m. Values are standardised.

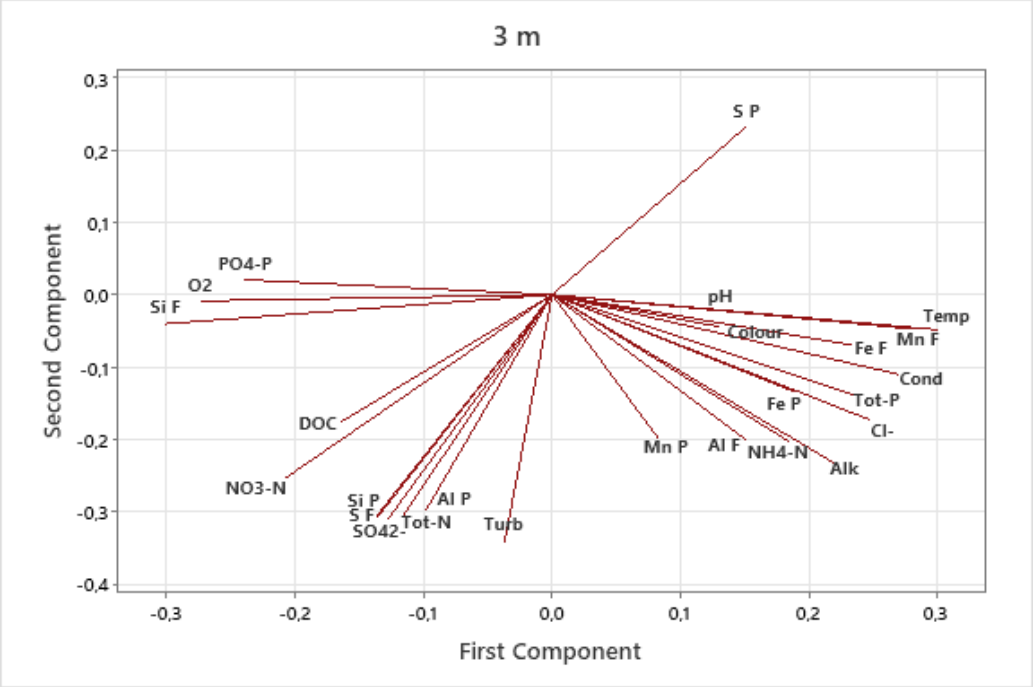

Figure 33. Principal component analysis (PCA) of dissolved Fe (Fe F), particulate Fe (Fe P), temperature (Temp), oxygen saturation (O2), conductivity (Cond), colour, turbidity (Turb), DOC, Tot-P, dissolved Mn (Mn F), particulate Mn (Mn P), dissolved Al (Al F), particulate Al (Al P), dissolved S (S F), particulate S (S P), Cl^-, Tot-N, NH_4-N, pH, alkalinity (Alk), SO_4^{2-}, dissolved Si (Si F), particulate Si (Si P), PO_4-P, and NO_3-N. Analysis was performed on parameters from 3 m. Values are standardised.

3.3.2 Paired t-test

A paired t-test of selected parameters (N=9) was performed to see if there was a significant difference between mean values in the surface layer (0.5 m and 1 m) and bottom layer (3 m) in the lake (Table 5 and 6).

Dissolved Fe, dissolved Al, oxygen saturation, pH, conductivity, and temperature had a significant difference in mean concentrations between 0.5 m and 3 m, and between 1 m and 3 m, while colour had a significant difference in mean concentrations between 0.5 m and 3 m ($p<0.05$).

Table 5. *Paired t-test of parameters (N=9) between 0.5 m and 3 m. Raw data was used for the test. Significance level = 0.05. P-values <0.05 is marked in bold.*

Parameter	Mean concentration (0.5m)	Mean concentration (3m)	Mean difference (0.5m - 3m)	P-value
Particulate Fe (mg/L)	0.148	0.248	-0.100	0.117
Particulate Al (mg/L)	0.080	0.097	-0.017	0.479
Particulate Mn (mg/L)	0.004	0.004	0.000	0.960
Particulate S (mg/L)	0.058	0.033	0.024	0.194
Particulate Si (mg/L)	0.240	0.288	-0.048	0.390
Dissolved Fe (mg/L)	0.230	0.378	-14.780	**0.033**
Dissolved Al (mg/L)	0.262	0.300	-0.038	**0.018**
Dissolved Mn (mg/L)	0.013	0.022	-0.009	0.105
Dissolved S (mg/L)	0.552	0.596	-0.043	0.146
Dissolved Si (mg/L)	0.763	0.723	0.039	0.285
O_2 saturation (%)	92.470	45.960	46.510	**0.001**
pH	6.212	5.984	0.228	**0.000**
DOC (mg/L)	10.724	10.424	0.300	0.209
Colour (mg Pt/L)	81.660	87.810	-6.160	**0.046**
Conductivity (µS/cm)	21.607	24.573	-2.967	**0.005**
Temperature (∘C)	18.490	13.480	5.010	**0.002**

Table 6. *Paired t-test of parameters (N=9) between 1 m and 3 m. Raw data was used for the test. Significance level = 0.05. P-values <0.05 is marked in bold.*

Parameter	Mean concentration (1m)	Mean concentration (3m)	Mean difference (1m - 3m)	P-value
Particulate Fe (mg/L)	0.230	0.248	-0.018	0.771
Particulate Al (mg/L)	0.072	0.097	-0.024	0.359
Particulate Mn (mg/L)	0.004	0.004	0.000	0.928
Particulate S (mg/L)	0.043	0.033	0.010	0.688
Particulate Si (mg/L)	0.359	0.288	0.071	0.125
Dissolved Fe (mg/L)	0.230	0.378	-0.148	**0.033**
Dissolved Al (mg/L)	0.260	0.300	-0.040	**0.005**
Dissolved Mn (mg/L)	0.013	0.022	-0.009	0.104
Dissolved S (mg/L)	0.563	0.596	-0.032	0.377
Dissolved Si (mg/L)	0.761	0.723	0.102	0.300
O_2 saturation (%)	92.180	45.960	46.220	**0.001**
pH	6.157	5.984	0.172	**0.005**
DOC (mg/L)	10.438	10.424	0.013	0.935
Colour (mg Pt/L)	82.120	87.810	-5.700	0.058
Conductivity (µS/cm)	21.784	24.573	-2.789	**0.014**
Temperature (∘C)	18.100	13.480	4.620	**0.003**

4. Discussion

4.1 Seasonal Variations of Fe at Different Depths

4.1.1 External loading of Fe during spring

Early spring was drier than normal in the study area, with a reduction in mean precipitation of 21.2, 4.9, and 32.8 mm in February, March, and April, respectively, from the normal (1991-2021). Weather and climate data suggest that ice and snow melt happened in March, and that the lake's catchment experienced a normal or small spring flood (Table 1-3).

Fe is usually associated with clay and silt mineral particles during spring floods in catchments dominated by woodland, due to the erosion of silt deposits in stream banks (Björkvald et al., 2008). In May, when the mean precipitation was 28.7 mm higher than normal (1991-2021), the lake had increased concentrations of Tot-P, total Si, total Al, dissolved S, and SO_4^{2-} (Fig. 24, 27-29). Fe incorporated in silicate minerals, such as aluminosilicates, Fe sulfides, and other clay fractions may have entered the lake from the catchment following the spring flood and an increased discharge in May, as reported from high flow periods in other studies (Davison, 1993; Shaked et al., 2004; Björnerås et al., 2021). By mid-May, both dissolved and particulate Fe concentrations saw an increase at 3 m in the lake (Fig. 16-19).

Moreover, DOC concentrations also increased during May, which would enhance the solubility and mobility of Fe (Cameron and Liss, 1984) in the catchment. Along with Fe (oxy)hydroxides, Fe-OM complexes are one of the main Fe phases in boreal river and stream mouths (Herzog et al., 2017), and are therefore likely to be an important carrier of Fe to the lake Vindlandstjernet.

In the beginning of May, the lake had similar temperatures at all depths in the water column, which would suggest a full spring circulation (Fig. 11, 12). By the end of May, the surface and bottom layers had an approximate 10°C temperature difference. As the water column became increasingly thermally stratified, the oxygen saturation at the bottom layer started to decline (Fig. 13, 14). There was also an increase in colour and turbidity at all depths in May. This may have contributed to the decline in oxygen by inducing a stronger thermal stratification, restricting photosynthesis, and increasing microbial activity as reported in other studies (Richardson et al., 2017; Couture et al., 2015; Arzel et al., 2020).

4.1.2 Remobilisation of Fe during summer stratification

The catchment area experienced 40.2 mm less precipitation in June than normal (1991-2021). During the first half of June, the oxygen saturation dropped to 35% and 1% at 3 m and 3.5 m, respectively. June saw a decline in parameters associated with precipitation and high flow, i.e. DOC, colour, and turbidity, which would be expected in a boreal catchment during dry periods (Hongve et al., 2004). Moreover, the pH in the lake saw an increase at all depths, from a mean of 5.8 on the 2nd of June to a mean of 6.2 on the 30th of June (Fig. 15). This is also expected as the pH in freshwater tends to increase along with increased primary production in the summer (Tank et al., 2009).

During the second half of June, the lake was thermally stratified with an oxygen saturation of 16% and 0.8% at 3 m and 3.5 m, respectively. Fe concentrations saw a sharp increase at 3 m on the 30th of June (Fig. 16-19 and Table 4), likely due to anoxic conditions. 65% of the total Fe concentration at 3 m was particulate which suggests that the redox boundary was located in the sediment column, as described in the conceptual model of Davison (1985). When reduced Fe is released from the sediment, it will oxidise to particulate oxides suspended in the bottom layer of the water column and transported vertically by random processes. Moreover, Cl^-, conductivity, and Tot-P concentrations increased at 3 m, likely due to an accumulation at the bottom layer following stratification, as well as internal loading of P. The negative correlation between Fe and PO_4^{3-} ($p<0.05$), and the low concentrations of PO_4^{3-} during summer stratification, suggest that the release of PO_4^{3-} is limited by adsorption onto Fe (oxy)hydroxides.

The lake's southern inlet stream (IN1) (Fig. 3) also saw a similar increase in particulate Fe two weeks earlier, which means the lake could have had an input of Fe coming from this stream (Pålsrud, 2022). However, as the Fe concentrations in the stream were low before and after the sudden increase, it may be explained by particulates from the sediment entering the sample.

During the first half of July, the surface and bottom layers had a peak temperature difference of 14°C. The lake saw a strong increase of dissolved Fe concentrations at 3 m (Fig. 18 and 19, Table 4), which would suggest a migration of the redox boundary from the sediment to the water column. However, because the oxygen saturation at 3.5 m was not sampled, it is difficult to say for certain. Dissolved Mn concentrations also saw an increase at 3 m, which would indicate a common driver due to the similar chemical behaviour of Fe and Mn (Stumm and Morgan, 1996). Although the oxygen saturation at 3 m was 35% during the peak of dissolved Fe concentrations at 3 m, organic complexation could have supported Fe solubility and

prevented a loss of Fe from the water column, which is typical for catchments dominated by woodland (Maranger et al., 2006; Heikkinen et al., 2022). Further, the water colour also saw a strong increase at 3 m, which did not follow the trend of DOC concentrations at the time (Fig. 20 and 21). It did, however, have a positive correlation to dissolved Fe at 3 m ($p<0.05$), which suggests that increased concentrations of Fe contributed to the increase in colour at 3 m through organic complexation, as reported by Xiao and Riise (2021).

On the 28th of July, a heavy rainfall event (46 mm) diluted most parameters, including total Fe concentrations which declined at 3 m (Fig. 16-19). The heavy rainfall is also likely to have lowered the surface layer temperature, weakening the thermal stratification in the lake and encouraging a mixing of the water column as documented by Liu et al. (2020). Particulate Si, however, increased at all depths except for 0.5 m (Fig. 29). This would suggest an increased particulate transport from the catchment following erosion during heavy rainfall.

4.1.3 Circulation of the water column during autumn

August was especially dry with a total precipitation of 14.6 mm, which is 82.9 mm less than normal (1991-2021). Following heavy rainfall in the end of July, most parameters in the lake increased, including pH, total Si, total Al, total Mn, Tot-N, conductivity, Cl^-, turbidity, DOC, and total Fe (see Chapter 3.2). The concentration of these parameters was more equally distributed in the water column, and the oxygen saturation at 3 m increased from 18% in the end of July to 54% in the beginning of September. This would suggest a circulation of the water column encouraged by heavy rainfall and the surface layer temperature declining by 10°C.

DOC concentrations and colour followed the same trend during August, where both increased following heavy rainfall and eventually declined somewhat, while the turbidity remained low at all depths. Particulate Fe also saw a slight increase throughout the water column in August, possibly due to the export of Fe (oxy)hydroxides and Fe-OM complexes from the catchment following heavy rainfall.

4.2 Retention of Fe at Different Stratification and Runoff Conditions

This study shows that the lake Vindlandstjernet is highly dynamic where the input, retention, and export of Fe vary on a short time scale. This is supported by other studies on the biogeochemical cycling of Fe in lakes (e.g. Shaked et al., 2004; Weyhenmeyer et al., 2014).

The water retention time of lakes varies with depth (Weyhenmeyer et al., 2014; Tong et al., 2019), which would make Vindlandstjernet less likely to retain Fe during high flow events. In boreal catchments, Fe is usually transported to lakes as Fe (oxy)hydroxides, Fe-OM complexes, or with aluminosilicates (Davison, 1993; Shaked et al., 2004). During spring floods in boreal catchments dominated by woodland, erosion in river and stream banks will lead to Fe loading in lakes (Björkvald et al., 2008). High flow periods will also make Fe more mobile while organically complexed (Cameron and Liss, 1984; Jansen et al., 2002). The total Fe concentration in the lake had a slight increase during May when the catchment experienced more precipitation than normal, and a decrease in June which was drier than normal. The lake's outlet stream (UT) (Fig. 3) did not see a significant increase in Fe concentrations during spring (Pålsrud, 2022), which would suggest the lake acted as a sink despite increased runoff conditions. Overall, total Fe concentrations in the lake remained low until the end of June.

The lake's inlet stream (IN1) (Fig. 3) saw a sharp increase in particulate Fe from 0.08 mg/L on the 2nd of June to 1.07 mg/L on the 16th of June (Pålsrud, 2022). This may have led to the increase in particulate Fe at 3 m in the lake on the 30th of June. At this point, the lake was anoxic at 3.5 m, which would have led to the remobilisation of sedimentary Fe to the water column. The lake's outlet stream (UT) also saw an increase in Fe concentrations during this time, suggesting an influx of Fe from the lake. Another possibility would be Fe loading to the outlet stream from an adjacent inlet stream (IN3), which saw a significant increase in June.

It is not known if the thermal stratification and anoxic conditions observed during the summer are typical for the lake, or if it is due to extremities in weather and climate. June was very dry and had a mean temperature which was 2.6°C higher than normal (1991-2021). The surface layer in the lake may therefore have been warmed more rapidly during June, which could have led to an earlier and stronger thermal stratification. This could in turn have exacerbated the decline in oxygen at the bottom layer in the lake during the summer months. If the bottom layer had higher oxygen levels, the lake could have been a more efficient sink as Fe would be more readily removed from the water column through sedimentation, aggregation, and hydrolysis.

The Fe concentration along the aquatic continuum will decline with increasing water retention time (Weyhenmeyer et al., 2014). A shorter water retention time due to increased precipitation can therefore limit a lake's ability to retain Fe (Dillon et al., 1988). Following, and during, the heavy rainfall event on the 28th of July, the lake's outlet stream (UT) saw a sharp increase in particulate Fe concentrations. However, because the outlet stream is adjacent to an inlet stream (IN3) (Fig. 3) that also saw a significant increase in Fe concentrations at the time, it is not certain to what degree the lake contributed to the influx of Fe. Agricultural soil treatment in the catchment area of the adjacent inlet stream (IN3) has most likely caused an increased mobilisation of Fe (Pålsrud, 2022).

4.3 Potential Impacts on Aquatic Fauna

4.3.1 The noble crayfish

In many freshwater ecosystems, crayfish are considered keystone species due to their importance to the food web (Momot, 1995; Usio, 2000). As polytrophic consumers, their diet includes benthic organisms, macrophytes, algae, fish eggs, detritus, and carrion (Dorn and Wojdak, 2004). Crayfish can therefore significantly affect the abundance and species richness of organisms in freshwater ecosystems (Ercoli et al., 2014).

The Norwegian population of the noble crayfish (*Astacus astacus*) has been reduced by an approximate 90% since the 1960's (Miljødirektoratet, 2020). One of the species' biggest threats is the crayfish plague (*Aphanomyces astaci*), carried by the invasive signal crayfish (*Pasifastacus leniusculus*). The noble crayfish is listed as vulnerable on the IUCN Red List (2010) and as very threatened on the Norwegian Red List (2021). The population of the noble crayfish is also heavily influenced by water quality (Pârvulescu et al., 2011), but due to how many chemical water parameters interact with each other in natural freshwater, it is difficult to set a specific limit for toxicity.

Increased concentrations of metals such as Fe and Al can lead to hypoxia and osmoregulatory stress in crayfish (Svobodová et al., 2017). Previous studies on the toxicity of Al on crayfish have found that concentrations above 0.18 mg/L, with a labile Al fraction of 0.02 mg/L, to be lethal, and an approximate 0.5 mg/L to be sub-lethal (Alexopoulos et al., 2003; Ward et al., 2006). Fe concentrations above 0.5 mg/L and 1 mg/L are often considered to negatively impact

crayfish populations (Edsman et al., 2018). The toxicity of Fe and Al depend on speciation, making it difficult to assess if the concentrations in the lake Vindlandstjernet are damaging to the local noble crayfish population. Total Al concentrations ranged between a mean of 0.34 mg/L at 0.5 m and 0.40 mg/L at 3 m, while total Fe concentrations ranged between a mean of 0.38 mg/L at 0.5 m and 0.63 mg/L at 3 m. The lake's Fe and Al concentrations can therefore potentially impact the noble crayfish population negatively.

The noble crayfish are vulnerable to low oxygen concentrations, and dissolved oxygen concentrations less than 4 mg/L can be lethal (Souty-Grosset et al., 2006). The anoxic and hypoxic conditions in the bottom layer of the lake during summer stratification can therefore have adverse impacts on the population and act as a bottleneck for the catchment. The pH in the lake ranged from a mean of 6.2 at 0.5 m to 5.9 at 3 m. A pH below 6 is usually considered a limiting factor for crayfish (Nyström, 2002), which means the seasonal variations in the lake pH can also negatively impact the crayfish population. Moreover, the lake is considered to be poor in calcium (Ca), with a mean concentration of 1.8 mg/L. A Ca concentration above 5 mg/L is considered as necessary to support crayfish populations (Edsman et al., 2018).

Further, the noble crayfish are heavily reliant on shelter, such as stone, aquatic vegetation, submerged logs and roots (Souty-Grosset et al., 2006). Although the lake has an abundance of macrophytes and riparian vegetation in many areas, there are few stones and other similar hiding places, which may be a limiting factor.

4.3.2 Fish species

Among fish species found in the lake are perch (*Perca fluviatilis*) and pike (*Esox lucius*).

Metals such as Fe and Al can accumulate in and on gill tissue, which at high concentrations will inhibit osmoregulation and ionregulation. As with the noble cray fish, it is difficult to determine a specific limit for the toxicity of metals to fish species due to the dynamic chemical nature of freshwaters. For example, the toxicity of Fe is reduced in water with high concentrations of humic acid (Peuranen et al., 1994). Fe and Al will also exacerbate the relative toxicity of each other (Vuorinen et al., 1999). Moreover, Fe is more toxic in its bioavailable species as Fe(II) and will therefore be more toxic under anoxic conditions and in water bodies with a short water retention time as Fe does not get enough time to oxidise and precipitate. In general, total Fe concentrations have shown to be toxic to fish at concentrations above 0.05 mg/L under unfavoured conditions (Åtland et al., 2003).

The remobilisation of Fe as Fe(II) from the sediment during summer stratification, as well as more particulate Fe in solution in the water column, can potentially be a limiting factor on fish populations in the lake Vindlandstjernet. Depending on several factors, including the ratio between Fe and humic acid, the total Fe concentrations observed during the study period could be considered toxic.

5. Conclusion

As a humic and shallow lake, Vindlandstjernet is highly dynamic where the biogeochemical cycling and retention of Fe vary on a short time scale. The distribution and cycling of Fe in the water column seem to be highly dependent on weather and climate, with an external loading of Fe from the catchment during high flow and a remobilisation of Fe in the lake while thermally stratified.

The weather and climate prior to and during the study period were characterised as warm and dry, which would have led to less Fe export from the catchment overall. During periods of high flow, the lake did see an increase in total Fe concentrations and associated parameters such as Si, Al, S, P, and DOC. Further, the degree of thermal stratification was unexpected as the lake is very shallow. However, as a humic lake, the warm and dry climate during the study period, as well as increased DOC concentrations and turbidity following high flow in May, could have induced a stronger summer stratification than normal.

The redox boundary in the lake seems to have migrated from the sediment to the water column during summer, as suggested by the high concentrations of particulate Fe at 3 m in June and high concentrations of dissolved Fe at 3 m in July. Organic complexation may also have been essential in keeping Fe in solution and preventing a loss of Fe from the water column under oxic conditions. A heavy rainfall event in the end of July most likely induced an early circulation during August. As the lake is very shallow, a surface water temperature decrease of 10°C would readily induce a mixing of the water column in autumn. Fe concentrations declined as the hypolimnion became more oxic, with a slight upwards trend in particulate Fe following the heavy rainfall event.

Although the study lake experienced relatively high increases of Fe during the summer months, the concentrations are still below the mean in lakes located in south eastern Norway (Hindar et al., 2019). Any adverse impacts on aquatic fauna would highly depend on speciation and several physicochemical properties, making it difficult to assess the relative toxicity of Fe.

The results from this study confirm the first hypothesis that thermal stratification affects the distribution and cycling of Fe in the water column. Further, the results indicate that the lake acts as a Fe sink in the catchment, but more data on the total Fe budget of the lake would be needed to reject the second hypothesis. It is not clear how much the lake contributed as a Fe source to its outlet stream during high flow due to significant Fe increases nearby in the catchment.

References

ALEXOPOULOS, E., MCCROHAN, C. R., POWELL, J. J., JUGDAOHSINGH, R. & WHITE, K. N. 2003. Bioavailability and Toxicity of Freshly Neutralized Aluminium to the Freshwater Crayfish Pacifastacus leniusculus. *Archives of Environmental Contamination and Toxicology,* 45**,** 509-514. doi: 10.1007/s00244-003-0228-9

ARZEL, C., NUMMI, P., ARVOLA, L., PÖYSÄ, H., DAVRANCHE, A., RASK, M., OLIN, M., HOLOPAINEN, S., VIITALA, R., EINOLA, E. & MANNINEN-JOHANSEN, S. 2020. Invertebrates are declining in boreal aquatic habitat: The effect of brownification? *Science of The Total Environment,* 724**,** 138199. doi: https://doi.org/10.1016/j.scitotenv.2020.138199

BJÖRKVALD, L., BUFFAM, I., LAUDON, H. & MÖRTH, C.-M. 2008. Hydrogeochemistry of Fe and Mn in small boreal streams: The role of seasonality, landscape type and scale. *Geochimica et Cosmochimica Acta,* 72**,** 2789-2804. doi: https://doi.org/10.1016/j.gca.2008.03.024

BJÖRNERÅS, C., PERSSON, P., WEYHENMEYER, G. A., HAMMARLUND, D. & KRITZBERG, E. S. 2021. The lake as an iron sink - new insights on the role of iron speciation. *Chemical Geology,* 584**,** 120529. doi: https://doi.org/10.1016/j.chemgeo.2021.120529

BJÖRNERÅS, C., WEYHENMEYER, G. A., EVANS, C. D., GESSNER, M. O., GROSSART, H. P., KANGUR, K., KOKORITE, I., KORTELAINEN, P., LAUDON, H., LEHTORANTA, J., LOTTIG, N., MONTEITH, D. T., NÕGES, P., NÕGES, T., OULEHLE, F., RIISE, G., RUSAK, J. A., RÄIKE, A., SIRE, J., STERLING, S. & KRITZBERG, E. S. 2017. Widespread Increases in Iron Concentration in European and North American Freshwaters. *Global Biogeochemical Cycles,* 31**,** 1488-1500. doi: https://doi.org/10.1002/2017GB005749

CAMERON, A. J. & LISS, P. S. 1984. The stabilization of "dissolved" iron in freshwaters. *Water Research,* 18**,** 179-185. doi: https://doi.org/10.1016/0043-1354(84)90067-8

COUTURE, R.-M., DE WIT, H. A., TOMINAGA, K., KIURU, P. & MARKELOV, I. 2015. Oxygen dynamics in a boreal lake responds to long-term changes in climate, ice phenology, and DOC inputs. *Journal of Geophysical Research: Biogeosciences,* 120**,** 2441-2456. doi: https://doi.org/10.1002/2015JG003065

CUNHA, T., GEMAQUE, COSTA, D. P. D., PEREIRA, L. V. & FILHO, K. C. I. 2019. Evaluation of Iron Toxicity in the Tropical Fish Leporinus friderici. *Journal of Scientific & Technical Research,* 18. doi: 10.26717/BJSTR.2019.18.003127

DAVISON, W. 1985. Conceptual models for transport at a redox boundary. *In:* STUMM, W. (ed.) *Chemical processes in lakes.* 1st ed.: Wiley-Interscience.

DAVISON, W. 1993. Iron and manganese in lakes. *Earth-Science Reviews,* 34**,** 119-163. doi: https://doi.org/10.1016/0012-8252(93)90029-7

DILLON, P. J., EVANS, H. E. & SCHOLER, P. J. 1988. The effects of acidification on metal budgets of lakes and catchments. *Biogeochemistry,* 5**,** 201-220. doi: 10.1007/BF02180228

DORN, N. J. & WOJDAK, J. M. 2004. The role of omnivorous crayfish in littoral communities. *Oecologia,* 140**,** 150-159. doi: 10.1007/s00442-004-1548-9

EDSMAN, L., P, N., T, J., MANNONEN, A. & JUSSILA, J. 2018. *Krätfodlingens ABC.* ed.

EKSTRÖM, S., REGNELL, O., READER, H., NILSSON, A., STEFAN, L. & KRITZBERG, E. 2016. Increasing concentrations of iron in surface waters as a consequence of reducing conditions in the catchment area. *Journal of Geophysical Research: Biogeosciences,* 121. doi: 10.1002/2015JG003141

ERCOLI, F., RUOKONEN, T. J., HÄMÄLÄINEN, H. & JONES, R. I. 2014. Does the introduced signal crayfish occupy an equivalent trophic niche to the lost native noble crayfish in boreal lakes? *Biological Invasions,* 16**,** 2025-2036. doi: 10.1007/s10530-014-0645-x

EVANS, C., MONTEITH, D. & COOPER, D. 2005. Long-term increases in surface water dissolved organic carbon: Observations, possible causes and environmental impacts. *Environmental pollution (Barking, Essex : 1987),* 137**,** 55-71. doi: 10.1016/j.envpol.2004.12.031

FINSTAD, A. G., ANDERSEN, T., LARSEN, S., TOMINAGA, K., BLUMENTRATH, S., DE WIT, H. A., TØMMERVIK, H. & HESSEN, D. O. 2016. From greening to browning: Catchment vegetation development and reduced S-deposition promote organic carbon load on decadal time scales in Nordic lakes. *Scientific Reports,* 6**,** 31944. doi: 10.1038/srep31944

GAVIN, A. L., NELSON, S. J., KLEMMER, A. J., FERNANDEZ, I. J., STROCK, K. E. & MCDOWELL, W. H. 2018. Acidification and Climate Linkages to Increased Dissolved Organic Carbon in High-Elevation Lakes. *Water Resources Research,* 54**,** 5376-5393. doi: https://doi.org/10.1029/2017WR020963

GOULET, R. R. & PICK, F. R. 2001. Changes in dissolved and total Fe and Mn in a young constructed wetland: Implications for retention performance. *Ecological Engineering,* 17**,** 373-384. doi: https://doi.org/10.1016/S0925-8574(00)00161-0

HEIKKINEN, K., SAARI, M., HEINO, J., RONKANEN, A. K., KORTELAINEN, P., JOENSUU, S., VILMI, A., KARJALAINEN, S. M., HELLSTEN, S., VISURI, M. & MARTTILA, H. 2022. Iron in boreal river catchments: Biogeochemical, ecological and management implications. *Science of The Total Environment,* 805**,** 150256. doi: https://doi.org/10.1016/j.scitotenv.2021.150256

HERZOG, S. D., PERSSON, P. & KRITZBERG, E. S. 2017. Salinity Effects on Iron Speciation in Boreal River Waters. *Environmental Science & Technology,* 51**,** 9747-9755. doi: 10.1021/acs.est.7b02309

HINDAR, A., GARMO, Ø., AUSTNES, K. & SAMPLE, J. E. 2019. Nasjonal innsjøundersøkelse 2019. Norsk institutt for vannforskning (NIVA). doi:

HONGVE, D., RIISE, G. & KRISTIANSEN, J. 2004. Increased colour and organic acid concentrations in Norwegian forest lakes and drinking water—a result of increased precipitation? Aquat Sci. *Aquatic Sciences - Research Across Boundaries,* 66**,** 231-238. doi: 10.1007/s00027-004-0708-7

HAALAND, S., HONGVE, D., LAUDON, H., RIISE, G. & VOGT, R. D. 2010. Quantifying the Drivers of the Increasing Colored Organic Matter in Boreal Surface Waters. *Environmental Science & Technology,* 44**,** 2975-2980. doi: 10.1021/es903179j

JANSEN, B., NIEROP, K. G. J. & VERSTRATEN, J. M. 2002. Influence of pH and metal/carbon ratios on soluble organic complexation of Fe(II), Fe(III) and Al(III) in soil solutions determined by diffusive gradients in thin films. *Analytica Chimica Acta,* 454**,** 259-270. doi: https://doi.org/10.1016/S0003-2670(01)01551-3

KNORR, K.-H., LISCHEID, G. & BLODAU, C. 2009. Dynamics of redox processes in a minerotrophic fen exposed to a water table manipulation. *Geoderma,* 153**,** 379-392. doi: 10.1016/j.geoderma.2009.08.023

KOKORITE, I., KLAVINS, M., RODINOV, V. & SPRINGE, G. 2012. Trends of natural organic matter concentrations in river waters of Latvia. *Environmental Monitoring and Assessment,* 184**,** 4999-5008. doi: 10.1007/s10661-011-2315-0

KRITZBERG, E. S. 2017. Centennial-long trends of lake browning show major effect of afforestation. *Limnology and Oceanography Letters,* 2**,** 105-112. doi: https://doi.org/10.1002/lol2.10041

KRITZBERG, E. S. & EKSTRÖM, S. M. 2012. Increasing iron concentrations in surface waters - a factor behind brownification? *Biogeosciences,* 9**,** 1465-1478. doi: 10.5194/bg-9-1465-2012

KRITZBERG, E. S., HASSELQUIST, E. M., ŠKERLEP, M., LÖFGREN, S., OLSSON, O., STADMARK, J., VALINIA, S., HANSSON, L.-A. & LAUDON, H. 2020. Browning of freshwaters: Consequences to ecosystem services, underlying drivers, and potential mitigation measures. *Ambio,* 49**,** 375-390. doi: 10.1007/s13280-019-01227-5

LALONDE, K., MUCCI, A., MORITZ, A., OUELLET, A. & GELINAS, Y. 2011. The Rusty Sink: Iron Promotes the Preservation of Organic Matter in Sediments. *AGU Fall Meeting Abstracts***,** 0311. doi:

LIU, M., ZHANG, Y., SHI, K., ZHANG, Y., ZHOU, Y., ZHU, M., ZHU, G., WU, Z. & LIU, M. 2020. Effects of rainfall on thermal stratification and dissolved oxygen in a deep drinking water reservoir. *Hydrological Processes,* 34**,** 3387-3399. doi: https://doi.org/10.1002/hyp.13826

LUEDER, U., JØRGENSEN, B. B., KAPPLER, A. & SCHMIDT, C. 2020. Photochemistry of iron in aquatic environments. *Environmental Science: Processes & Impacts,* 22**,** 12-24. doi: 10.1039/C9EM00415G

MALONEY, K. O., MORRIS, D. P., MOSES, C. O. & OSBURN, C. L. 2005. The Role of Iron and Dissolved Organic Carbon in the Absorption of Ultraviolet Radiation in Humic Lake Water. *Biogeochemistry,* 75**,** 393-407. doi: 10.1007/s10533-005-1675-3

MARANGER, R., CANHAM, C. D., PACE, M. L. & PAPAIK, M. J. 2006. A spatially explicit model of iron loading to lakes. *Limnology and Oceanography,* 51**,** 247-256. doi: https://doi.org/10.4319/lo.2006.51.1.0247

MOMOT, W. T. 1995. Redefining the role of crayfish in aquatic ecosystems. *Reviews in Fisheries Science,* 3**,** 33-63. doi: 10.1080/10641269509388566

MONTEITH, D., STODDARD, J., EVANS, C., DE WIT, H., FORSIUS, M., HØGÅSEN, T., WILANDER, A., SKJELKVÅLE, B. L., JEFFRIES, D., VUORENMAA, J., KELLER, B., KOPÁČEK, J. & VESELY, J. 2007. Dissolved organic carbon trends resulting from changes in atmospheric deposition chemistry. *Nature,* 450**,** 537-40. doi: 10.1038/nature06316

MORTIMER, C. H. 1941. The Exchange of Dissolved Substances Between Mud and Water in Lakes. *Journal of Ecology,* 29**,** 280-329. doi: 10.2307/2256395

NEAL, C., LOFTS, S., EVANS, C., REYNOLDS, B., TIPPING, E. & NEAL, M. 2008. Increasing Iron Concentrations in UK Upland Waters. *Aquatic Geochemistry,* 14**,** 263-288. doi: 10.1007/s10498-008-9036-1

NYSTRÖM, P. 2002. Ecology. *In:* HOLDICH, D. M. (ed.) *Biology of freshwater crayfish.* Oxford: Blackwell Science.

PÂRVULESCU, L., PACIOGLU, O. & HAMCHEVICI, C. 2011. The assessment of the habitat and water quality requirements of the stone crayfish (Austropotamobius torrentium) and noble crayfish (Astacus astacus) species in the rivers from the Anina Mountains (SW Romania). *Knowl. Managt. Aquatic Ecosyst.***,** 03. doi:

PEURANEN, S., VUORINEN, P. J., VUORINEN, M. & HOLLENDER, A. 1994. The effects of iron, humic acids and low pH on the gills and physiology of Brown Trout (Salmo trutta). *Annales Zoologici Fennici,* 31**,** 389-396. doi:

PÅLSRUD, S. H. 2022. *Kilder og variasjoner i jern langs et borealt vassdrag i Sørøst-Norge under en tørkeperiode.* Norges miljø- og naturvitenskapelige universitet (NMBU).

RICHARDSON, D. C., MELLES, S. J., PILLA, R. M., HETHERINGTON, A. L., KNOLL, L. B., WILLIAMSON, C. E., KRAEMER, B. M., JACKSON, J. R., LONG, E. C., MOORE, K., RUDSTAM, L. G., RUSAK, J. A., SAROS, J. E., SHARMA, S., STROCK, K. E., WEATHERS, K. C. & WIGDAHL-PERRY, C. R. 2017. Transparency, Geomorphology and Mixing Regime Explain Variability in Trends in Lake Temperature and Stratification across Northeastern North America (1975–2014). *Water,* 9**,** 442. doi:

SARKKOLA, S., NIEMINEN, M., KOIVUSALO, H., LAURÉN, A., KORTELAINEN, P., MATTSSON, T., PALVIAINEN, M., PIIRAINEN, S., STARR, M. & FINÉR, L. 2013. Iron concentrations are increasing in surface waters from forested headwater catchments in eastern Finland. *Science of The Total Environment,* 463-464**,** 683-689. doi: https://doi.org/10.1016/j.scitotenv.2013.06.072

SHAKED, Y., EREL, Y. & SUKENIK, A. 2004. The biogeochemical cycle of iron and associated elements in Lake Kinneret1, 21Associate editor: M. L. Machesky2See

Electronic Annex (Elsevier Web site; Science Direct). *Geochimica et Cosmochimica Acta,* 68**,** 1439-1451. doi: https://doi.org/10.1016/j.gca.2003.09.018

SHAPIRO, J. 1966. The relation of humic color to iron in natural waters. *SIL Proceedings, 1922-2010,* 16**,** 477-484. doi: 10.1080/03680770.1965.11895719

SMEDBERG, E., MÖRTH, C.-M., SWANEY, D. P. & HUMBORG, C. 2006. Modeling hydrology and silicon-carbon interactions in taiga and tundra biomes from a landscape perspective: Implications for global warming feedbacks. *Global Biogeochemical Cycles,* 20. doi: https://doi.org/10.1029/2005GB002567

SOUTY-GROSSET, C., HOLDICH, D. M., NÖEL, P. Y., REYNOLDS, J. & HAFFNER, P. H. 2006. *Atlas of Crayfish in Europe.* ed.

STUMM, W. & MORGAN, J. 1996. *Aquatic Chemistry: Chemical Equilibria and Rates in Natural Waters.* 3rd ed. New York, John Wiley & Sons.

SVOBODOVÁ, J., DOUDA, K., FISCHER, D., LAPŠANSKÁ, N. & VLACH, P. 2017. Toxic and heavy metals as a cause of crayfish mass mortality from acidified headwater streams. *Ecotoxicology,* 26**,** 261-270. doi: 10.1007/s10646-017-1760-0

TANK, S. E., LESACK, L. F. W. & MCQUEEN, D. J. 2009. Elevated pH regulates bacterial carbon cycling in lakes with high photosynthetic activity. *Ecology,* 90**,** 1910-1922. doi: https://doi.org/10.1890/08-1010.1

TONG, Y., LI, J., QI, M., ZHANG, X., WANG, M., LIU, X., ZHANG, W., WANG, X., LU, Y. & LIN, Y. 2019. Impacts of water residence time on nitrogen budget of lakes and reservoirs. *Science of The Total Environment,* 646**,** 75-83. doi: https://doi.org/10.1016/j.scitotenv.2018.07.255

USIO, N. 2000. Effects of crayfish on leaf processing and invertebrate colonisation of leaves in a headwater stream: decoupling of a trophic cascade. *Oecologia,* 124**,** 608-614. doi: 10.1007/s004420000422

VUORI, K.-M. 1995. Direct and indirect effects of iron on river ecosystems. *Annales Zoologici Fennici,* 32**,** 317-329. doi:

VUORINEN, P. J., KEINÄNEN, M., PEURANEN, S. & TIGERSTEDT, C. 1999. Effects of iron, aluminium, dissolved humic material and acidity on grayling (Thymallus thymallus) in laboratory exposures, and a comparison of sensitivity with brown trout (Salmo trutta). *BOREAL ENVIRONMENT RESEARCH,* 3**,** 405–419. doi:

WAITE, T. D. & MOREL, F. M. M. 1984. Photoreductive dissolution of colloidal iron oxides in natural waters. *Environmental Science & Technology,* 18**,** 860-868. doi: 10.1021/es00129a010

WARD, R. J. S., MCCROHAN, C. R. & WHITE, K. N. 2006. Influence of aqueous aluminium on the immune system of the freshwater crayfish Pacifasticus leniusculus. *Aquatic Toxicology,* 77**,** 222-228. doi: 10.1016/j.aquatox.2005.12.006

WARREN, L. A. & HAACK, E. A. 2001. Biogeochemical controls on metal behaviour in freshwater environments. *Earth-Science Reviews,* 54**,** 261-320. doi: https://doi.org/10.1016/S0012-8252(01)00032-0

WEBER, T., ALLARD, T., TIPPING, E. & BENEDETTI, M. F. 2006. Modeling Iron Binding to Organic Matter. *Environmental Science & Technology,* 40**,** 7488-7493. doi: 10.1021/es0607077

WEYHENMEYER, G. A., PRAIRIE, Y. T. & TRANVIK, L. J. 2014. Browning of Boreal Freshwaters Coupled to Carbon-Iron Interactions along the Aquatic Continuum. *PLOS ONE,* 9**,** e88104. doi: 10.1371/journal.pone.0088104

XIAO, Y. & RIISE, G. 2021. Coupling between increased lake color and iron in boreal lakes. *Science of The Total Environment,* 767**,** 145104. doi: https://doi.org/10.1016/j.scitotenv.2021.145104

ÅTLAND, Å., KROGLUND, F. & RØYSET, O. 2003. Avgiftning av jern ved dosering av flytende silikat - en pilotstudie. Oslo: Norsk institutt for vannforskning (NIVA). doi:

Online Resources

Artsdatabanken. 2021. *Edelkreps Astacus astacus (Linnaeus, 1758)*. Available at: https://artsdatabanken.no/lister/rodlisteforarter/2021/4463 [Accessed 14.02.2021].

IUCN. 2010. *IUCN Red List of Threatened Species: Noble Crayfish*. Available at: https://www.iucnredlist.org/species/2191/9338388 [Accessed 14.02.2022].

Kartverket. 2021. *Norgeskart*. Available at: https://www.norgeskart.no/#!?project=norgeskart&layers=1002&zoom=3&lat=7197864.00&lon=396722.00 [Accessed 13.04.2021].

Miljødirektoratet. 2020. *Edelkreps*. Available at: https://miljostatus.miljodirektoratet.no/Edelkreps/ [Accessed 14.02.2022].

Norges Geologiske Undersøkelse (NGU). 2021. *Kart på nett*. Available at: https://www.ngu.no/emne/kart-pa-nett [Accessed 12.11.2021].

Norges vassdrags- og energidirektorat (NVE). 2021a. *Vassdrag - Innsjødatabase*. Available at: https://temakart.nve.no/link/?link=innsjodatabase [Accessed 15.11.2021].

Norges vassdrags- og energidirektorat (NVE). 2021b. *NEVINA Nedbørsfelt-Vannføring-INdeks-Analyse*. Available at: https://nevina.nve.no/ [Accessed 15.11.2021].

Norges vassdrags- og energidirektorat (NVE). 2021c. *SeNorge*. Available at: http://retro.senorge.no/ [Accessed 09.05.2022].

The Norwegian Meteorological Institute. 2021. *Seklima*. Available at: https://seklima.met.no/ [Accessed 15.01.2022].

Vann-nett. 2021. *Ulverudåa*. Available at: https://www.vann-nett.no/portal/#/waterbody/002-3656-R [Accessed 15.11.2021].

Vannområdet Øyeren. n.d. *Om vannområdet*. Available at: http://xn--vo-yeren-74a.no/om-vannomradet [Accessed 12.11.2021].

APPENDIX A

Raw data from samples taken between May – September 2021.

		Total	Filtered	Total	Filtered	Total	Filtered	Total	Filtered	Total	Filtered	Total	Filtered	Total	Filtered	Total	Filtered	Total	Filtered
Date	**Depth**	**Fe**	**Fe**	**Al**	**Al**	**Ca**	**Ca**	**K**	**K**	**Mg**	**Mg**	**Mn**	**Mn**	**Na**	**Na**	**S**	**S**	**Si**	**Si**
	m	**mg/L**	**mg/L**	**mg/L**	**mg/L**	**mg/L**	**mg/L**	**mg/L**	**mg/L**	**mg/L**	**mg/L**	**mg/L**	**mg/L**	**mg/L**	**mg/L**	**mg/L**	**mg/L**	**mg/L**	**mg/L**
05.05.21	**0.5**	0.27	0.16	0.34	0.29	1.4	1.5	0.22	0.15	0.38	0.38	0.016	0.016	1.7	1.6	0.56	0.55	1.4	1.2
05.05.21	**1**	0.27	0.17	0.33	0.28	1.4	1.6	0.21	0.19	0.38	0.40	0.016	0.016	1.7	1.9	0.58	0.66	1.4	1.2
05.05.21	**2**	0.29	0.17	0.35	0.29	1.5	1.5	0.22	0.14	0.39	0.38	0.016	0.016	1.7	1.6	0.59	0.55	1.5	1.2
05.05.21	**3**	0.26	0.17	0.32	0.29	1.4	1.5	0.21	0.14	0.37	0.38	0.015	0.016	1.7	1.6	0.56	0.53	1.3	1.2
19.05.21	**0.5**	0.32	0.20	0.42	0.30	1.8	1.6	0.30	0.16	0.47	0.40	0.016	0.013	1.9	1.6	0.64	0.58	1.6	1.2
19.05.21	**1**	0.31	0.21	0.39	0.31	1.6	1.6	0.30	0.16	0.43	0.40	0.015	0.014	1.8	1.7	0.61	0.56	2.2	1.2
19.05.21	**2**	0.35	0.23	0.42	0.31	1.6	1.5	0.26	0.15	0.43	0.38	0.016	0.014	1.8	1.6	0.62	0.53	1.6	1.3
19.05.21	**3**	0.51	0.26	0.60	0.34	2.6	2.2	0.46	0.24	0.64	0.51	0.017	0.012	2.4	2.1	0.77	0.83	2.1	1.4
02.06.21	**0.5**	0.31	0.19	0.42	0.32	1.8	1.6	0.26	0.15	0.45	0.41	0.016	0.014	1.9	1.7	0.61	0.56	1.4	1.1
02.06.21	**1**	0.33	0.19	0.42	0.32	1.9	1.6	0.26	0.15	0.47	0.41	0.017	0.014	2	1.7	0.64	0.55	1.6	1.1
02.06.21	**2**	0.32	0.20	0.40	0.32	1.8	1.7	0.26	0.16	0.45	0.42	0.014	0.013	1.9	1.7	0.60	0.55	1.4	1
02.06.21	**3**	0.44	0.27	0.43	0.33	1.9	1.8	0.29	0.18	0.48	0.45	0.013	0.012	2.0	1.8	0.62	0.57	1.3	1
16.06.21	**0.5**	0.34	0.21	0.38	0.29	1.8	1.6	0.27	0.16	0.47	0.42	0.020	0.016	2	1.7	0.63	0.54	1.1	0.79
16.06.21	**1**	0.39	0.21	0.43	0.28	2.0	1.6	0.27	0.17	0.52	0.42	0.021	0.016	2.2	1.7	0.66	0.53	1.1	0.79
16.06.21	**2**	0.33	0.22	0.35	0.29	1.7	1.6	0.24	0.16	0.44	0.42	0.018	0.017	1.9	1.8	0.58	0.56	0.96	0.79
16.06.21	**3**	0.59	0.33	0.42	0.33	1.8	1.8	0.28	0.18	0.48	0.46	0.020	0.018	2.1	1.9	0.62	0.57	0.87	0.67
30.06.21	**0.5**	0.32	0.18	0.31	0.27	1.6	1.7	0.23	0.16	0.41	0.43	0.018	0.017	1.8	1.8	0.58	0.54	0.79	0.64
30.06.21	**1**	0.34	0.19	0.31	0.26	1.7	1.7	0.23	0.16	0.43	0.43	0.019	0.017	1.9	1.8	0.57	0.57	0.83	0.64
30.06.21	**2**	0.33	0.19	0.30	0.27	1.6	1.7	0.22	0.18	0.41	0.43	0.019	0.018	1.8	1.8	0.56	0.54	0.74	0.63
30.06.21	**3**	1.00	0.35	0.48	0.32	2.0	1.8	0.33	0.19	0.54	0.49	0.056	0.046	2.4	2.1	0.66	0.59	0.81	0.52
14.07.21	**0.5**	0.38	0.26	0.29	0.24	1.7	1.7	0.27	0.14	0.44	0.44	0.020	0.015	2.0	1.9	0.58	0.54	0.62	0.44
14.07.21	**1**	0.39	0.26	0.28	0.26	1.7	1.7	0.24	0.14	0.45	0.44	0.020	0.015	2.0	1.9	0.58	0.53	0.63	0.44
14.07.21	**2**	0.40	0.27	0.31	0.26	1.7	1.7	0.25	0.14	0.45	0.43	0.021	0.016	2.0	2.0	0.59	0.53	0.61	0.44
14.07.21	**3**	1.10	0.85	0.41	0.37	1.8	1.9	0.28	0.19	0.48	0.49	0.055	0.055	2.2	2.5	0.58	0.57	0.49	0.32
28.07.21	**0.5**	0.43	0.27	0.27	0.19	1.9	1.7	0.28	0.15	0.50	0.44	0.017	0.005	2.1	2.5	0.62	0.53	0.53	0.36
28.07.21	**1**	0.38	0.27	0.23	0.19	1.7	1.7	0.23	0.15	0.44	0.45	0.014	0.004	1.9	2.0	0.56	0.54	0.79	0.35
28.07.21	**2**	0.38	0.27	0.28	0.19	1.7	1.8	0.26	0.15	0.45	0.46	0.014	0.004	2.0	2.0	0.57	0.55	0.87	0.36
28.07.21	**3**	0.51	0.37	0.25	0.22	1.7	1.8	0.26	0.17	0.46	0.47	0.020	0.009	2.0	2.1	0.57	0.57	0.78	0.32
11.08.21	**0.5**	0.43	0.30	0.29	0.25	1.8	1.9	0.25	0.16	0.47	0.48	0.015	0.009	2.0	2.1	0.59	0.57	0.81	0.65
11.08.21	**1**	0.48	0.31	0.32	0.24	2.0	1.9	0.26	0.15	0.52	0.47	0.017	0.009	2.2	2.0	0.63	0.56	0.87	0.66
11.08.21	**2**	0.51	0.30	0.33	0.24	2.1	1.9	0.29	0.15	0.55	0.48	0.018	0.009	2.3	2.1	0.65	0.54	0.86	0.64
11.08.21	**3**	0.63	0.44	0.32	0.27	1.9	1.9	0.24	0.18	0.50	0.49	0.025	0.019	2.1	2.1	0.60	0.56	0.75	0.61
01.09.21	**0.5**	0.60	0.30	0.36	0.21	2.3	1.9	0.31	0.15	0.60	0.49	0.017	0.011	2.6	2.0	0.68	0.56	0.77	0.48
01.09.21	**1**	0.50	0.26	0.28	0.20	1.9	1.9	0.25	0.15	0.51	0.48	0.015	0.010	2.2	2.0	0.63	0.57	0.66	0.47
01.09.21	**2**	0.60	0.27	0.37	0.20	2.3	1.9	0.29	0.15	0.60	0.49	0.019	0.011	2.6	2.0	0.69	0.58	0.78	0.47
01.09.21	**3**	0.59	0.36	0.34	0.23	2.2	1.9	0.27	0.17	0.57	0.49	0.017	0.011	2.5	2.1	0.68	0.57	0.7	0.47

Date	Depth	Conductivity	Temperature	O_2*	O_2 saturation*	pH	Alk corr.	Turbidity	OD245	OD410	Colour	DOC	Tot-P	Tot-N	PO_4-P	NH_4-N	NO_3-N	Cl^-	SO_4^{2-}
	m	µS/cm	°C	mg/L	%		mmol/L	FNU			mg Pt/L	mg/L	µg/L	mg/L	µg/L	mg/L	mg/L	mg/L	mg/L
05.05.21	**0.5**	19.00	8.669	10.86	97.2	6.13	0.0416	1.62	0.424	0.215	80.827	10.18	6.68	0.378	0.689	0.017081	0.03	1.7	1.3
05.05.21	**1**	19.00	8.578	10.85	97.0	5.99	0.0369	1.17	0.429	0.217	81.579	10.29	7.16	0.368	1.61	0.01978	0.03	1.9	1.7
05.05.21	**2**	19.00	8.461	10.86	96.9	5.91	0.0512	1.11	0.433	0.216	81.203	10.20	6.88	0.336	1.44	0.015301	0.03	1.7	1.4
05.05.21	**3**	19.10	8.379	10.86	96.8	5.94	0.0504	0.98	0.421	0.216	81.203	10.10	7.88	0.368	1.669	0.015826	0.03	1.7	1.3
19.05.21	**0.5**	20.20	12.479	9.95	94.6	5.99	0.0546	1.66	0.432	0.222	83.400	10.79	10.48	0.347	1.146	0.016931	0.05	1.7	1.4
19.05.21	**1**	19.90	11.879	9.99	94.5	5.94	0.05	1.63	0.440	0.228	85.660	11.15	12.30	0.420	1.116	0.013614	0.06	1.7	1.4
19.05.21	**2**	20.70	10.408	10	92.8	5.9	0.0502	2.00	0.488	0.255	95.800	11.97	7.44	0.368	2.744	0.016913	0.05	1.7	1.4
19.05.21	**3**	22.80	9.084	9.08	81.3	5.9	0.0683	2.63	0.464	0.238	89.410	11.58	8.97	0.525	1.543	0.01933	0.12	2.1	2.1
02.06.21	**0.5**	20.40	19.977	8.84	96.1	5.88	0.0516	1.26	0.481	0.256	97.710	12.21	6.11	0.368	1.558	0.016107	0.02	1.7	1.4
02.06.21	**1**	20.40	19.176	8.85	95.6	5.79	0.0546	1.17	0.485	0.253	96.560	11.88	8.68	0.410	0.667	0.008517	0.02	1.7	1.4
02.06.21	**2**	20.60	15.391	8.77	88.2	5.83	0.0579	1.14	0.483	0.253	96.560	11.74	8.69	0.420	0.615	0.01309	0.03	1.7	1.3
02.06.21	**3**	22.70	10.771	4.4	46.8	5.77	0.0633	1.67	0.474	0.247	94.270	11.63	9.18	0.389	1.138	0.014683	0.05	1.8	1.4
16.06.21	**0.5**	20.80	19.125	8.43	91.3	6.13	0.0613	1.04	0.487	0.239	93.730	11.84	8.36	0.357	1.109	0.024503	<0.02	1.8	1.3
16.06.21	**1**	20.80	19.000	8.28	90.3	6.13	0.0608	0.99	0.480	0.242	94.900	10.59	7.65	0.347	-0.232	0.008386	<0.02	1.8	1.3
16.06.21	**2**	21.00	18.203	8.02	85.6	6.1	0.0604	1.31	0.479	0.245	96.080	10.58	8.43	0.368	0.335	0.008273	<0.02	1.8	1.4
16.06.21	**3**	25.60	12.033	3.80	35.8	5.86	0.0658	1.28	0.479	0.249	97.650	10.66	8.08	0.347	0.63	0.014514	0.03	2.1	1.4
30.06.21	**0.5**	21.30	21.779	8.12	93.0	6.31	0.0625	1.40	0.431	0.216	81.200	10.63	8.74	0.420	0.181	0.015882	<0.02	1.9	1.4
30.06.21	**1**	21.20	21.464	8.11	92.9	6.27	0.0604	1.11	0.428	0.215	80.830	11.36	8.24	0.410	-0.151	0.010128	<0.02	1.8	1.3
30.06.21	**2**	21.30	20.258	7.92	89.6	6.31	0.0608	1.42	0.435	0.22	82.710	10.01	7.90	0.389	-0.394	0.01011	<0.02	1.9	1.4
30.06.21	**3**	26.00	14.031	1.62	16.6	5.95	0.0725	1.78	0.452	0.236	88.720	10.34	12.27	0.389	0.077	0.022048	0.03	2.3	1.5
14.07.21	**0.5**	21.60	23.900	7.86	94.0	6.37	0.0596	1.36	0.411	0.202	75.370	10.01	7.05	0.420	1.234	0.007149	<0.02	1.9	1.3
14.07.21	**1**	21.70	22.892	7.84	93.0	6.35	0.0629	1.55	0.417	0.203	75.750	9.63	7.14	0.336	0.21	0.008873	<0.02	1.9	1.3
14.07.21	**2**	21.80	21.235	7.41	85.8	6.25	0.0613	1.59	0.419	0.206	76.870	9.99	6.18	0.368	-0.365	0.007036	<0.02	1.9	1.3
14.07.21	**3**	27.10	15.356	2.94	35.2	5.97	0.0764	1.76	0.499	0.269	100.370	10.28	10.90	0.410	0.998	0.022179	0.02	2.6	1.4
28.07.21	**0.5**	22.40	22.125	7.46	87.5	6.3	0.0665	1.25	0.382	0.182	68.420	10.26	7.83	0.368	0.077	0.013614	<0.02	2.3	1.3
28.07.21	**1**	22.40	22.046	7.50	87.7	6.33	0.0627	1.26	0.385	0.182	68.420	8.74	7.65	0.294	0.099	0.012415	<0.02	2	1.3
28.07.21	**2**	22.90	16.611	6.56	74.0	6.37	0.0692	1.14	0.388	0.183	68.800	8.93	8.13	0.368	-0.453	0.010841	<0.02	2	1.3
28.07.21	**3**	28.40	16.611	1.81	18.0	6.21	0.07	1.33	0.402	0.195	73.310	8.96	7.96	0.347	-0.07	0.015376	<0.02	2	1.4
11.08.21	**0.5**	22.76	19.692	*	*	6.3	0.0671	1.27	0.466	0.217	80.370	10.30	7.64	0.347	-0.21	0.01129	<0.02	2	1.4
11.08.21	**1**	22.66	19.119	*	*	6.3	0.0708	1.29	0.455	0.223	82.590	10.17	7.13	0.368	-0.357	0.010897	<0.02	2	1.4
11.08.21	**2**	22.63	18.792	*	*	6.28	0.0683	1.16	0.447	0.219	81.110	11.15	6.79	0.431	-0.085	0.011497	<0.02	2	1.4
11.08.21	**3**	23.76	16.788	*	*	6.06	0.0721	1.31	0.467	0.235	87.040	10.24	7.95	0.389	-0.21	0.020005	<0.02	2.1	1.4
01.09.21	**0.5**	26.00	18.701	8.73	91.0	6.5	0.0708	1.21	0.410	0.198	73.880	10.30	9.28	0.410	0.018	0.013446	<0.02	2.1	1.4
01.09.21	**1**	28.00	18.706	8.78	90.8	6.31	0.0845	1.24	0.414	0.195	72.760	10.13	8.49	0.326	0.262	0.009979	<0.02	2.1	1.4
01.09.21	**2**	25.50	18.400	8.64	89.2	6.25	0.0897	1.15	0.419	0.198	73.880	10.97	6.58	0.410	0.085	0.010091	<0.02	2.1	1.4
01.09.21	**3**	26.20	18.266	7.90	53.9	6.2	0.16	1.10	0.432	0.21	78.360	10.03	6.34	0.347	0.21	0.009716	<0.02	2.2	1.4

* O_2 samples were taken at 3.5 m on the 16th and 30th of June with an oxygen saturation (%) of 1.1 and 0.8, respectively.

APPENDIX B

LOD and LOQ of filtered samples.

	Al (µg/L)	Ca (mg/L)	Fe (µg/L)	K (mg/L)	Mg (mg/L)	Mn (µg/L)	Na (mg/L)	S (mg/L)	Si (mg/L)
LOD	24.44975397	0.067323469	2.400948214	0	0	2.187409862	0.427077284	0.106904497	0.262261953
LOQ	24.44975397	0.067323469	2.400948214	0	0	2.18741	0.427077	0.106904	0.262262

LOD and LOQ of unfiltered samples.

	Al (µg/L)	Ca (mg/L)	Fe (µg/L)	K (mg/L)	Mg (mg/L)	Mn (µg/L)	Na (mg/L)	S (mg/L)	Si (mg/L)
LOD	0.895991071	0.009165151	3.00813896	0.018	0	0.337194306	0.018	0.01698089	0.034641016
LOQ	2.986636905	0.030550505	10.02712987	0.06	0	1.12398102	0.06	0.056602968	0.115470054

APPENDIX C

Principal Component Analysis (PCA) 0.5 m

Eigenvectors

Variable	PC1	PC2	PC3	PC4	PC5	PC6	PC7	PC8	PC9	PC10	PC11	PC12
Fe F	0,244	0,067	0,047	0,099	0,177	-0,237	-0,183	-0,172	0,279	-0,091	-0,256	0,237
Fe P	0,249	-0,014	-0,026	0,063	-0,488	0,179	-0,087	0,367	-0,038	0,099	-0,200	0,118
Temp	0,182	-0,229	0,244	-0,049	0,033	-0,081	0,350	0,004	0,215	0,210	-0,234	0,128
O_2	-0,210	-0,181	0,161	-0,149	-0,462	-0,084	0,094	-0,058	0,216	0,186	0,323	0,119
Cond	0,245	-0,058	-0,236	-0,118	-0,025	-0,205	0,132	0,042	0,453	0,182	0,046	-0,263
Colour	0,146	-0,272	0,016	0,066	-0,038	0,540	-0,329	-0,354	0,247	-0,311	0,146	-0,020
Turb	-0,095	0,310	0,128	0,097	-0,120	-0,113	-0,135	0,104	0,275	-0,223	-0,325	-0,362
DOC	0,175	-0,239	-0,088	0,093	-0,277	0,032	-0,087	-0,056	0,015	0,312	-0,355	0,027
Tot-P	0,107	0,303	0,018	0,218	0,201	-0,018	-0,138	0,073	0,165	0,390	0,397	0,239
Mn F	-0,239	-0,096	0,054	0,215	-0,206	-0,118	-0,321	-0,055	-0,110	0,168	-0,006	0,086
Mn P	0,239	0,096	-0,278	0,073	-0,092	-0,159	0,111	-0,058	-0,193	-0,207	-0,041	-0,025
Al F	0,181	-0,230	-0,202	-0,067	0,282	0,121	-0,107	-0,023	0,276	0,158	0,106	-0,236
Al P	0,242	0,079	-0,097	-0,071	0,164	0,337	0,365	0,005	-0,222	0,150	-0,019	0,265
S F	0,195	0,208	0,019	-0,175	-0,087	0,119	-0,108	0,361	0,105	-0,206	0,146	0,121
S P	0,247	0,049	0,158	-0,288	-0,082	-0,087	-0,391	-0,084	-0,306	0,297	0,221	-0,248
Cl-	-0,134	-0,283	-0,047	-0,307	0,003	-0,215	0,048	-0,143	0,012	-0,072	-0,079	0,165
Tot-N	-0,195	-0,208	0,171	0,325	0,046	0,185	0,254	0,397	0,089	-0,050	0,187	-0,241
NH_4-N	-0,146	0,272	-0,244	0,050	-0,302	0,184	0,090	-0,180	0,312	-0,048	0,076	0,322
pH	-0,219	0,160	0,005	0,003	0,162	-0,194	-0,118	0,111	0,225	0,140	0,009	0,155
Alk	0,245	0,060	0,072	0,154	-0,262	-0,286	0,329	-0,302	-0,027	-0,187	0,378	-0,205
SO_4^{2-}	0,249	-0,014	-0,303	0,025	-0,104	-0,153	-0,103	0,315	-0,010	-0,130	0,124	0,000
Si F	-0,115	0,297	-0,058	-0,083	-0,077	0,306	0,130	-0,128	0,048	0,340	-0,154	-0,413
Si P	0,221	0,155	0,638	-0,317	-0,010	0,077	0,030	0,049	0,117	-0,124	-0,020	0,064
PO_4-P	0,214	-0,171	0,261	0,557	0,054	-0,062	-0,048	0,011	-0,032	0,065	0,004	0,021
NO_3-N	0,093	0,311	0,097	0,241	-0,060	0,040	0,076	-0,330	-0,070	0,090	-0,099	-0,010

Variable	PC13	PC14	PC15	PC16	PC17	PC18	PC19	PC20	PC21	PC22	PC23	PC24	PC25
Fe F	0,018	0,356	-0,188	0,134	-0,066	-0,171	0,093	0,021	-0,327	0,268	-0,272	0,099	0,284
Fe P	-0,283	0,303	0,143	0,018	-0,133	0,173	-0,023	0,212	0,336	0,046	-0,190	-0,020	0,136
Temp	0,236	-0,214	-0,064	0,105	0,285	-0,064	0,101	-0,213	0,423	-0,172	-0,053	0,099	0,287
O_2	-0,370	0,050	0,014	-0,084	0,273	-0,259	0,044	-0,176	-0,244	0,131	-0,064	0,182	-0,083
Cond	0,088	0,088	0,314	0,393	-0,092	-0,103	-0,167	0,220	-0,048	0,011	0,292	-0,015	-0,209
Colour	0,085	-0,068	0,378	0,043	0,092	0,001	0,082	-0,075	0,036	-0,033	-0,040	-0,010	0,114
Turb	-0,082	-0,289	0,129	-0,303	0,099	-0,157	-0,422	-0,032	0,015	0,013	-0,085	0,125	0,123
DOC	0,105	-0,296	-0,068	-0,280	-0,107	0,206	0,104	-0,061	-0,441	0,051	0,287	-0,225	0,060
Tot-P	0,069	0,077	0,180	-0,205	0,037	0,214	-0,264	-0,306	0,103	0,178	0,105	-0,129	0,153
Mn F	0,300	0,062	-0,015	0,066	-0,154	-0,595	-0,085	0,024	0,209	-0,092	0,001	-0,371	-0,028
Mn P	-0,076	-0,235	0,133	0,021	0,042	-0,182	0,252	-0,295	0,243	0,599	0,009	-0,109	-0,161
Al F	-0,300	-0,019	-0,451	-0,361	-0,024	-0,158	0,031	0,139	0,256	0,024	-0,119	-0,171	-0,118
Al P	-0,042	-0,173	0,226	-0,132	-0,088	-0,439	-0,259	0,191	-0,234	-0,037	-0,203	0,041	0,033
S F	0,232	0,062	-0,142	-0,252	-0,103	-0,292	0,300	-0,005	0,009	-0,085	0,456	0,297	0,066
S P	0,175	-0,273	-0,078	0,145	0,073	0,035	-0,026	0,244	0,011	0,191	-0,169	0,280	0,142
Cl-	0,367	0,224	0,233	-0,500	-0,066	0,138	-0,137	0,168	0,161	0,221	-0,098	0,157	-0,171
Tot-N	0,286	-0,004	-0,050	0,010	0,076	0,008	0,085	0,264	-0,146	0,436	-0,098	-0,095	0,159
NH_4-N	0,227	-0,294	-0,384	0,157	-0,116	0,158	-0,127	0,169	0,101	0,086	-0,148	0,093	-0,163
pH	-0,125	-0,327	0,372	-0,082	-0,132	0,026	0,558	0,270	0,013	-0,124	-0,232	-0,054	-0,004
Alk	0,023	0,020	-0,012	-0,205	-0,335	0,047	0,067	0,072	0,001	-0,233	-0,100	-0,133	0,296
SO_4^{2-}	0,280	0,027	-0,007	-0,061	0,424	0,045	0,012	-0,130	-0,212	-0,316	-0,415	-0,161	-0,212
Si F	0,232	0,292	0,046	-0,065	-0,163	-0,044	0,268	-0,323	-0,030	-0,012	-0,258	0,110	-0,112
Si P	0,032	-0,031	-0,040	0,031	-0,104	0,060	-0,017	-0,032	-0,049	0,091	-0,078	-0,447	-0,375
PO_4-P	-0,009	-0,060	0,004	-0,035	-0,199	0,006	-0,001	-0,056	0,020	-0,086	-0,062	0,458	-0,512
NO_3-N	0,008	0,203	0,014	-0,153	0,568	-0,020	0,160	0,439	0,063	-0,008	0,223	-0,074	-0,136

Eigenanalysis of the correlation matrix

Eigenvalue	16,094	8,906	0,000	0,000	0,000	0,000	0,000	0,000	0,000	0,000	0,000
Proportion	0,644	0,356	0,000	0,000	0,000	0,000	0,000	0,000	0,000	0,000	0,000
Cumulative	0,644	1,000	1,000	1,000	1,000	1,000	1,000	1,000	1,000	1,000	1,000
Eigenvalue	0,000	0,000	0,000	-0,000	-0,000	-0,000	-0,000	-0,000	-0,000	-0,000	
Proportion	0,000	0,000	0,000	-0,000	-0,000	-0,000	-0,000	-0,000	-0,000	-0,000	
Cumulative	1,000	1,000	1,000	1,000	1,000	1,000	1,000	1,000	1,000	1,000	
Eigenvalue	-0,000	-0,000	-0,000	-0,000							
Proportion	-0,000	-0,000	-0,000	-0,000							
Cumulative	1,000	1,000	1,000	1,000							

Principal Component Analysis (PCA) 1 m

Eigenvectors

Variable	PC1	PC2	PC3	PC4	PC5	PC6	PC7	PC8	PC9	PC10	PC11	PC12
Fe F	0,163	-0,277	0,225	0,083	-0,262	-0,098	0,023	0,431	0,040	0,227	0,013	0,130
Fe P	0,167	0,270	-0,010	0,132	-0,210	0,018	-0,145	-0,002	0,089	-0,074	-0,326	0,390
Temp	0,209	0,173	-0,055	0,268	0,243	0,204	0,071	0,108	0,251	0,286	0,122	-0,141
O_2	-0,178	0,250	0,379	-0,315	0,135	0,087	-0,292	0,330	0,076	0,196	-0,047	0,098
Cond	0,233	0,033	0,188	0,230	0,056	0,342	-0,119	0,059	-0,005	-0,179	-0,219	-0,305
Colour	0,204	0,187	0,008	-0,169	-0,011	0,285	0,229	0,218	-0,091	0,137	0,270	-0,219
Turb	0,058	-0,375	-0,308	-0,091	0,485	0,072	-0,276	0,247	0,138	0,078	-0,282	0,089
DOC	0,229	0,078	-0,214	-0,351	-0,149	-0,011	0,014	-0,070	0,324	-0,105	-0,161	0,217
Tot-P	0,120	-0,331	-0,219	0,234	-0,227	-0,128	-0,036	0,253	0,019	-0,276	0,288	-0,039
Mn F	-0,225	0,105	0,057	-0,083	0,135	0,187	0,188	-0,040	0,402	-0,098	0,114	0,022
Mn P	0,212	0,164	-0,056	0,126	-0,044	0,195	0,381	0,103	-0,304	0,157	-0,017	0,313
Al F	0,234	-0,012	-0,022	-0,339	0,023	0,351	-0,004	0,182	0,080	-0,503	0,172	-0,048
Al P	0,232	0,052	0,055	-0,037	-0,159	-0,147	0,032	0,113	0,181	-0,005	0,140	0,231
S F	-0,229	0,074	0,166	0,284	0,061	0,095	-0,380	-0,112	0,072	-0,136	0,393	0,121
S P	0,233	-0,018	-0,165	-0,157	-0,011	0,035	-0,313	-0,249	-0,028	0,207	0,541	0,143
Cl-	-0,225	0,105	0,039	0,168	0,126	-0,108	0,293	0,228	-0,000	-0,420	0,057	0,025
Tot-N	0,209	-0,173	0,170	-0,102	-0,105	0,208	0,039	-0,502	-0,110	-0,052	-0,161	-0,162
NH_4-N	-0,229	-0,075	0,049	0,155	-0,043	0,358	0,165	-0,161	0,186	0,068	0,030	0,339
pH	-0,202	-0,196	-0,027	-0,270	0,009	-0,098	0,338	0,002	0,096	0,288	0,110	-0,181
Alk	0,234	-0,008	0,195	-0,102	0,582	-0,291	0,208	-0,140	-0,209	-0,182	0,120	0,336
SO_4^{2-}	-0,225	0,105	-0,128	-0,190	-0,074	0,198	-0,179	0,175	-0,607	-0,031	0,008	0,102
Si F	-0,167	-0,270	0,009	0,026	-0,081	0,307	0,110	-0,019	0,030	0,042	0,024	0,324
Si P	0,138	-0,313	0,648	-0,073	-0,050	-0,028	-0,030	0,007	-0,009	-0,021	0,021	0,027
PO_4-P	-0,228	-0,085	0,000	-0,319	-0,217	-0,005	0,040	0,001	0,042	-0,163	-0,014	0,015
NO_3-N	-0,037	-0,382	-0,077	0,062	0,137	0,285	0,032	-0,001	-0,138	0,021	-0,025	0,101

Variable	PC13	PC14	PC15	PC16	PC17	PC18	PC19	PC20	PC21	PC22	PC23	PC24	PC25
Fe F	-0,150	0,059	-0,303	0,261	-0,161	0,091	-0,131	0,017	-0,043	-0,286	0,067	-0,274	-0,322
Fe P	-0,062	-0,329	0,024	-0,015	-0,031	0,203	-0,314	0,183	-0,261	0,279	0,315	0,094	0,052
Temp	-0,444	-0,030	0,069	0,154	-0,299	-0,173	0,108	0,113	-0,008	0,095	-0,087	0,405	-0,064
O_2	-0,067	-0,015	0,010	-0,156	0,330	-0,167	0,210	0,326	0,073	0,172	-0,084	-0,120	-0,117
Cond	0,039	0,224	0,219	-0,068	0,175	0,427	0,304	-0,121	-0,213	-0,118	0,142	-0,038	-0,199
Colour	0,134	-0,175	0,186	0,004	0,193	0,262	-0,547	-0,005	0,136	-0,028	-0,231	-0,033	0,061
Turb	0,222	-0,240	-0,030	-0,180	-0,025	0,026	-0,106	-0,016	-0,006	-0,285	-0,042	0,162	0,008
DOC	-0,091	0,151	0,106	0,337	0,019	0,294	0,248	0,170	0,368	-0,169	-0,159	-0,006	0,185
Tot-P	-0,246	-0,287	-0,020	-0,087	0,485	0,006	0,197	0,092	0,043	0,150	-0,073	0,106	0,065
Mn F	0,051	-0,182	-0,197	0,415	0,325	-0,129	0,024	-0,205	-0,405	-0,205	0,131	-0,027	0,133
Mn P	0,391	-0,036	-0,208	-0,035	0,148	-0,152	0,317	0,033	0,193	-0,111	0,203	0,243	-0,058
Al F	-0,039	-0,005	-0,234	-0,167	-0,346	-0,202	0,019	-0,103	0,092	0,197	0,237	-0,149	-0,017
Al P	0,315	-0,151	0,384	-0,098	-0,218	-0,150	0,234	-0,213	-0,358	0,047	-0,416	-0,092	-0,108
S F	0,265	-0,293	0,048	0,226	-0,185	0,199	0,056	0,008	0,379	-0,059	0,055	0,021	-0,186
S P	0,027	0,292	-0,062	-0,147	0,069	0,073	-0,026	0,256	-0,333	-0,187	0,195	0,057	0,035
Cl-	0,064	0,131	0,108	-0,101	-0,178	0,029	-0,064	0,593	-0,157	-0,312	-0,065	0,021	0,071
Tot-N	-0,078	-0,422	-0,044	0,012	0,013	-0,220	0,027	0,357	-0,040	-0,226	-0,188	-0,088	-0,231
NH_4-N	-0,180	0,054	-0,321	-0,436	-0,035	0,300	0,024	-0,100	-0,000	0,021	-0,374	-0,068	0,046
pH	0,026	-0,322	0,115	-0,120	-0,205	0,381	0,297	0,140	-0,070	0,165	0,352	-0,055	-0,023
Alk	-0,266	-0,043	0,037	0,068	0,122	0,184	-0,027	-0,135	0,005	0,078	-0,007	-0,055	-0,227
SO_4^{2-}	-0,289	-0,190	0,044	0,195	-0,179	0,117	0,194	-0,129	-0,224	-0,178	-0,142	0,066	0,181
Si F	-0,217	0,096	0,619	-0,052	0,079	-0,260	-0,125	-0,075	0,144	-0,141	0,296	-0,099	-0,040
Si P	0,058	0,016	0,007	-0,003	-0,075	0,034	-0,018	-0,038	0,016	-0,027	0,018	0,402	0,526
PO_4-P	0,031	0,142	-0,008	0,027	0,051	0,073	-0,133	-0,057	-0,069	0,052	-0,070	0,631	-0,549
NO_3-N	0,242	0,213	0,004	0,425	-0,011	0,027	-0,014	0,275	-0,157	0,533	-0,175	-0,103	0,012

Eigenanalysis of the correlation matrix

Eigenvalue	18,310	6,690	0,000	0,000	0,000	0,000	0,000	0,000	0,000	0,000	0,000
Proportion	0,732	0,268	0,000	0,000	0,000	0,000	0,000	0,000	0,000	0,000	0,000
Cumulative	0,732	1,000	1,000	1,000	1,000	1,000	1,000	1,000	1,000	1,000	1,000
Eigenvalue	0,000	-0,000	-0,000	-0,000	-0,000	-0,000	-0,000	-0,000	-0,000	-0,000	
Proportion	0,000	-0,000	-0,000	-0,000	-0,000	-0,000	-0,000	-0,000	-0,000	-0,000	
Cumulative	1,000	1,000	1,000	1,000	1,000	1,000	1,000	1,000	1,000	1,000	
Eigenvalue	-0,000	-0,000	-0,000	-0,000							
Proportion	-0,000	-0,000	-0,000	-0,000							
Cumulative	1,000	1,000	1,000	1,000							

Principal Component Analysis (PCA) 2 m

Eigenvectors

Variable	PC1	PC2	PC3	PC4	PC5	PC6	PC7	PC8	PC9	PC10	PC11	PC12
Fe F	0,023	0,296	-0,157	0,102	0,038	0,045	-0,539	0,087	0,029	0,316	-0,016	0,101
Fe P	0,269	-0,025	-0,185	-0,062	0,195	-0,032	0,069	-0,287	-0,024	0,145	0,304	-0,121
Temp	0,265	0,057	0,086	0,045	0,143	-0,030	0,072	0,354	-0,076	0,219	0,412	0,207
O_2	-0,248	-0,118	0,106	0,153	0,393	-0,489	0,271	0,113	0,108	0,269	-0,125	0,218
Cond	0,142	0,253	-0,207	-0,042	-0,347	-0,123	0,190	0,160	-0,009	-0,132	0,033	0,536
Colour	0,164	0,237	-0,362	0,024	0,191	0,224	0,264	0,088	0,010	0,098	-0,053	-0,022
Turb	-0,108	0,273	0,068	-0,297	0,103	-0,102	0,429	-0,101	-0,177	-0,134	0,174	-0,098
DOC	0,127	0,263	0,083	0,520	-0,061	0,024	0,001	-0,134	0,035	-0,220	0,054	0,112
Tot-P	0,264	0,065	0,115	-0,128	0,202	0,044	-0,169	-0,000	0,008	0,233	0,082	0,261
Mn F	-0,218	-0,175	-0,187	-0,198	0,142	0,052	-0,195	0,120	-0,214	0,060	0,037	-0,123
Mn P	0,023	0,296	-0,001	-0,200	-0,074	-0,108	-0,032	-0,305	0,008	-0,136	0,233	0,040
Al F	0,218	0,175	-0,025	-0,009	-0,250	-0,415	-0,073	0,068	-0,193	-0,106	-0,230	-0,208
Al P	-0,008	0,297	0,090	0,209	0,591	0,095	-0,126	-0,080	0,080	-0,404	-0,080	-0,089
S F	0,115	-0,269	-0,117	0,147	-0,052	0,158	0,073	0,043	0,349	-0,000	0,243	-0,010
S P	-0,067	0,288	0,065	0,250	-0,196	-0,035	0,248	-0,026	0,166	0,475	0,133	-0,511
Cl-	-0,115	0,269	0,067	-0,336	0,066	0,022	-0,170	0,240	0,418	-0,069	0,207	-0,105
Tot-N	0,258	0,087	-0,042	0,008	0,223	0,135	0,212	0,317	-0,307	0,014	-0,317	-0,115
NH_4-N	-0,235	0,147	0,023	0,138	0,032	-0,077	-0,180	-0,298	-0,489	0,277	0,113	0,138
pH	-0,270	-0,009	0,143	0,120	-0,062	0,082	0,011	0,482	-0,278	-0,152	0,342	-0,035
Alk	0,265	-0,060	0,131	-0,280	-0,006	0,329	0,091	-0,153	-0,121	0,190	-0,165	0,034
SO_4^{2-}	-0,269	0,025	0,116	0,043	0,017	0,208	0,229	-0,207	0,199	0,125	-0,140	0,357
Si F	-0,247	0,121	0,083	0,105	-0,139	0,517	0,093	0,005	-0,184	-0,002	0,042	0,031
Si P	0,269	-0,025	0,760	-0,002	-0,062	0,013	-0,053	0,019	-0,007	0,032	-0,017	-0,022
PO_4-P	-0,200	0,200	0,138	-0,370	0,040	-0,033	0,006	-0,003	0,027	0,040	-0,023	0,054
NO_3-N	-0,115	0,269	0,017	-0,048	-0,109	0,069	-0,050	0,210	0,185	0,175	-0,404	0,003

Variable	PC13	PC14	PC15	PC16	PC17	PC18	PC19	PC20	PC21	PC22	PC23	PC24	PC25
Fe F	-0,092	0,279	-0,184	-0,152	-0,134	0,425	-0,068	0,188	0,177	0,029	0,189	-0,087	-0,087
Fe P	-0,261	-0,285	-0,461	-0,151	-0,126	-0,053	-0,280	-0,056	-0,235	0,287	-0,094	-0,049	0,012
Temp	0,116	-0,326	0,064	0,369	-0,086	0,064	0,056	-0,150	0,401	0,053	0,083	0,173	0,022
O_2	-0,115	0,111	-0,326	-0,058	0,066	-0,054	0,203	0,184	0,039	-0,156	-0,134	0,012	0,033
Cond	-0,102	0,109	-0,105	-0,030	-0,063	-0,394	-0,128	0,073	-0,091	-0,050	0,314	-0,210	-0,013
Colour	0,251	-0,086	0,040	-0,224	0,147	0,123	0,398	-0,213	-0,054	-0,081	-0,152	-0,442	-0,130
Turb	-0,162	0,152	0,261	-0,273	0,071	0,234	-0,159	0,215	0,366	0,191	0,051	-0,043	0,139
DOC	0,022	-0,207	0,015	-0,146	0,195	0,025	-0,311	0,182	0,152	-0,311	-0,393	0,105	-0,179
Tot-P	-0,258	0,188	0,495	-0,258	-0,133	-0,209	0,100	-0,069	-0,248	-0,054	-0,306	0,209	0,066
Mn F	-0,111	-0,003	0,048	0,084	-0,167	-0,323	-0,305	-0,041	0,329	-0,339	-0,252	-0,413	-0,021
Mn P	0,264	0,259	-0,170	0,423	-0,268	0,068	0,204	0,151	-0,090	-0,102	-0,384	-0,048	0,179
Al F	-0,272	0,129	-0,148	-0,024	0,059	0,031	0,119	-0,557	0,213	0,001	-0,176	0,114	-0,002
Al P	0,038	0,134	-0,052	0,039	-0,159	-0,332	0,035	-0,176	0,103	0,108	0,282	0,035	0,037
S F	-0,038	0,547	-0,040	0,121	0,303	-0,139	-0,061	-0,050	0,225	0,336	-0,200	-0,045	-0,152
S P	0,026	0,130	0,123	0,041	-0,191	-0,240	-0,075	-0,023	-0,079	-0,187	0,182	0,034	-0,041
Cl-	-0,163	-0,111	-0,107	0,057	0,504	0,024	-0,083	-0,091	-0,171	-0,261	0,037	0,012	0,224
Tot-N	-0,107	0,215	-0,008	0,414	0,110	0,158	-0,316	0,163	-0,319	-0,022	-0,057	0,053	-0,046
NH_4-N	0,149	0,038	0,075	0,133	0,522	-0,175	-0,029	-0,127	-0,101	0,182	0,071	-0,075	0,082
pH	0,257	0,189	-0,212	-0,351	-0,153	0,035	-0,084	-0,163	-0,241	0,065	-0,153	0,101	0,075
Alk	0,289	0,159	-0,363	-0,225	0,127	-0,175	-0,041	0,003	0,261	-0,287	0,086	0,311	0,129
SO_4^{2-}	-0,044	0,067	0,007	0,112	-0,174	0,299	-0,339	-0,545	-0,019	-0,061	-0,030	-0,058	0,106
Si F	-0,567	-0,072	-0,197	0,124	-0,023	-0,070	0,401	0,095	0,081	0,008	-0,078	0,077	-0,012
Si P	-0,030	0,009	-0,084	-0,024	0,014	0,011	0,025	0,022	-0,019	0,067	0,013	-0,568	-0,052
PO_4-P	0,087	-0,049	-0,060	0,035	-0,010	-0,079	-0,040	-0,047	-0,032	0,108	-0,068	0,161	-0,829
NO_3-N	0,168	-0,225	-0,029	-0,022	-0,051	-0,233	-0,110	0,125	0,127	0,501	-0,334	0,009	0,277

Eigenanalysis of the correlation matrix

Eigenvalue	13,700	11,300	0,000	0,000	0,000	0,000	0,000	0,000	0,000	0,000	0,000
Proportion	0,548	0,452	0,000	0,000	0,000	0,000	0,000	0,000	0,000	0,000	0,000
Cumulative	0,548	1,000	1,000	1,000	1,000	1,000	1,000	1,000	1,000	1,000	1,000
Eigenvalue	0,000	-0,000	-0,000	-0,000	-0,000	-0,000	-0,000	-0,000	-0,000	-0,000	
Proportion	0,000	-0,000	-0,000	-0,000	-0,000	-0,000	-0,000	-0,000	-0,000	-0,000	
Cumulative	1,000	1,000	1,000	1,000	1,000	1,000	1,000	1,000	1,000	1,000	
Eigenvalue	-0,000	-0,000	-0,000	-0,000							
Proportion	-0,000	-0,000	-0,000	-0,000							
Cumulative	1,000	1,000	1,000	1,000							

Principal Component Analysis (PCA) 3 m

Eigenvectors

Variable	PC1	PC2	PC3	PC4	PC5	PC6	PC7	PC8	PC9	PC10	PC11	PC12
Fe F	0,233	-0,069	0,339	0,098	0,108	0,056	0,088	0,294	0,042	0,264	0,035	0,112
Fe P	0,188	-0,134	-0,393	-0,012	-0,053	0,343	0,228	0,084	-0,329	0,007	0,249	0,209
Temp	0,300	-0,048	0,059	-0,056	0,045	0,159	0,106	0,010	-0,104	-0,373	-0,343	0,314
O_2	-0,273	-0,009	0,136	0,242	-0,007	-0,245	0,112	-0,135	-0,007	0,004	-0,073	-0,067
Cond	0,270	-0,110	0,062	-0,174	-0,272	-0,082	-0,108	0,121	0,048	-0,269	-0,158	0,099
Colour	0,174	-0,071	0,331	-0,338	-0,190	0,170	0,061	-0,063	0,032	0,432	-0,191	-0,119
Turb	-0,037	-0,340	0,022	-0,031	0,200	-0,039	0,358	0,024	0,257	0,033	-0,034	-0,056
DOC	-0,164	-0,175	0,061	-0,392	0,353	0,008	0,062	0,158	0,216	-0,249	-0,031	-0,173
Tot-P	0,235	-0,139	-0,182	0,081	0,527	0,038	-0,054	-0,038	0,037	0,144	-0,218	-0,062
Mn F	0,282	-0,047	0,026	0,219	0,176	0,060	-0,077	0,014	0,257	-0,304	0,267	-0,287
Mn P	0,082	-0,197	-0,444	-0,036	-0,072	0,190	-0,174	-0,512	0,127	0,126	-0,320	-0,119
Al F	0,150	-0,199	0,359	-0,121	0,047	-0,038	0,056	-0,572	-0,318	-0,240	0,256	-0,162
Al P	-0,098	-0,297	-0,214	-0,086	-0,125	0,106	0,046	0,122	0,046	0,131	0,421	-0,261
S F	-0,136	-0,307	0,002	0,031	-0,193	0,093	0,216	-0,016	0,072	0,185	0,044	-0,027
S P	0,151	0,232	-0,248	-0,210	0,149	-0,092	-0,006	-0,042	0,267	-0,021	0,321	0,313
Cl-	0,247	-0,173	0,135	0,101	-0,204	0,095	-0,159	0,045	0,480	0,119	0,020	0,171
Tot-N	-0,116	-0,306	0,079	0,133	0,164	-0,153	0,270	-0,159	0,121	-0,064	0,036	0,376
NH_4-N	0,184	-0,202	-0,045	0,323	0,250	-0,201	-0,086	0,151	-0,356	0,239	-0,148	-0,070
pH	0,129	-0,044	-0,029	0,553	-0,289	-0,056	0,087	-0,072	0,164	-0,133	0,054	-0,019
Alk	0,219	-0,232	0,078	-0,103	-0,006	-0,138	-0,256	0,110	-0,266	0,075	0,307	0,101
SO_4^{2-}	-0,128	-0,311	-0,029	0,039	-0,183	0,203	-0,089	0,338	-0,109	-0,363	-0,197	-0,224
Si F	-0,302	-0,040	-0,052	0,051	0,086	0,142	-0,036	0,167	-0,087	0,000	-0,067	0,172
Si P	-0,137	-0,306	-0,057	-0,074	-0,003	-0,337	-0,600	0,004	0,069	0,010	0,019	0,124
PO_4-P	-0,239	0,020	0,289	0,209	0,224	0,643	-0,359	-0,128	0,032	0,006	0,134	0,161
NO_3-N	-0,207	-0,252	0,005	-0,065	-0,110	-0,052	0,033	-0,101	-0,065	-0,015	-0,007	0,428

Variable	PC13	PC14	PC15	PC16	PC17	PC18	PC19	PC20	PC21	PC22	PC23	PC24	PC25
Fe F	-0,442	-0,084	0,019	-0,276	-0,090	-0,254	0,288	0,074	0,231	-0,127	0,216	0,046	0,252
Fe P	0,170	0,256	0,057	0,065	-0,143	0,164	-0,026	0,215	0,189	-0,006	-0,052	0,065	0,399
Temp	-0,008	-0,141	-0,110	-0,304	0,136	0,112	0,058	-0,138	-0,402	0,356	0,048	0,139	0,094
O_2	0,192	0,041	-0,246	-0,098	-0,219	0,211	0,347	0,470	0,067	0,249	0,070	0,365	-0,015
Cond	0,219	-0,011	-0,303	0,023	0,086	-0,233	0,190	0,056	0,378	-0,248	-0,435	0,100	-0,139
Colour	-0,055	0,057	-0,339	0,192	-0,005	0,245	-0,380	0,046	0,105	0,219	0,040	0,060	0,019
Turb	0,259	-0,280	0,119	-0,330	-0,359	-0,101	-0,292	0,070	0,049	0,075	-0,264	-0,253	-0,016
DOC	-0,221	0,581	0,032	0,019	0,060	-0,089	-0,002	0,175	-0,163	-0,013	-0,120	0,136	0,047
Tot-P	0,182	0,069	-0,270	0,329	-0,285	-0,012	0,291	-0,336	0,022	-0,022	0,142	-0,055	-0,080
Mn F	0,120	0,026	-0,178	-0,224	0,310	0,308	-0,192	0,061	0,267	-0,073	0,325	-0,061	-0,044
Mn P	-0,315	-0,011	0,140	-0,257	0,041	-0,051	0,063	0,179	0,155	-0,029	0,016	0,093	-0,125
Al F	-0,119	-0,125	-0,037	0,117	-0,140	0,009	0,102	0,049	-0,167	-0,258	-0,047	-0,124	0,140
Al P	-0,127	-0,218	-0,288	0,012	0,256	-0,082	0,340	-0,096	-0,146	0,369	-0,170	-0,098	-0,014
S F	0,259	0,045	-0,056	-0,144	0,114	-0,091	-0,046	-0,266	-0,273	-0,464	0,222	0,473	-0,033
S P	-0,152	-0,300	-0,266	0,142	-0,172	-0,140	-0,203	0,284	-0,186	-0,100	0,102	0,261	-0,118
Cl-	0,126	0,053	0,293	0,225	-0,010	0,283	0,268	0,249	-0,332	-0,095	-0,064	-0,189	0,002
Tot-N	-0,200	-0,114	0,201	0,363	0,316	0,144	-0,054	-0,164	0,333	0,124	-0,091	0,215	-0,045
NH_4-N	0,002	-0,040	-0,054	0,076	0,358	-0,130	-0,236	0,384	-0,257	-0,103	-0,190	-0,006	-0,060
pH	-0,308	0,347	-0,241	0,059	-0,281	-0,167	-0,238	-0,178	-0,123	0,108	-0,171	-0,002	0,022
Alk	-0,031	0,173	0,234	-0,203	-0,254	0,134	-0,029	-0,117	0,028	0,182	0,005	0,191	-0,557
SO_4^{2-}	-0,139	-0,304	0,102	0,350	-0,239	-0,054	-0,105	0,159	0,028	0,002	0,316	0,073	-0,092
Si F	-0,319	-0,084	-0,305	-0,162	-0,105	0,553	0,023	-0,052	-0,038	-0,389	-0,247	-0,153	-0,138
Si P	0,049	-0,055	-0,081	-0,089	-0,084	0,057	-0,158	-0,137	0,018	0,053	0,022	0,070	0,550
PO_4-P	0,157	-0,019	-0,046	-0,005	0,013	-0,245	-0,084	0,054	0,039	0,104	-0,177	0,130	-0,058
NO_3-N	0,073	0,234	-0,255	-0,045	0,099	-0,225	-0,006	0,157	0,023	0,023	0,426	-0,494	-0,193

Eigenanalysis of the correlation matrix

Eigenvalue	10,645	8,319	3,046	2,502	0,488	0,000	0,000	0,000	0,000	0,000	0,000
Proportion	0,426	0,333	0,122	0,100	0,020	0,000	0,000	0,000	0,000	0,000	0,000
Cumulative	0,426	0,759	0,880	0,980	1,000	1,000	1,000	1,000	1,000	1,000	1,000
Eigenvalue	0,000	-0,000	-0,000	-0,000	-0,000	-0,000	-0,000	-0,000	-0,000	-0,000	
Proportion	0,000	-0,000	-0,000	-0,000	-0,000	-0,000	-0,000	-0,000	-0,000	-0,000	
Cumulative	1,000	1,000	1,000	1,000	1,000	1,000	1,000	1,000	1,000	1,000	
Eigenvalue	-0,000	-0,000	-0,000	-0,000							
Proportion	-0,000	-0,000	-0,000	-0,000							
Cumulative	1,000	1,000	1,000	1,000							

APPENDIX D

Pearson correlation coefficient (p <0.05) – all depths, selected parameters

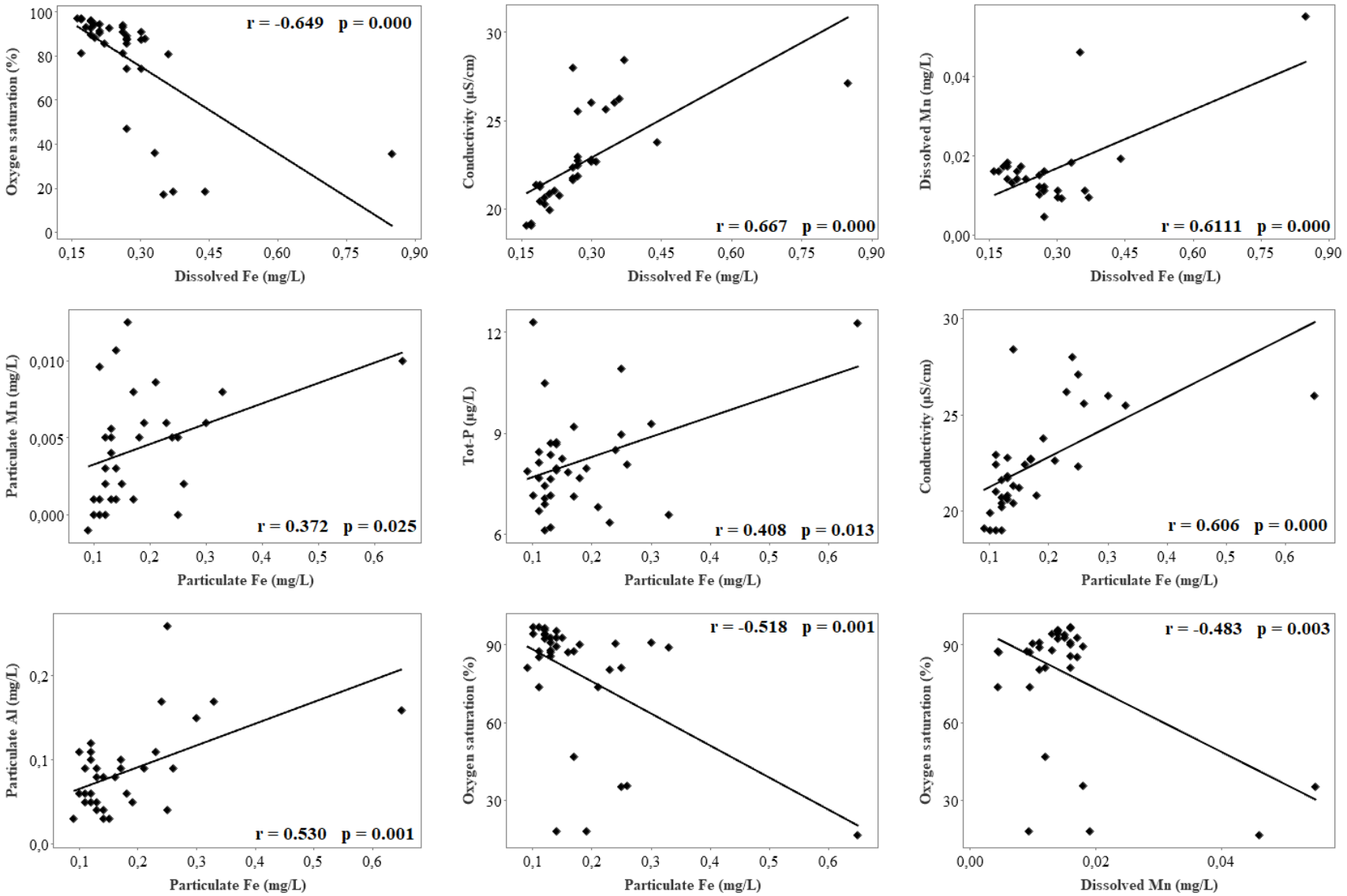

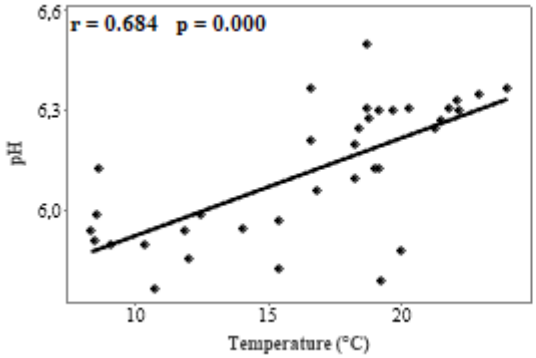
r = 0.684 p = 0.000
pH
6,6
6,3
6,0
10
15
20
Temperature (°C)

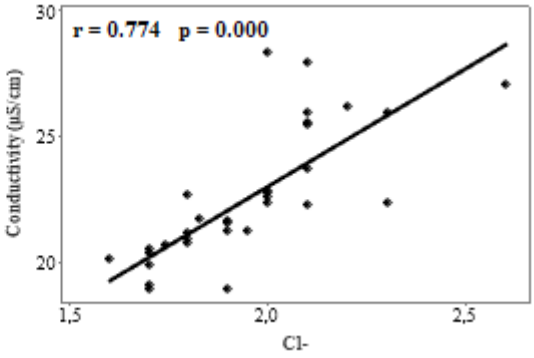
r = 0.774 p = 0.000
Conductivity (µS/cm)
30
25
20
1,5
2,0
2,5
Cl-

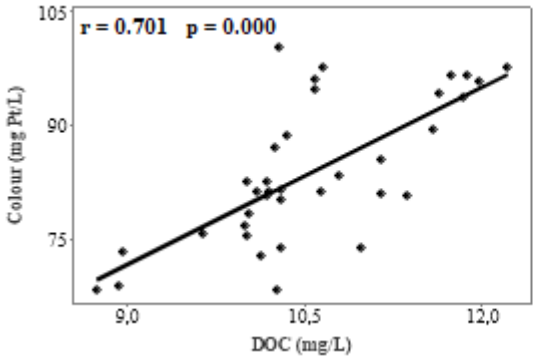
r = 0.701 p = 0.000
Colour (mg Pt/L)
105
90
75
9,0
10,5
12,0
DOC (mg/L)

APPENDIX E

Pearson correlation coefficient (p <0.05) – 0.5 m

Dis = dissolved; Part = particulate; Cond = conductivity; Turb = turbidity

	Dis Fe	Part Fe	Temp	O_2	Cond	Colour	Turb	DOC	Tot-P	Dis Mn	Part Mn	Dis Al	Part Al	Dis S	Part S	Cl-	Tot-N	NH4-N	pH	Alk	SO_4^{2-}	Dis Si	Part Si	PO_4-P
Part Fe	0,575																							
Temp	0,501	0,159																						
O_2	-0,780	-0,344	-0,511																					
Cond	0,848	0,894	0,459	-0,632																				
Colour	-0,561	-0,418	-0,160	0,460	-0,507																			
Turb	-0,477	-0,351	-0,665	0,571	-0,500	-0,167																		
DOC	-0,424	-0,230	0,046	0,258	-0,324	0,910	-0,389																	
Tot-P	0,136	0,384	-0,151	-0,228	0,311	-0,221	0,171	-0,146																
Dis Mn	-0,695	-0,332	-0,242	0,746	-0,504	0,568	0,225	0,310	-0,080															
Part Mn	0,741	0,351	0,495	-0,799	0,550	-0,607	-0,444	-0,295	0,097	-0,895														
Dis Al	-0,783	-0,602	-0,462	0,715	-0,750	0,881	0,309	0,669	-0,140	0,703	-0,822													
Part Al	0,188	0,647	-0,157	0,031	0,424	0,087	-0,155	0,300	0,491	-0,206	0,180	-0,052												
Dis S	0,057	0,045	-0,477	0,169	0,031	0,264	0,389	0,101	0,350	0,001	-0,320	0,397	0,374											
Part S	0,412	0,741	0,282	-0,390	0,633	-0,163	-0,555	0,177	0,475	-0,368	0,545	-0,454	0,789	-0,160										
Cl^-	0,747	0,547	0,584	-0,815	0,728	-0,721	-0,503	-0,461	0,007	-0,747	0,845	-0,941	-0,015	-0,476	0,453									
Tot-N	0,041	0,374	0,391	0,204	0,322	-0,373	-0,011	-0,377	-0,066	0,334	-0,127	-0,337	-0,125	-0,460	0,076	0,241								
NH_4-N	-0,566	-0,138	-0,399	0,175	-0,388	0,622	-0,168	0,665	0,213	0,343	-0,315	0,528	0,253	-0,033	0,238	-0,405	-0,426							
pH	0,685	0,631	0,427	-0,550	0,764	-0,774	-0,277	-0,720	0,189	-0,281	0,441	-0,848	-0,097	-0,344	0,289	0,752	0,605	-0,512						
Alk	0,816	0,621	0,687	-0,853	0,859	-0,435	-0,627	-0,212	0,404	-0,530	0,666	-0,722	0,202	-0,127	0,596	0,770	0,172	-0,268	0,699					
SO_4^{2-}	0,089	0,286	0,008	-0,009	0,310	0,212	0,114	0,185	0,375	0,001	-0,265	0,213	0,306	0,706	0,007	-0,155	-0,046	-0,095	-0,098	0,237				
Dis Si	-0,749	-0,480	-0,794	0,724	-0,724	0,651	0,565	0,447	-0,044	0,472	-0,718	0,879	0,105	0,546	-0,422	-0,890	-0,478	0,497	-0,846	-0,832	0,186			
Part Si	-0,215	0,114	-0,409	0,339	-0,107	0,491	0,094	0,544	0,478	0,162	-0,207	0,476	0,797	0,566	0,421	-0,551	-0,411	0,502	-0,548	-0,194	0,271	0,555		
PO_4-P	-0,547	-0,492	-0,134	0,713	-0,615	0,653	0,135	0,599	-0,240	0,530	-0,420	0,689	0,165	0,074	-0,110	-0,728	-0,109	0,261	-0,710	-0,613	-0,196	0,547	0,553	
NO_3-N	0,549	0,333	-0,362	-0,814	0,205	-0,536	0,717	-0,399	0,998	-0,623	0,623	-0,366	0,581	0,869	0,505	-0,983	-0,869	0,535	0,115	0,532	0,333	0,650	0,760	-0,154

Pearson correlation coefficient (p <0.05) – 1 m

Dis = dissolved; Part = particulate; Cond = conductivity; Turb = turbidity

	Dis Fe	Part Fe	Temp	O_2	Cond	Colour	Turb	DOC	Tot-P	Dis Mn	Part Mn	Dis Al	Part Al	Dis S	Part S	Cl-	Tot-N	NH4-N	pH	Alk	SO_4^{2-}	Dis Si	Part Si	PO_4-P
Part Fe	0,349																							
Temp	0,506	0,361																						
O_2	-0,826	-0,420	-0,599																					
Cond	0,598	0,818	0,407	-0,531																				
Colour	-0,516	-0,020	-0,234	0,393	-0,525																			
Turb	0,309	-0,379	-0,113	0,127	-0,021	-0,318																		
DOC	-0,639	0,038	-0,256	0,594	-0,341	0,779	-0,173																	
Tot-P	-0,264	-0,211	-0,380	0,317	-0,128	0,213	0,513	0,464																
Dis Mn	-0,743	-0,114	-0,300	0,724	-0,513	0,579	-0,129	0,660	0,113															
Part Mn	0,853	0,284	0,675	-0,920	0,478	-0,415	-0,051	-0,685	-0,429	-0,816														
Dis Al	-0,675	-0,404	-0,443	0,741	-0,741	0,840	0,089	0,786	0,424	0,738	-0,715													
Part Al	-0,182	0,430	-0,120	-0,098	-0,019	0,755	-0,487	0,456	0,184	0,181	-0,035	0,352												
Dis S	-0,463	-0,238	-0,779	0,540	-0,230	-0,076	-0,163	0,102	-0,095	0,250	-0,584	0,114	-0,229											
Part S	0,328	0,500	0,480	-0,409	0,256	0,462	-0,055	0,189	0,144	-0,087	0,399	0,118	0,686	-0,821										
Cl^-	0,692	0,482	0,229	-0,603	0,758	-0,760	-0,058	-0,753	-0,527	-0,645	0,602	-0,908	-0,317	0,106	-0,171									
Tot-N	-0,570	-0,256	-0,381	0,617	-0,519	0,643	0,100	0,911	0,560	0,621	-0,720	0,811	0,205	0,202	-0,026	-0,781								
NH_4-N	-0,326	-0,551	-0,822	0,401	-0,376	-0,222	0,105	-0,167	0,060	0,024	-0,418	0,054	-0,336	0,869	-0,837	0,082	0,056							
pH	0,706	0,377	0,608	-0,725	0,589	-0,746	0,046	-0,706	-0,483	-0,418	0,644	-0,838	-0,417	-0,292	-0,016	0,747	-0,665	-0,252						
Alk	0,723	0,836	0,652	-0,707	0,918	-0,375	-0,035	-0,283	-0,170	-0,487	0,638	-0,670	0,093	-0,525	0,514	0,631	-0,453	-0,651	0,665					
SO_4^{2-}	-0,401	-0,268	-0,857	0,574	-0,276	0,073	-0,062	0,103	-0,057	0,199	-0,540	0,244	-0,097	0,934	-0,656	0,055	0,184	0,846	-0,459	-0,565				
Dis Si	-0,704	-0,430	-0,817	0,754	-0,664	0,686	0,023	0,676	0,481	0,530	-0,771	0,846	0,343	0,510	-0,175	-0,690	0,737	0,480	-0,920	-0,759	0,635			
Part Si	-0,200	-0,465	-0,360	0,231	-0,346	0,272	0,519	0,301	0,900	-0,050	-0,240	0,460	0,196	-0,187	0,186	-0,587	0,434	0,112	-0,566	-0,341	-0,063	0,511		
PO_4-P	-0,593	-0,550	-0,839	0,808	-0,426	0,094	0,293	0,205	0,386	0,279	-0,707	0,462	-0,189	0,693	-0,574	-0,300	0,317	0,756	-0,669	-0,721	0,789	0,736	0,407	
NO_3-N	0,596	-0,803	-0,583	-0,516	-0,243	-0,618	0,918	-0,354	0,764	-0,115	-0,564	-0,127	-0,289	-0,033	-0,112	-0,115	0,300	0,347	0,636	-0,138	-0,115	0,803	0,705	0,372

Pearson correlation coefficient (p <0.05) – 2 m

Dis = dissolved; Part = particulate; Cond = conductivity; Turb = turbidity

	Dis Fe	Part Fe	Temp	O_2	Cond	Colour	Turb	DOC	Tot-P	Dis Mn	Part Mn	Dis Al	Part Al	Dis S	Part S	Cl-	Tot-N	NH4-N	pH	Alk	SO_4^{2-}	Dis Si	Part Si	PO_4-P
Part Fe	0,468																							
Temp	0,509	0,289																						
O_2	-0,756	-0,060	-0,527																					
Cond	0,750	0,807	0,569	-0,468																				
Colour	-0,485	-0,374	-0,306	0,400	-0,571																			
Turb	-0,010	-0,293	-0,127	0,312	-0,214	0,374																		
DOC	-0,074	0,241	-0,294	0,339	-0,103	0,721	0,324																	
Tot-P	-0,430	-0,486	-0,077	-0,094	-0,300	0,517	-0,136	0,043																
Dis Mn	-0,643	-0,252	-0,022	0,724	-0,548	0,521	0,364	0,209	-0,034															
Part Mn	0,908	0,518	0,413	-0,774	0,816	-0,728	-0,265	-0,298	-0,357	-0,836														
Dis Al	-0,683	-0,540	-0,432	0,600	-0,823	0,889	0,396	0,576	0,333	0,690	-0,890													
Part Al	0,470	0,759	-0,133	-0,054	0,697	-0,190	-0,075	0,382	-0,247	-0,533	0,530	-0,438												
Dis S	0,020	0,622	0,072	0,050	0,523	-0,188	-0,626	-0,030	0,102	-0,203	0,198	-0,407	0,576											
Part S	0,569	0,724	-0,020	-0,052	0,489	-0,064	0,156	0,615	-0,613	-0,248	0,435	-0,178	0,716	0,076										
Cl^-	0,666	0,696	0,601	-0,565	0,896	-0,704	-0,306	-0,342	-0,277	-0,524	0,805	-0,898	0,444	0,405	0,308									
Tot-N	0,438	0,577	0,478	-0,425	0,522	0,064	-0,278	0,461	0,070	-0,310	0,385	-0,165	0,366	0,195	0,529	0,445								
NH_4-N	-0,398	-0,164	-0,903	0,418	-0,454	0,352	0,218	0,490	0,104	-0,071	-0,317	0,430	0,213	-0,202	0,221	-0,463	-0,153							
pH	0,621	0,317	0,746	-0,655	0,667	-0,751	-0,193	-0,656	-0,263	-0,367	0,710	-0,832	0,002	0,089	-0,025	0,864	0,179	-0,688						
Alk	0,617	0,858	0,538	-0,390	0,959	-0,593	-0,444	-0,153	-0,277	-0,489	0,737	-0,817	0,666	0,701	0,410	0,876	0,509	-0,481	0,622					
SO_4^{2-}	-0,189	0,335	-0,229	0,345	-0,021	0,214	0,115	0,311	-0,186	0,357	-0,231	0,109	0,163	0,213	0,290	0,130	-0,029	0,269	-0,061	0,027				
Dis Si	-0,645	-0,363	-0,840	0,660	-0,740	0,729	0,338	0,619	0,196	0,410	-0,727	0,820	-0,076	-0,243	0,044	-0,798	-0,283	0,829	-0,910	-0,729	0,351			
Part Si	0,114	-0,035	-0,418	-0,240	0,143	-0,221	-0,316	-0,083	0,292	-0,772	0,361	-0,279	0,456	0,245	-0,015	0,007	0,002	0,396	-0,174	0,140	-0,499	0,026		
PO_4-P	-0,401	-0,219	-0,856	0,612	-0,503	0,586	0,531	0,623	0,026	0,235	-0,496	0,617	0,206	-0,214	0,243	-0,637	-0,337	0,847	-0,802	-0,565	0,358	0,913	0,137	
NO_3-N	0,866	-0,500	-0,245	0,033	0,545	0,461	1,000	0,600	-0,216	-0,189	0,866	0,189	0,918	-1,000	0,982	1,000	-0,143	0,817	0,397	-0,600	0,500	0,756	-0,500	0,923

Pearson correlation coefficient (p <0.05) – 3 m

Dis = dissolved; Part = particulate; Cond = conductivity; Turb = turbidity

	Dis Fe	Part Fe	Temp	O_2	Cond	Colour	Turb	DOC	Tot-P	Dis Mn	Part Mn	Dis Al	Part Al	Dis S	Part S	Cl-	Tot-N	NH4-N	pH	Alk	SO_4^{2-}	Dis Si	Part Si	PO_4-P
Part Fe	0,526																							
Temp	0,526	0,130																						
O_2	-0,402	-0,372	-0,464																					
Cond	0,586	0,324	0,780	-0,591																				
Colour	0,444	0,245	-0,289	-0,165	-0,032																			
Turb	0,102	0,340	-0,343	0,081	-0,031	0,394																		
DOC	-0,213	0,099	-0,619	0,351	-0,504	0,638	0,619																	
Tot-P	0,383	0,735	-0,145	-0,451	0,169	0,526	0,519	0,219																
Dis Mn	0,728	0,612	0,169	-0,410	0,324	0,542	0,203	-0,055	0,826															
Part Mn	-0,104	0,465	0,540	-0,453	0,561	-0,551	0,110	-0,444	0,085	-0,077														
Dis Al	0,318	0,295	-0,540	0,008	-0,214	0,914	0,588	0,692	0,666	0,574	-0,553													
Part Al	-0,315	0,469	-0,348	0,347	-0,155	0,163	0,799	0,646	0,242	-0,075	0,234	0,331												
Dis S	-0,170	0,135	-0,376	0,371	-0,163	0,110	0,881	0,539	0,118	-0,156	0,154	0,314	0,873											
Part S	-0,049	0,256	0,454	-0,093	0,184	-0,106	-0,667	-0,209	-0,156	0,062	0,060	-0,332	-0,296	-0,689										
Cl^-	0,843	0,518	0,537	-0,325	0,671	0,404	0,304	-0,124	0,487	0,764	0,183	0,323	0,113	0,106	0,030									
Tot-N	0,015	0,117	-0,456	0,319	-0,324	0,304	0,917	0,633	0,321	0,083	-0,068	0,534	0,748	0,907	-0,738	0,160								
NH_4-N	0,467	0,473	-0,101	-0,465	0,029	0,446	0,534	0,120	0,809	0,733	0,072	0,578	0,148	0,240	-0,455	0,482	0,507							
pH	0,181	-0,128	0,780	-0,098	0,522	-0,757	-0,397	-0,825	-0,426	-0,153	0,596	-0,828	-0,312	-0,205	0,194	0,214	-0,367	-0,266						
Alk	0,136	0,070	0,641	0,308	0,389	-0,319	-0,226	-0,201	-0,408	-0,121	0,252	-0,466	0,101	-0,061	0,569	0,335	-0,238	-0,539	0,595					
SO_4^{2-}	-0,175	0,187	-0,368	0,340	-0,164	0,109	0,889	0,535	0,157	-0,127	0,188	0,317	0,887	0,998	-0,674	0,119	0,911	0,280	-0,206	-0,071				
Dis Si	-0,649	-0,247	-0,881	0,657	-0,883	0,082	0,391	0,685	-0,122	-0,428	-0,417	0,315	0,508	0,554	-0,444	-0,609	0,599	-0,035	-0,592	-0,387	0,547			
Part Si	-0,248	0,083	-0,225	0,174	0,085	-0,163	0,772	0,283	0,073	-0,309	0,429	0,034	0,726	0,867	-0,662	-0,025	0,677	0,076	-0,006	-0,063	0,858	0,354		
PO_4-P	-0,210	-0,321	-0,857	0,694	-0,695	0,331	0,340	0,581	0,056	-0,059	-0,754	0,577	0,250	0,368	-0,459	-0,313	0,501	0,021	-0,636	-0,370	0,338	0,777	0,161	
NO_3-N	-0,385	-0,135	-0,552	0,583	-0,320	-0,164	0,789	0,775	-0,271	-0,565	0,235	0,110	0,855	0,947	-0,797	-0,186	0,869	-0,048	-0,267	0,022	0,936	0,734	0,953	0,441

Norges miljø- og biovitenskapelige universitet
Noregs miljø- og biovitskapelege universitet
Norwegian University of Life Sciences

Postboks 5003
NO-1432 Ås
Norway